University of Nevada, Reno

ortho-Tolyl(trifluoromethyl)carbenes

Generation, Calculations, and Reactions through Quantum Mechanical Tunneling

A thesis submitted in partial fulfillment of the requirements for the

degree of Master of Science in Chemistry

by

Chengliang Zhu

Dr. Robert S. Sheridan/ Thesis Advisor

August 2012

University of Nevada, Reno
Statewide • Worldwide

THE GRADUATE SCHOOL

We recommend that the thesis
prepared under our supervision by

Chengliang Zhu

entitled

o-Tolyl(trifluoromethyl)carbenes: Generation, Calculations, and Reaction through Quantum Mechanical Tunneling

be accepted in partial fulfillment of the
requirements for the degree of

MASTER OF SCIENCE

Robert S. Sheridan, Ph. D., Advisor

Christopher S. Jeffrey, Ph. D., Committee Member

Paula J Noble, Ph. D., Graduate School Representative

Marsha H. Read, Ph. D., Dean, Graduate School

August, 2012

Abstract

We synthesized *o*-tolyl(trifluoromethyl)diazirine, trideuteriomethyl-*o*-tolyl(trifluoromethyl)diazirine and *p*-methoxy-*o*-tolyl(trifluoromethyl)diazirine precursors and generated the corresponding carbene species photochemically in low temperature nitrogen matrices. 1, 4-Hydrogen shifts in thermal decay and other photochemical reactivities were investigated both experimentally and theoretically. All carbene species as well as their subsequent rearranged products were characterized with IR and UV-vis spectroscopy and confirmed by comparison with frequency and TD DFT calculations at the B3LYP/6-31G** level of theory.

Acknowledgments

I would like to express my deepest gratitude to my graduate program advisor, Professor Robert S. Sheridan, for his tremendous guidance and support in my three-year graduate study, and particularly in the most recent months when this thesis is being written. Without his fatherly understanding and encouragement, this work can never be accomplished on time.

My appreciation also goes to all the current and former group members in Sheridan's lab. In particular, I want to thank Rajendra Ghimire for numerous help in my study and research, as well as his encouragement in my hard times. I also appreciate all the help I obtained from Dr. Peter Zuev for guiding me in the synthetic work and introducing me to the computational chemistry. Part of the calculations and theoretical analysis in this thesis were accomplished with the help from Yao Xu and the stimulating talk with him.

Finally, I would like to thank my parents and Chuanyu, for their love, understanding and support whenever I need in my life.

Table of Contents

1. Introduction

In the past 30 years, a number of experimental studies have shown that a quantum mechanical tunneling pathway might be more reasonable than a classical transition state mechanism in many carbene reactions at very low temperatures. Although direct spectroscopic observations of 1, 4-hydrogen shifts in aryl carbenes involving quantum mechanical tunneling pathways have been recorded for both triplets and singlets by chemists, the recent advances in matrix isolation and spectroscopy techniques as well as merging of high-level computational methods allow us to do more research in this area.[1,2] Most recently, aryl carbenes with trifluoromethyl groups have been demonstrated to favor the singlet state versus triplet in energy compared to hydrogen. In addition, both density functional theory (DFT) calculations and experimental observations have noted that *para*-methoxyphenyl(trifluoromethyl)carbene is a ground state singlet. The previous work and experimental techniques encouraged us to investigate the energetics and 1, 4-hydrogen migration of the *o*-tolyl(trifluoromethyl)carbenes family in more detail.

2. Background

2.1 Carbene basics

Reactive intermediates exist in many chemical processes and studies of these transient species give insight into the underlying mechanisms in those transformations. As early as 1954, Doering and Hoffman for the first time proposed dichlorocarbene as a reaction intermediate in the hydrolysis of chloroform under basic conditions.[3] From then on, this neutral reactive intermediate family has been studied heavily. Thanks to high-level computational methods, matrix isolation techniques and time resolved spectroscopic tools, numerous facile carbene species were detected, trapped and investigated. However, it is appropriate to emphasize that not all carbenes are highly reactive. Those having bulky and/or strong electron-donating substituents are even bench-stable. On account of its unique electronics and ambiphilic reactivities (both electrophilic and nucleophilic), this “fleeting” species has found application in various interdisciplinary research fields other than chemistry, including molecular biology, pharmaceuticals and interstellar physics. In addition, many nitrogen heterocyclic carbenes (NHC) have found use as ligands for important transition

metal catalysts in new organic transformations. This chapter will discuss the basics in carbene chemistry, such as electronic structures, generation and reactivity, as well as the classical tools in carbene study.

2.1.1 Electronics and structures

Carbenes can be defined as a family of neutral carbon-based reactive intermediates, which feature a carbon center (also called carbenic carbon) with 6 valence electrons and 2 substituents. The simplest carbene is methylene ($:CH_2$) and other carbene species can be simply thought of as methylene derivatives with different substituents. (Figure 2-1)

Figure 2-1 Generic carbene structure and the simplest carbene-methylene

The electronic configuration of methylene is simply pictured in Figure 2-2. Besides two bonding orbitals with hydrogens, the carbenic carbon has another two orbitals (**σ** and **p**) as well as 2 unshared electrons. Thus, there are at least 4 different ways to distribute the nonbonding electrons into orbitals and therefore two types of spin states would be produced: either both electrons are paired, or remain unpaired. These two electron spin states are termed singlet (**S**) and triplet (**T**). If both electrons are spin paired, either in the same orbital or in different orbitals, it is called a singlet state (**S**). On the contrary, if the nonbonding electrons are in separate orbitals and spin parallel, its multiplicity is called triplet (**T**). Evidence that this triplet is the ground state in methylene was provided by IR, UV-vis, and particularly electron paramagnetic resonance (EPR) spectra. Unpaired electrons in triplet states give EPR signals, while singlets are unobservable.

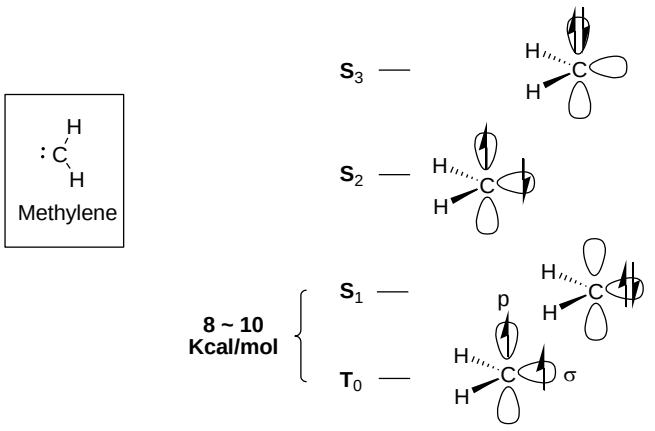

Figure 2-2 Electronic configurations in methylene

Pioneering work to unravel methylene's structure and energetics started as early as 1959.[4] Foster and Boys predicted a nonlinear structure of triplet methylene based on their ab initio calculations.[5] Two years later, Herzberg obtained the electronic spectrum of methylene and verified its triplet ground state. After careful analysis of his experimental data, Herzberg made conclusions that triplet methylene is linear rather than bent.[6] In 1966, Pople and Segal used semiempirical methods to predict that the bond angle of triplet methylene is 141.4 ^{o} in agreement with Foster and Boys' prediction of a bent structure.[7] Bender and Schaefer also studied the methylene problem by using higher-level computational methods in 1970, and their calculated results clearly showed that methylene in its ground state is bent with bond angle of 135.1^{o}.[8] However, before any compelling experimental evidence was acquired, theoretical chemists chose to avoid challenging Herzberg's conclusion. Two following EPR studies of methylene made by Bernheim and Wasserman, and Yager and Kuck, not only strongly suggested a bent structure with the most probable bond angle of 136^{o}, but also forced Herzberg to reexamine his previous experimental data and finally agree with the bent structure.[9,10,11] The most precise bond angle of triplet methylene, 133.8^{o} $\pm$ 0.1^{o}, was obtained from laser magnetic resonance experiments by Bunker and Jensen in 1983. [12] The energy gap between triplet ground state and lowest singlet state(ΔE_{T-S}) in methylene was also debated for many years.[4] In 1982, Lee reported the methylene singlet-triplet energy splitting to be 8.5$\pm$ 0.8 kcal/mol by direct experimental measurement. [13] This value is in very close agreement with computational predictions and an average of 8-10 kcal/mol is accepted by most chemists.

Like the parent carbene methylene, most carbene species are bent suggesting a sp^n hybridized carbenic center. Experimentally, carbenic center bond angles in triplet states (130^o -150^o) are usually found to be greater than those in singlet states (100^o -110^o). The smaller bond angles in singlet carbenes result from more electron-electron repulsions between the lone pair and bonding electrons. (Figure 2-3)

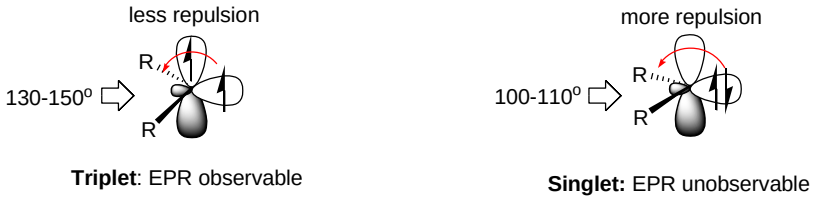

Figure 2-3 Bond angle differences in triplet and singlet carbenes

Hund's rule and the Pauli Exclusion Principle predict triplet state more stable than singlet, and this is indeed the case in methylene as well as many methylene derivatives. However, a variety of experimental evidence shows that the triplet-singlet splitting of many carbene species could be reduced or even overturned by appropriate substituents at the carbenic center. A guideline to determine the ground state of carbene species is comparing the energy required to promote an electron from the sp^n orbital to the p orbital with the electron-electron repulsion energy. If the energy gained by putting both electrons in the sp^n orbital is sufficient to overcome the repulsion between two electrons in a single orbital, singlet states are then preferred to triplets. Considering that the carbenic carbon only has six electrons, electron-donating substituents, such as halogen, alkoxy group etc., could stabilize the electron-deficient carbene to some extent, by partial delocalization of lone pair electrons onto the carbenic carbon. In fact, many electron donating substituents with lone pairs adjacent to the carbenic center have been found to lower the singlet state even below the triplet, which can be rationalized by an intuitive model in Figure 2-4. The nonbonding orbitals of electron-donating substituents (N, O, or halogen) interact with the p orbital (typically, resonance interaction is involved) and are stabilized

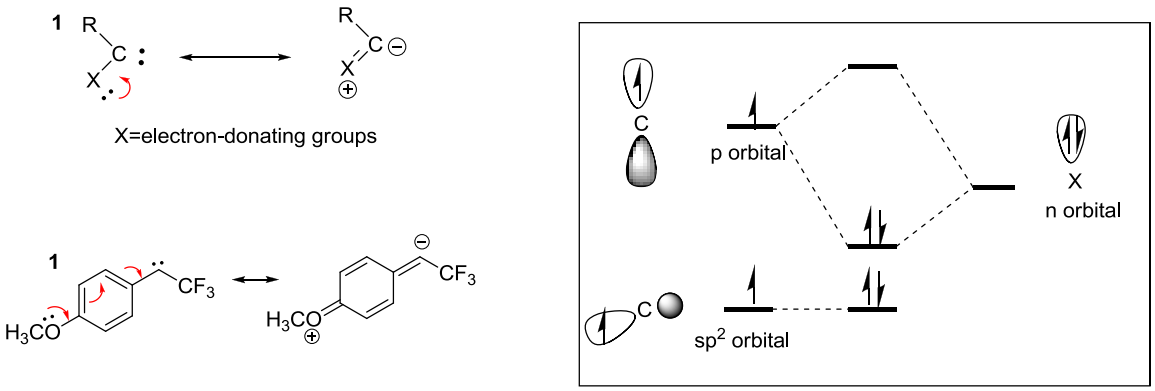

Figure2-4 Resonance-stabilized singlet state by electron-donating substituents

Methylmethoxycarbene (**1**) is the first directly observed singlet alkyl carbene with only one alkoxy stabilizing substituent.[14] Like alkoxy groups, halogen atoms as weaker electron donors were also found to stabilize the singlet states of chlorocyclopropyl carbene (**2**).[15] More recently, Sheridan's group showed that appropriate electron-rich substituents could switch aryl carbene ground states from triplet to singlet via a resonance interaction between the substituents and carbenic center. 2-Benzothienyl(trifluoromethyl)carbene (**3**) and *para*-methoxyphenyl(trifluoromethyl)carbene (**4**) were proved to be ground state singlets both theoretically and experimentally. [16,17] (Figure 2-5) However, *meta*-methoxyphenyl(trifluoromethyl)carbene, where resonance interaction between the methoxy group and carbene is not obtained is a triplet.

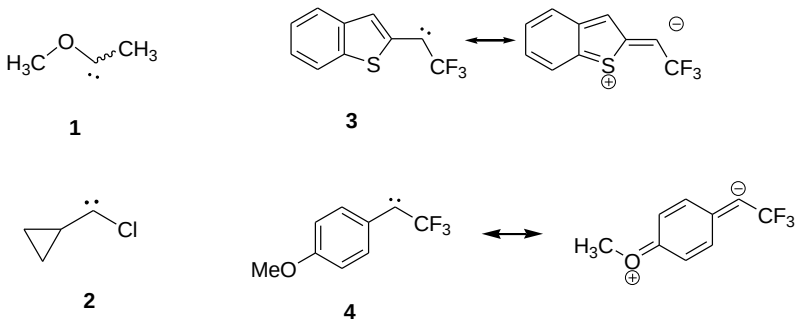

Figure 2-5 Carbene species with singlet ground state

2.1.2 Generation and chemical reactivity

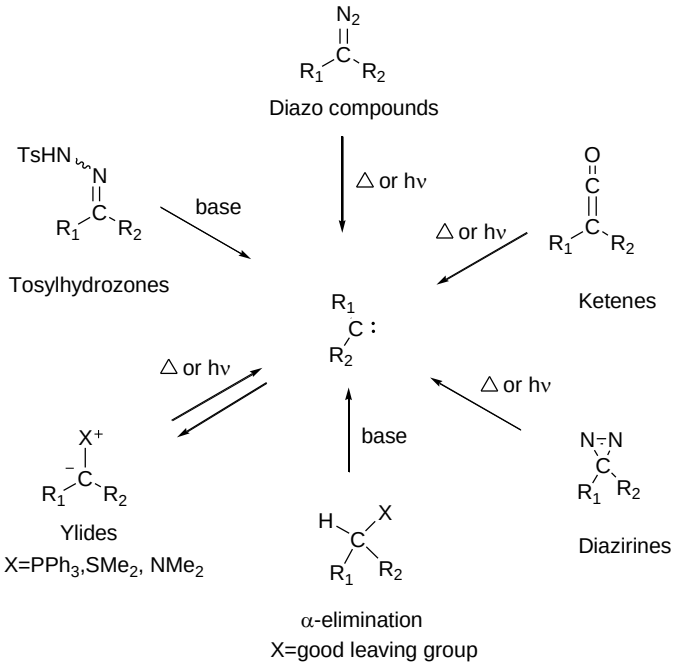

Figure 2-5 Generation of carbene species

There are several methods for generation of carbenes. (Figure 2-6) In general, carbenes are formed from precursors by loss of a small, stable molecule. Although carbenes can be formed in many similar reactions, for example, photolysis of diazo compounds, pyrolysis of tosylhydrazone sodium salts, loss of carbon monoxide from ketenes and α-elimination of leaving groups, the use of diazirines as carbene precursors has increased dramatically over the past twenty years. First synthesized and characterized in the early 1960s, diazirines were found easy to prepare, stable under various physical and chemical conditions, and form carbene species photochemically cleanly upon irradiation by UV light after irreversible nitrogen molecule release.[18,19]

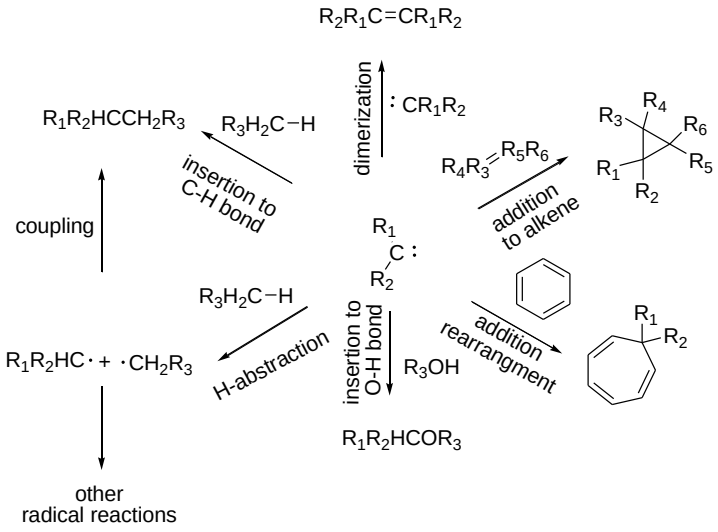

Figure 2-6 Typical carbene reactions

Carbenes undergo many types of reactions and the reactivities strongly depend on their spin states. Dimerization between two triplet carbenes is a spin-allowed process and usually fast and exothermic. Cycloaddition to alkenes' double bonds to form cyclopropanes is another characteristic reaction of both singlet and triplet carbenes, in which the stereochemistry is quite spin-dependent. Skell and Woodworth studied the 1, 2-cycloaddition of carbenes to alkenes, and summarized that a singlet carbene can add to a double bond in a single step and is stereospecific, while the triplet carbene cannot since it is spin-forbidden. [20] This argument indicates that cycloaddition of singlet is a concerted process with stereochemistry retained, while triplet cycloaddition is step-wise and a nonstereospecific process. The 1, 2-cycloaddition of methylene to an arbitrary olefin distinguishes these two different reaction types clearly. [21](Scheme 2-1) Singlet methylene gives stereospecific product, while triplet cycloaddition leads to a stereochemical mixture.

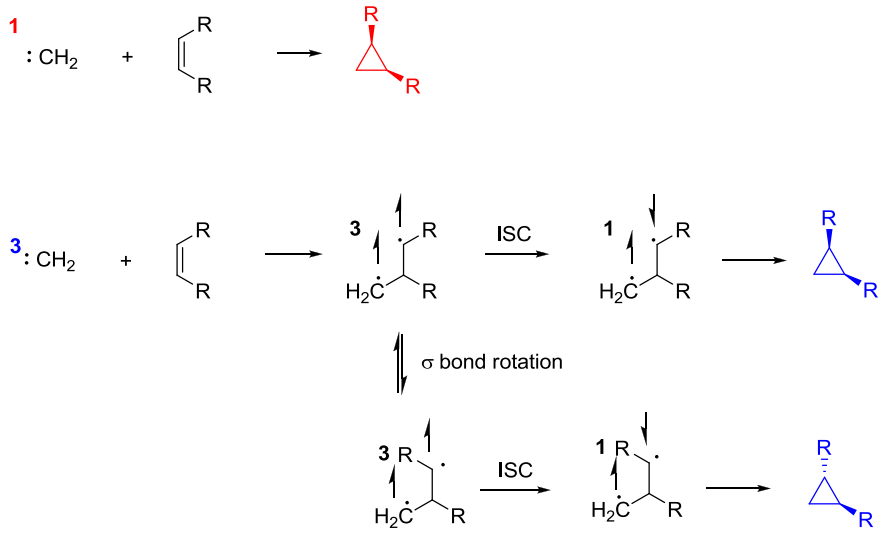

Scheme 2-1 Spin multiplicities dependent stereochemistry control in methylene 1, 2-cycloaddition

Considering its electron-deficiency at carbenic carbon, carbene species, either triplets or singlets are electrophilic. C-X bond insertion (X=H or O; also termed as H-abstraction as well, when X=H), is one of the characteristic reactions of carbenes. To fulfill the octet rule, the carbenic centers are desperate to insert into almost any singlet bonds, even the inert C-H σ bonds in alkanes. Again, two paths are proposed depending on the spin multiplicity, of which the stereochemistry is preserved in singlet carbene insertion, while lost in triplet insertion. (Scheme2-2)

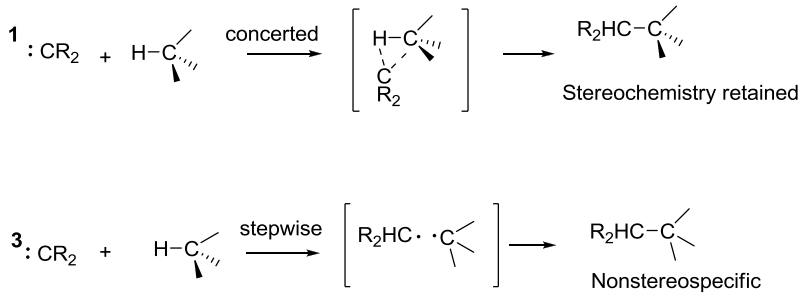

Scheme 2-2 Spin multiplicities dependent stereochemistry control in methylene C-H insertion

The vacant p-orbital of carbenes allows for fast rearrangement to occur. Wolff rearrangement of diazoketones to ketenes is a famous example involving carbene intermediates.

As discussed in the previous section, carbenes ground spin multiplicity can be changed by tuning substituents. Likewise, the reactivity of the carbenic carbon may be changed or even reversed with different substituents installed. Although most carbenes are electron-deficient and often electrophilic, carbenes with heavily electron-donating substituents are less electrophilic than others. For instance, the diamino carbenes can be quite nucleophilic and ready to react with electrophiles.

2.2 Classical study methods and techniques in carbene chemistry

Most carbenes are too reactive to isolate. A practical question is how we know they exist and how we can study them. Several techniques have been developed and make the study of reactive intermediates more convenient.

Matrix isolation- Matrix isolation is a technique to isolate highly reactive molecules in solid inert gas or organic glasses under cryogenic conditions. The host-gases are usually nitrogen, argon or xenon of high purities. At low temperatures, reactive intermediates are isolated by solid host gas and both intra-or intermolecular reactions are remarkable diminished, which makes it possible to characterize the reactive molecules by using spectroscopic methods, such as IR, UV-vis and EPR, etc.[22]

Frequency calculations and TD calculations-High-level computational methods are able to estimate the relative energies of reactive intermediates quite precisely. In addition, density functional theory (DFT) calculations have been proved successful in prediction of molecular vibrational frequencies which are in very close agreement to experimental IR spectra. Time-dependent (TD) DFT methods for excited states are greatly used in UV–vis calculations, in which the f values are proportional to absorption intensities in experimental UV-vis spectra.

Spectroscopic methods-Along with the computational data, spectroscopic observations help chemists directly "see" the highly reactive intermediates and understand the nature of their chemistry. Three commonly used classical spectroscopies are IR, UV-vis and EPR. Like under conventional conditions, IR and UV-vis spectroscopies are also used in matrix studies to characterize the reactive molecules with information of bond vibrating modes and excited states. EPR spectroscopy is particular in detection of

those intermediates with triplet spin states and is extremely useful in carbene spin-multiplicity determination.

Trapping experiments-Trapping experiments are experimental probes for detecting carbene species, or the carbenes' spin multiplicities, based on their spin-dependent reactivities with trapping agents, such as oxygen, hydrogen and hydrogen chloride. Carbenes with different multiplicities show characteristic reactivities with different trapping agent-doped matrices at low temperatures. For instance, matrix-isolated singlet carbenes are found to react with hydrogen chloride with matrix annealing, but remain stable in oxygen and hydrogen. On the contrary, triplet carbenes are oxygen and hydrogen reactive at higher temperature but stay stable to hydrogen chloride.[23]

3. Quantum mechanical tunneling

3.1 Background

Transition state theory indicates reactant molecules must be activated to overcome an energy barrier before a chemical reaction proceeds. Quantum mechanical tunneling provides us another picture to understand how chemical reaction happens. On the atomic level, reactant molecules need not necessarily climb the activation energy barrier, but penetrate it to transform to products. This phenomenon is termed quantum mechanical tunneling (QMT). In certain cases if the de Broglie wavelength of reactant nuclei is large enough and the energy barrier is sufficiently "narrow", the wave function of reactants can then penetrate the barrier rather than pass over it. (Figure 2-7)

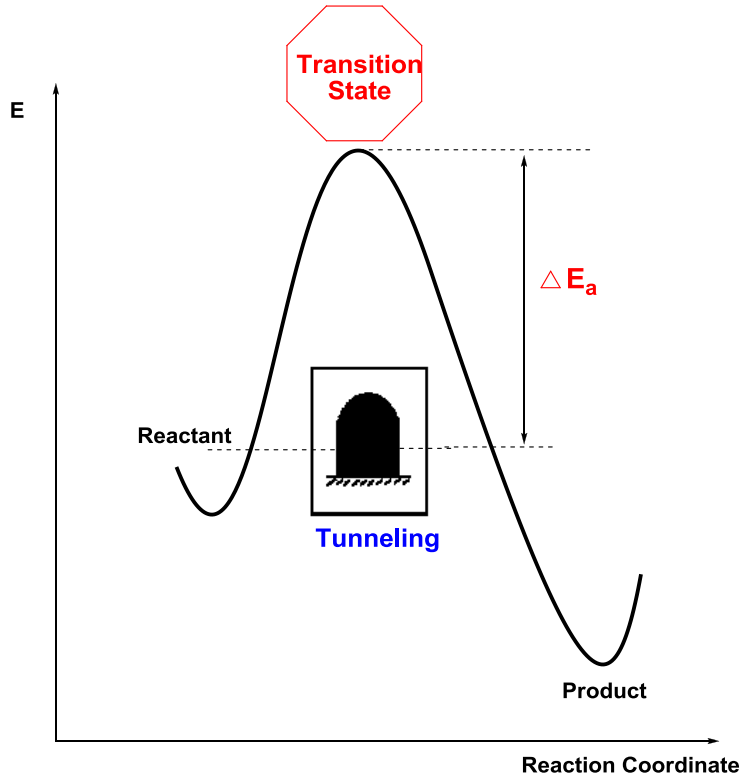

Figure 2-7 Transition state theory and quantum mechanical tunneling: climb the barrier or penetrate it

Theoretical treatment of tunneling shows that a light particle is more likely to tunnel than a heavy atom.[26] Thus, hydrogen tunneling was observed in many reactive intermediate transformations, but its isotope, deuterium is less often involved in tunneling pathways. In tunneling paths, a factor more important than the particle's mass is the barrier width. Carbon atoms, which are much heavier than hydrogen and deuterium, was also observed tunneling through a narrow barrier.[27]

In a recent review on quantum mechanical tunneling in organic reactive intermediates, Sheridan summarized the experimental signatures of tunneling.[25] Regular chemical reactions become dramatically sluggish as the temperature is lowered. However, the reaction rates in tunneling are independent of temperatures and faster than "expected". Since the tunneling is penetrating the energy barrier rather than passing over it, a nonlinear Arrhenius plot would be expected. (Figure 2-8a) In addition, "matrix effects" are also usually observed in many reactive intermediate reactions involving tunneling pathways. Matrix

effects refer to the nonexponetial kinetic measurements of reactive intermediate decays in matrices, in other words, the first-order plots of ln[intensity] versus time are “upward curved”.(Figure 2-8b)

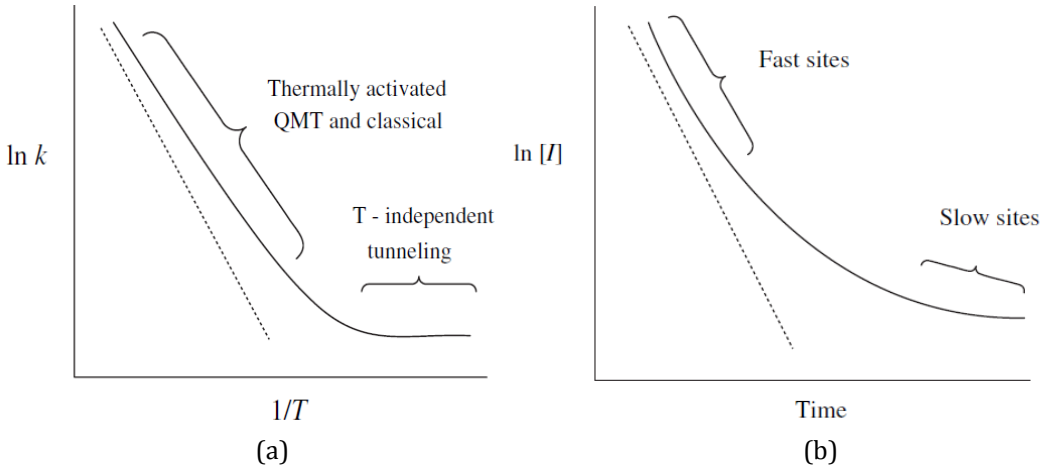

Figure 2-8 (a) Schematic Arrhenius plot with (solid line) and without (dotted line) tunneling; (b) First-order plots of ln[intensity] versus time (Figures are provided by Dr. Robert S. Sheridan)[25]

3.2 Quantum mechanical tunneling in aryl carbenes

Although quantum mechanical tunneling is uncommon under conventional reaction conditions, it is somewhat seen in reactive intermediate chemistry under cryogenic conditions. Tunneling pathways are proposed to be important in several aryl carbene intramolecular hydrogen migration reactions, which are supported by direct spectroscopic observations and/or computational evidence.

McMahon and Chapman studied the *o*-tolylmethylene system with low-temperature matrix-isolation techniques in 1987. [1] (Scheme 3-1) Obtained from irradiation of a matrix-isolated *o*-tolyldiazomethane (**5**) in inert gas matrices at cryogenic temperatures, *o*-tolylmethylene (**6**) was characterized by IR, UV-vis and particularly EPR spectrum. In addition, the unique thermal and photochemical reactivities of carbene (**6**) were investigated in great details.

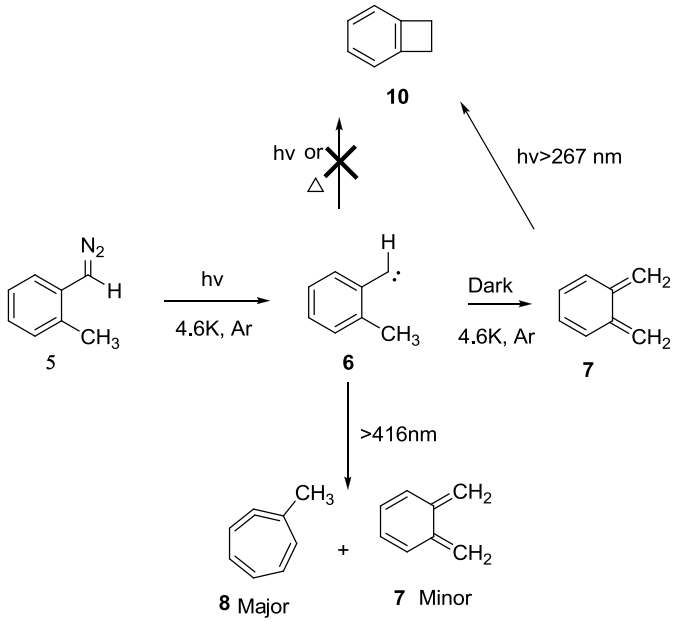

Scheme3-1 Photochemical and thermal reactivities of *o*-tolylmethylene

o-Tolylmethylene could be generated photolytically from diazo precursor under three different irradiation conditions. Long-wavelength irradiation (λ>470 nm) was found to produce triplet *o*-tolylmethylene (**6**), which was detected by UV-vis and EPR spectroscopy, along with the 1, 4–H shifted *o*- quinomethide product (**7**). The EPR data also distinguished two possible rotomers of the carbene (**6**), namely *anti* and *syn* with the *anti* being the major rotomer. Irradiation of diazo precursors at λ > 416 nm was found to generate the carbene (**6**) and *o*-quinomethide (**7**) as well as ring expended 1-methylcycloheptatetraene (**8**). Prolonged irradiation at this wavelength region consumed all of the carbene species, and afforded a mixture of *o*-quinomethide (**7**) and 1-methylcycloheptatetraene (**8**) with the ring expanded product as major. However, due to its facile nature, IR bands of the carbene (**6**) were not observed under either of these conditions (λ >470 nm and >416 nm). Flash irradiation (λ>200 nm, 1 min) of the diazo compound was found to generate a mixture of *o*-tolylmethylene (**6**), *o*-quinomethide (**7**) and 1-methylcycloheptatetraene (**8**), and the carbene species was detected by UV-vis, EPR and IR spectra.

Interestingly, after its generation, carbene (**6**) was found to decay thermally to give *o*-quinomethide (**7**) even at temperatures as low as 4.6 K in dark. This unusual 1, 4-H migration to *o*-quinomethide (**7**) was monitored spectroscopically. Kinetic analysis shows that the carbene disappearance follows the standard

(time)$^{1/2}$ dependence due to the "matrix effect". More precise kinetics measurements at a range of different temperatures of the carbene thermal decay indicated a negligible temperature-dependence and nonlinear Arrhenius plot. To investigate the isotopic effects, *o*-tolylmethylene with a perdeuterated methyl group was generated and the 1, 4 D-migration was not observed up to 19K in the Ar matrix, at which point the carbene dimerized. In Xe matrix this 1, 4 D-migration was shut down up to 65K, at which temperature the matrix became soft. By contrast, the H-analogue decays under the same conditions. (Scheme 3-2)

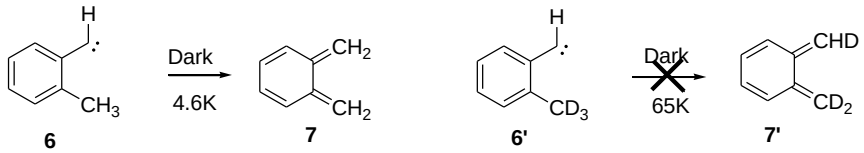

6 **7** **6'** **7'**

Scheme 3-2 Isotopic effects in *o*-tolylmethylene thermal decay

In their research, the thermal rearrangement at temperatures as low as 4.6 K, explicit matrix effects, negligible temperature dependence, non-Arrhenius plot and isotope effect, strongly suggest a quantum mechanical tunneling pathway for the 1, 4 H-migration in *o*-tolylmethylene.

3.3 A novel aryl carbene family: Aryl (trifluoromethyl) carbenes

By using high-level DFT computational methods, Song and Sheridan recently investigated the effects of trifluoromethyl groups as well as other charged substituents on the stability of carbenes' singlet spin states and singlet-triplet energies gaps. Both natural bond orbital (NBO) analysis and Bent's rule indicate that the electron-withdrawing trifluoromethyl group makes the atomic orbitals re-hybridize at the carbenic center and it was found that trifluoromethyl substituents increase the p_π and σ energy gap and stabilizes singlet to some extent.. In other words, compared with hydrogen atom, a trifluoromethyl group has small to moderate stabilizing effects on singlet carbenes.[28]

In addition to its singlet-stabilization effect, compared with aryl carbenes, aryl(trifluoromethyl)carbenes show different chemical reactivities. For example, 1, 2 hydrogen shifts from adjacent carbons to carbenic carbon are common in aryl carbenes, but corresponding 1, 2-F shifts are rarely observed. Moreover, ring expansion is strongly diminished in aryl(trifluoromethyl)carbene.(Scheme3-3) It was also found that

trifluoromethyl groups could affect carbene's chemical reactivities by increasing their electrophilicity and C-H insertion reactivity.

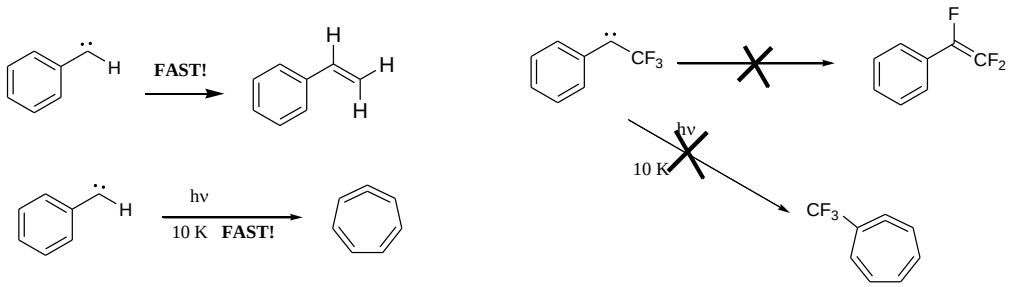

Scheme3-3 Unique reactivities of aryl(trifluoromethyl)carbene[29]

Practically, aryl(trifluoromethyl)carbenes as well as their precursors, aryl(trifluoromethyl)diazirines are widely used as labeling reagents in photoaffinity techniques to investigate structural and functional properties of biological systems. [30]

4. Research objectives

Our interests in exploring the energetics and reactivity of *o*-tolyl carbenes family was inspired by Chapman and McMahon's direct observation of 1, 4-H migration in triplet *o*-tolylmethylene (**8**) under tunneling conditions.[1] *o*-Tolyl(trifluoromethyl)carbene (**9**) was chosen to be our parent model, not only because it bears similarity to McMahon's prototypic carbene, but also the trifluoromethyl group was found to stabilize singlet versus triplet carbene state in comparison with hydrogen.(Figure 4-1) Finally, we have found in our group that the trifluoromethyl groups shut down other aryl carbene photochemical reactions, such as ring expansion.

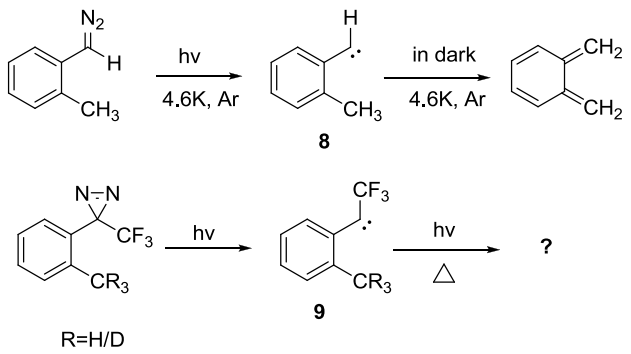

Figure 4-1Research objective1: *o*-tolyl(trifluoromethyl)carbene

According to the mechanisms proposed for the 1, 4-H shift in *o*-tolylmethylene, we also predicted two possible pathways for the same process in *o*-tolyl(trifluoromethyl)carbene: a classic transition state mechanism and a quantum mechanical tunneling pathway. (Figure 4-2)

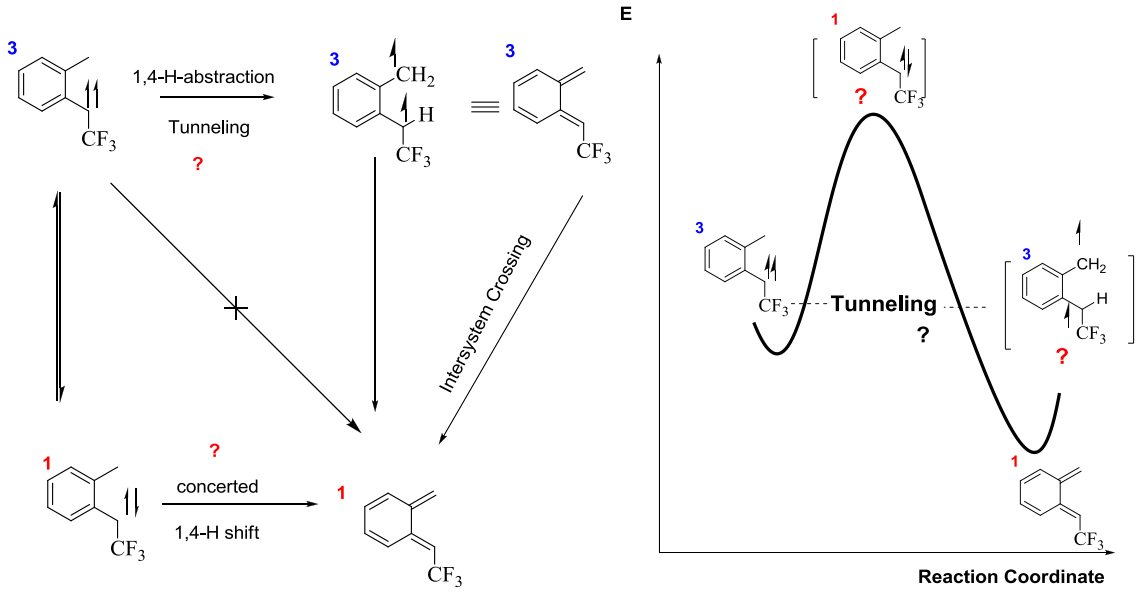

Figure 4-2 Proposed reaction pathways of *o*-tolyl(trifluoromethyl)carbene 1, 4-H migration

Our primary goal is to understand energetics of *o*-tolyl(trifluoromethyl)carbene and how it reacts under different thermal and photochemical conditions. To achieve this, the corresponding carbene will be generated and characterized spectroscopically. Trapping experiments are needed to confirm its spin multiplicity. In addition, DFT calculations are carried out to predict its ground spin state, vibrational frequencies and UV-vis absorptions. Its thermal and photochemical reactivity can be investigated by experimental observations together with theoretical predictions. To explore the tunneling effect in the

thermal 1, 4-H migration, precise kinetic measurements and isotope-labeling experiment are also needed.

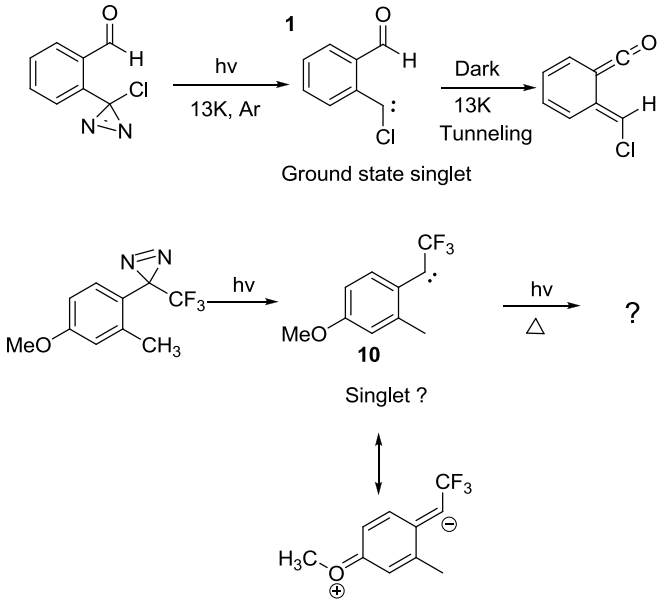

Figure 4-3 Research objective 2: *p*-methoxy-*o*-tolyl(trifluoromethyl)carbene

Tomioka and co-workers reported similar intramolecular 1, 4-H migration under tunneling conditions in thermal decay of singlet *o*-formylphenylcarbene shown in Fig.4-3.[2] Based on a simplified resonance picture, we predicted *p*-methoxy-*o*-tolyl(trifluoromethyl)carbene (**10**) to be ground state singlet, and might undergo the same 1, 4-H migration. To confirm this, the *p*-methoxy-*o*-tolyl(trifluoromethyl)carbene will be prepared, isolated and studied as in its parent *o*-tolyl(trifluoromethyl)carbene species. (Figure 4-3)

5. Results and Discussions

5.1 *o*-Tolyl (trifluoromethyl) carbene

Because of their advantages mentioned in the previous chapter, diazirines have been serving as primary carbene precursors in our research group for years. According to the typical procedure of diazirine synthesis reported in literature, aryl(trifluoromethyl)diazirines in this research are prepared from the corresponding aryl trifluoromethyl acetophenones, followed by oximation, mesylation, diaziridination and oxidation. [29b, 31] Among these, synthesis of the *o*-tolyl(trifluoromethyl)acetophenones is usually found to be the most challenging step.

5.1.1 Synthesis of *o*-tolyl (trifluoromethyl) diazirine precursor

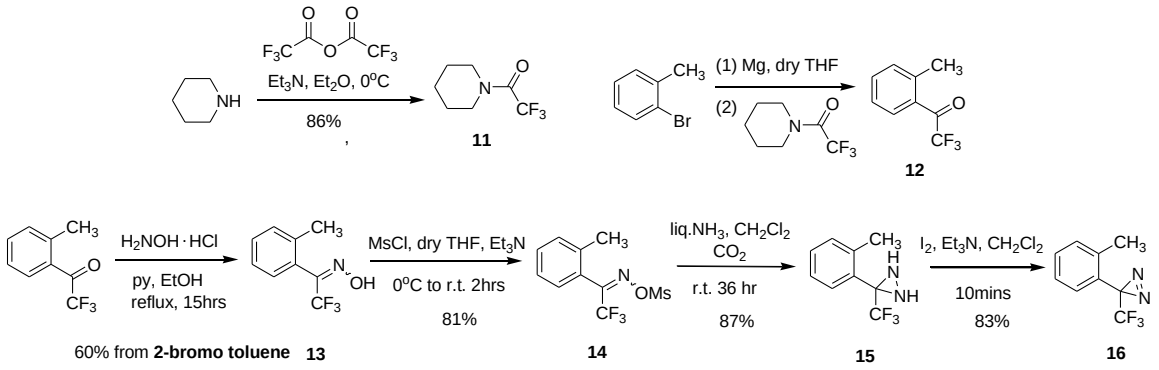

Scheme 5-1 Preparation of *o*-tolyl (trifluoromethyl) diazirine precursor

The desired *o*-tolyl (trifluoromethyl) diazirine precursor (**16**) was synthesized by following similar method of other group member's (Sean Ross) procedures with optimizations.[31,32] (Scheme 5-1) The synthesis starts from commercially available 2-bromotoluene, which was trifluoroacetylated by a Weinreb amide, *N*-trifluoroacetyl piperidine (**11**), via the Grignard reaction. As found in other organomagnesium mediated transformations, the activation of magnesium is essentially important to get reaction started. To achieve this, the magnesium turnings were washed with 1% HCl solution and acetone, and then dried under vacuum. The dry magnesium was abraded by stirring with magnetic bars overnight in the flasks under nitrogen before use. By following a classic procedure, the Grignard reaction was initiated with hot tap-water (ca. 40°C) and then acetylation agent was added with ice bath cooling. After the acylation, desired *o*-tolyl (trifluoromethyl) acetophenone (**12**) along with the excessive trifluoroacetyl piperidine (**11**) were co-

distilled out from the reaction mixture under high vacuum and used directly for oximation in the next step without further purification. Hydroxylamine hydrochloride and excessive pyridine were added to the two components mixture obtained in last step, and refluxed in ethanol. After prolonged reaction time and aqueous work-up, the remaining acylation agent could be removed from the system, presumably by forming water soluble salts and the *o*-tolyl (trifluoromethyl) acetophenone oxime (**13**) was obtained as fairly pure. The proton NMR spectrum shows that the *o*-tolyl (trifluoromethyl) acetophenone oxime was formed as two isomers with the hydroxyl group either *E* or *Z* to the trifluoromethyl group. The oxime was then mesylated with methanesulfonyl chloride in the presence of triethylamine, and white solid was obtained after recrystallization with hexane and dichloromethane. Again, two stereoisomers were formed for the mesylated oxime. The mesylated compound (**14**) was allowed to react with liquid ammonia in a high-pressure tube. After reacting at room temperature for 2 days, desired trifluoromethyl diaziridine (**1**5) was obtained as well as small amount of recovered oxime byproduct, which was produced by ammonia nucleophilic attack on the sulfur atom instead of imine carbon center. Because of their close polarities, it was impossible to purify the reaction mixture by column chromatography, which was directly oxidized by iodine under basic conditions. The 3-*o*-tolyl-3-trifluoromethyl-diazirine (**16**) as pale purple to pink liquid could be isolated easily by running a silica column. Both ^{1}H and ^{19}F NMR agree with other group member's data. And the ^{13}C NMR spectrum also matches the expected structure. After characterization, the diazirine was kept in solvent and stored in freezer for future matrix experiments.

To introduce the trifluoroacetyl group efficiently onto the aromatic ring, different acylation methods and agents have been tried. The classic lithiation acetylation method was first tried. However, neither lithium metal or organolithium reagent (i.e. n-BuLi) provided the desired product satisfactorily. For example, when n-BuLi and ethyl trifluoroacetate were used at low temperature, a mixture of *o*-tolyl (trifluoromethyl) acetophenone along with an unidentified side product was obtained. Despite side reactions, the purification was easily achieved by running a silica column. After the oximation process, excessive trifluoroacetyl piperidine can be converted to water-soluble salts in excessive pyridine after prolonged reaction time and purified by aqueous work up. In comparison to the tosylated oxime made by another group member, Sean Ross, mesylated oxime was chosen to avoid those drawbacks in its tosyl counterpart, such as the troubles in

purification and steric hindrance problems in the following diaziridination. Ammonation of mesylated oxime was carried out in liquid ammonia under high pressure and room temperature, and the reaction system was stirred for several days to drive all starting mesylated oxime to the product. Although prolonged reaction time could form small amount of oxime byproduct, both isomers of mesylated oxime are converted completely. In the tosyl case, in contrast it was found that one isomer was unreactive and was always left even after longer reaction time. A possible reason is that the mesyl substituent is much less bulky than tosyl group, in which the steric hindrance does not matter as much as that in tosyl oxime. It is worth pointing out that diaziridine could also be obtained by refluxing ammonia at -33^{o}C and less side product was observed. Presumably, under the low temperature condition, ammonia nucleophilic attack at sulfur center was inhibited and the reaction preferentially happened at the imine carbon. Iodine was chosen to oxidize diaziridine to diazirine and the oxidized product could be isolated easily isolated from the oxime by-product, which was made in last step. The diazirine is stable in solvents (e.g. $CDCl_3$, hexane, etc.) at low temperature and can be stored in the freezer for several weeks.

5.1.2 Computational studies

All possible geometries and electronic states of the diazirine precursors, carbene species and rearranged products were fully optimized. DFT calculations at the B3LYP 6-31+G ** level of theory were used to analyze their electronics and energetics. [33]Relative stability of those carbene species with different spin states or geometries could be partially understood with the calculated energies. Although DFT calculations of carbene species always overestimate the stability of triplet states by ca. 1-3 kcal/mol, no corrections were made for the overestimation in this work. Infrared and UV/vis spectra were predicted by frequency and TD calculations respectively and plotted out with Microsoft Excel in a manner of wavenumbers versus intensities (IR) or wavelength versus absorptions (UV). The calculated data are used to predict the most stable electronic state and confirm possible species produced in matrix by comparison with experimental results.

DFT calculations with the B3LYP 6-31+G** level of theory were first carried out for the *o*-tolyl (trifluoromethyl) diazirine precursor. In the vibrational frequency calculations, striking trifluoromethyl group vibration at 1146cm^{-1}, 1177cm^{-1} and N=N stretching at ~1700cm^{-1} were predicted. However, the

corresponding TD calculation shows a very small absorption at 332.03 nm (f=0.0006). This is uncommon for most diazirine species, which usually have a characteristic nπ * transition absorptions around 350-400 nm in their UV/vis spectra. The same phenomenon has also been observed in other group members' hindered aryl diazirine systems, which presumably comes from the steric effects of substituents which are *ortho* to the diazirine three-member heterocyclic ring. This "simple-minded" steric hindrance thought was supported by both electron population analysis of the HOMO-LUMO frontier orbitals and experimental observations. (Figure 5-1)

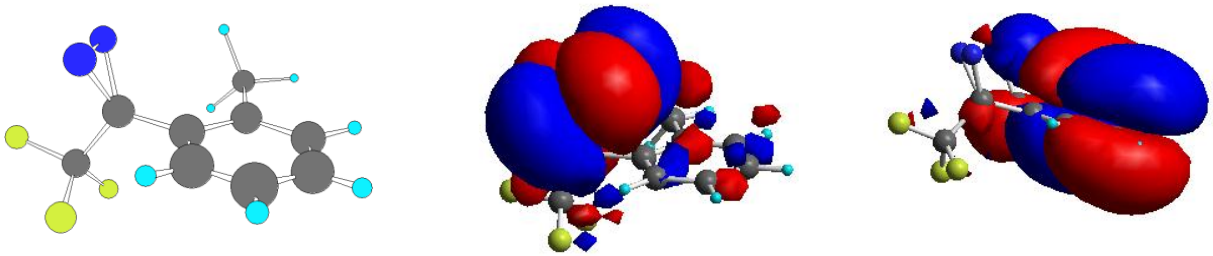

Figure 5-1 Geometry and frontier orbitals of *o*-tolyl (trifluoromethyl) diazirine

The most stable conformer of *o*-tolyl (trifluoromethyl) diazirine has the diazirine N=N bond rotated by the *ortho* methyl group to parallel the aromatic ring. The HOMO orbital mainly is aromatic π system, while the LUMO shows most character of the nitrogen N=N π*. The HOMO-LUMO pictures make us believe that, in its preferred geometry, there is poor mixing between the HOMO and LUMO, which produce a low nπ * transition strength. The TD B3LYP calculations predicted a small absorption at 332 nm (f=0.0006). For comparison, HOMO-LUMO molecular orbitals of its parent diazirine, phenyl (trifluoromethyl) diazirine, are shown below with permission from Dr. Sheridan. (Figure 5-2) In its energy minimum state, trifluoromethyl phenyl diazirine has the N=N bond bisected by the aromatic ring, which makes the best mixing of electrons from the aromatic ring and nitrogen's lone pairs. A strong nπ * transition at 388 nm (f = 0.0111) is predicted by the TD calculation with the same level of theory and supported by experimental observations.

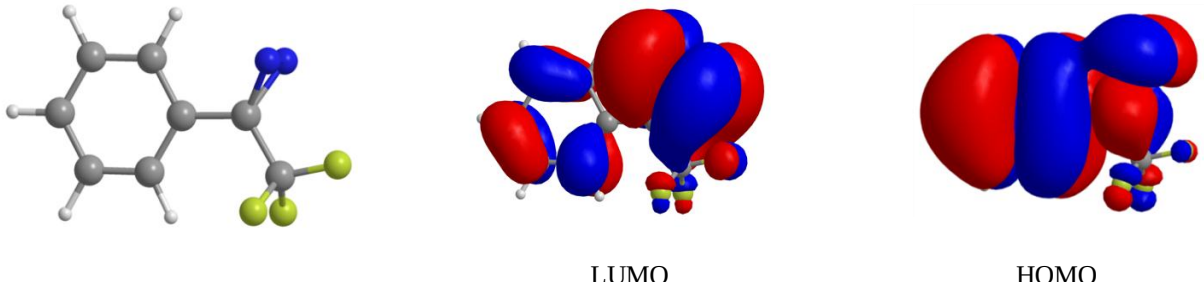

Figure 5-2 Geometry and frontier orbitals of trifluoromethyl phenyl diazirine

Geometry optimizations were also carried out on the carbene species to find their preferred conformations. An informal nomenclature used by other group members to distinguish carbene species with different conformations and spin states was followed in this research. Depending on the relative position of methyl group and trifluoromethyl group, from the one with lowest energy, the four conformers are respectively named as triplet *anti*, triplet *syn*, singlet *anti* and singlet *syn*. Sums of electronic and zero point energies of the four lowest-lying conformers were obtained by DFT calculations and *o*-tolyl (trifluoromethyl) carbene was found to be a ground state triplet with a favorable *anti* geometry. The triplet *anti* isomer was then set as zero and the relative energies of the other conformers were then calculated and listed in Figure 5-3. The energy diagram shows *o*-tolyl (trifluoromethyl) carbene is a ground state triplet, which is 4.13kcal/mol more stable than the lowest-lying singlet conformer.

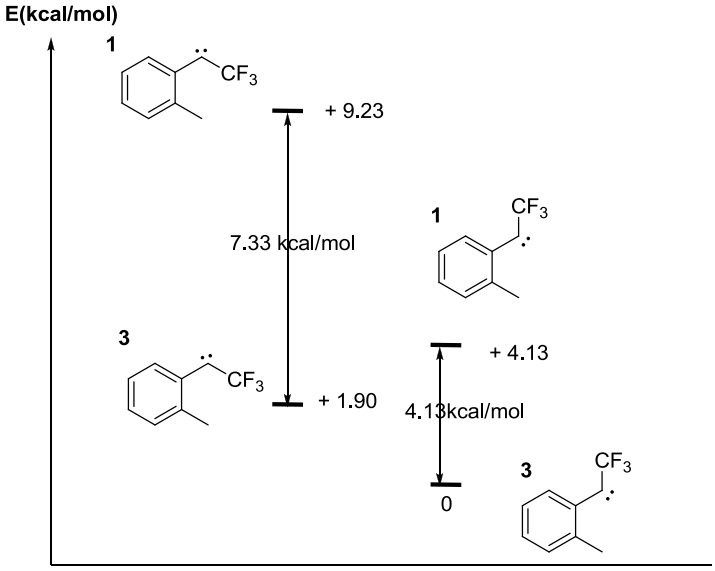

Figure 5-3 Geometries and relative energies (not corrected) of *o*-tolyl (trifluoromethyl) carbene

It is noteworthy to mention that the singlet and triplet energy gap of the two *syn*-conformers (7.33kcal/mol) is much greater than that between the two *anti*-isomers (4.13kcal/mol). One possible reason of this distinct discrepancy is the repulsion interactions between methyl and trifluoromethyl groups. As discussed in previous chapter and also supported by DFT calculations, singlet carbenes usually have smaller carbenic bond angles than their triplet counterparts. (Figure 5-4) A bond angle which is smaller in the singlet state adds more trifluoromethyl-methyl group repulsion strain than that in triplet. Therefore, the energy increased by this steric repulsion is more striking in the *syn*-conformers, presumably because of the more crowded environment.

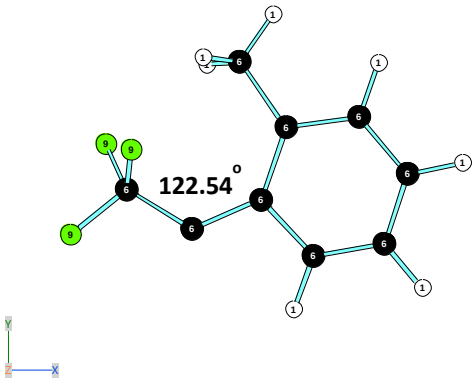

Syn-singlet *o*-tolyl (trifluoromethyl) carbene

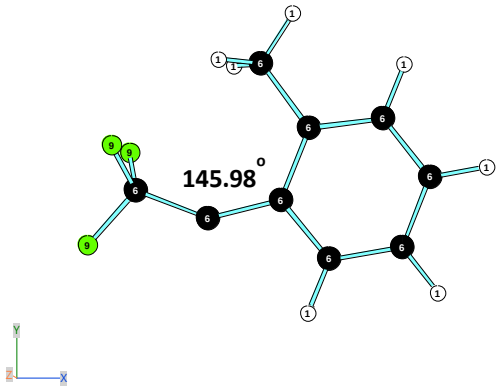

Syn-triplet *o*-tolyl (trifluoromethyl) carbene

Figure 5-4 Geometries of *syn*-*o*-tolyl (trifluoromethyl) carbenes

In addition to their geometries and relative energies, both frequency calculation and TD calculation of the four carbene conformers and possible rearranged products were predicted by DFT calculations respectively, and plotted out in the manner of 'intensity-wavenumber "(IR) and "intensity-wavelength" (UV/vis) with Excel to compare with experimental observations.

5.1.3 Matrix isolation and photo/thermal experiments

o-Tolyl (trifluoromethyl) diazirine was deposited in the matrix head by a "pre-mix" method. The purified diazirine was analyzed by NMR before use, and then solvent ($CDCl_3$) was removed under reduced pressure. To avoid losing diazirine, special attention should be paid during the removal of solvents and usually an ice bath is needed. Once concentrated to about 0.3ml or less, the solution was transferred into a pre-dried

deposition tube, which was then connected to the gas handling system in the matrix isolation apparatus. Air in the tube was removed by "freeze-thaw-pump" method. Then the deposition tube was placed in a cooling bath (about -50 ℃) made with ethanol and liquid nitrogen to remove the last trace of solvent. The pressure of system was monitored carefully and when there were no sharp jumps, vacuum was turned off and diazirine was sublimated into a 3L mixing bulb. Once the pressure reached about 0.4 torr, the mixing bulb was closed and the deposition tube was removed from the system. Inert gas (high purity nitrogen in this study) inlet was then connected to the gas handling system, which was flushed three times to get rid of air. The nitrogen gas was introduced slowly into the mixing bulb until the inner pressure reached 400 torr, at which point, a sample of ca. 0.1% diazirine in nitrogen was prepared in the mixing bulb. The closed-cycle helium refrigerator and cryogenics compressor were turned on to cool the system to its lowest minimum. The system was then warmed up to 21K and the premixed diazirine sample in nitrogen was deposited into the matrix head with a rate of 1.0 torr/min up to ca. 110 torr. The heater was then shut off to cool the system to its lowest minimum and the matrix-isolated diazirine was identified by IR and UV/vis spectra. As predicted by TD DFT calculations, no typical nπ * transition absorption was observed around 350-400 nm in the UV-vis spectrum.

Photochemistry was induced in the matrix-isolated diazirine samples by monochromatic light from a high-pressure mercury lamp equipped with monochromator, and the irradiation wavelength was carefully controlled. Light with wavelength at 313nm was chosen to irradiate the diazirine to release N_2. It is not only because the calculated UV/vis spectrum shows absorption at 308nm, but also because that 313nm light has been proved efficient to generate various carbene species from their diazirine precursors by other group members. After irradiating at 313nm for 1hr, a mixture of carbene, diazo compound and unreacted diazirine precursors was obtained. It was found that in IR difference spectra, characteristic diazirine bands at 938 cm^{-1}, 1164cm^{-1}, 1193cm^{-1} and 1243 cm^{-1} disappeared and new bands at 1099cm^{-1}, 1141cm^{-1}, and 1209 cm^{-1} grew. In addition, by comparing the UV/vis spectrum before and after irradiation, a new species with absorptions λ_{max} at 290nm, 299nm and 343nm were detected. The new species was then assigned to triplet carbene by comparing with the calculated results. Prolonged irradiation at 313nm for 2hrs or at 296nm for

0.5hr converted most of the diazirine to carbene with only trace amount of the isomeric diazo compound and rearranged product. (Figure 5-6 and 5-7)

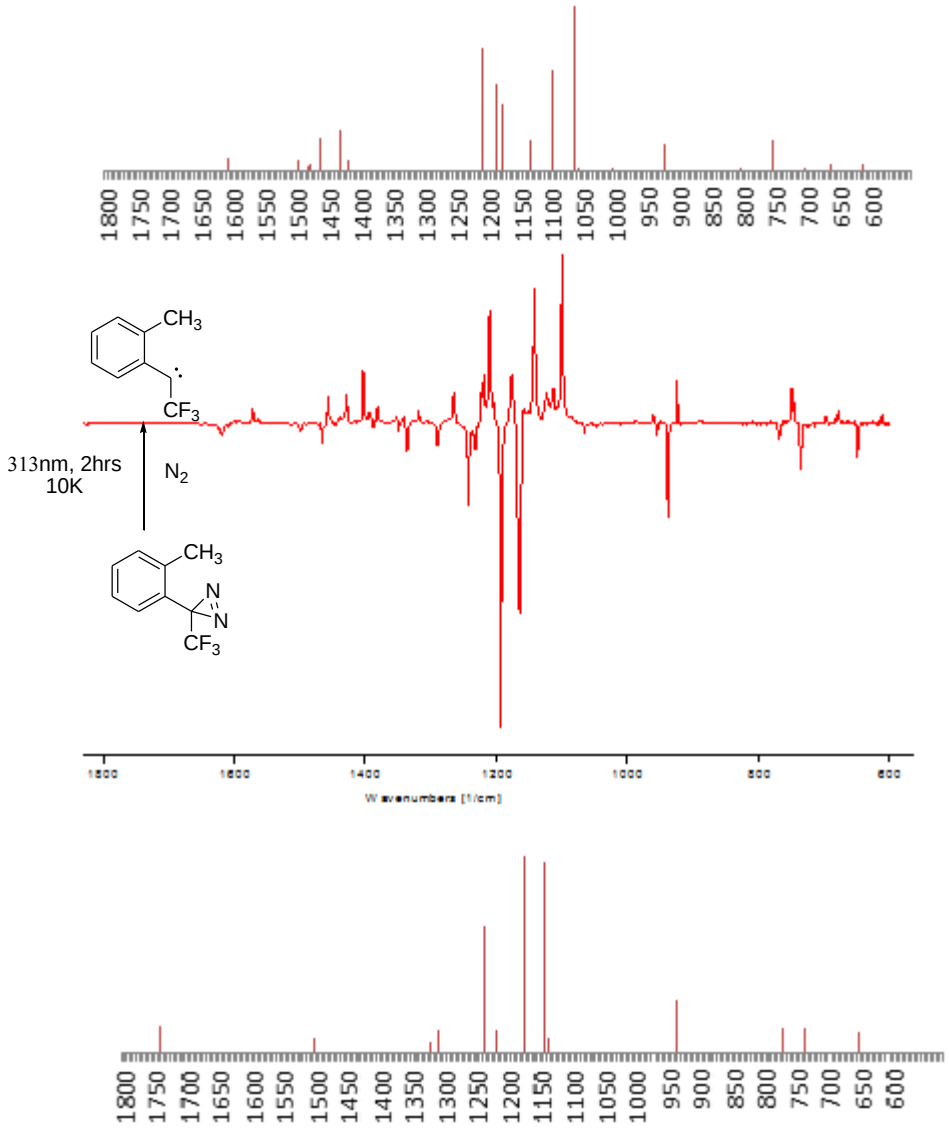

Figure 5-6 Top: calculated IR spectrum of anti-triplet *o*-tolyl (trifluoromethyl) carbene; Middle: difference IR spectrum of carbene generation from diazirine precursor; Bottom: calculated IR spectrum of *o*-tolyl (trifluoromethyl) diazirine

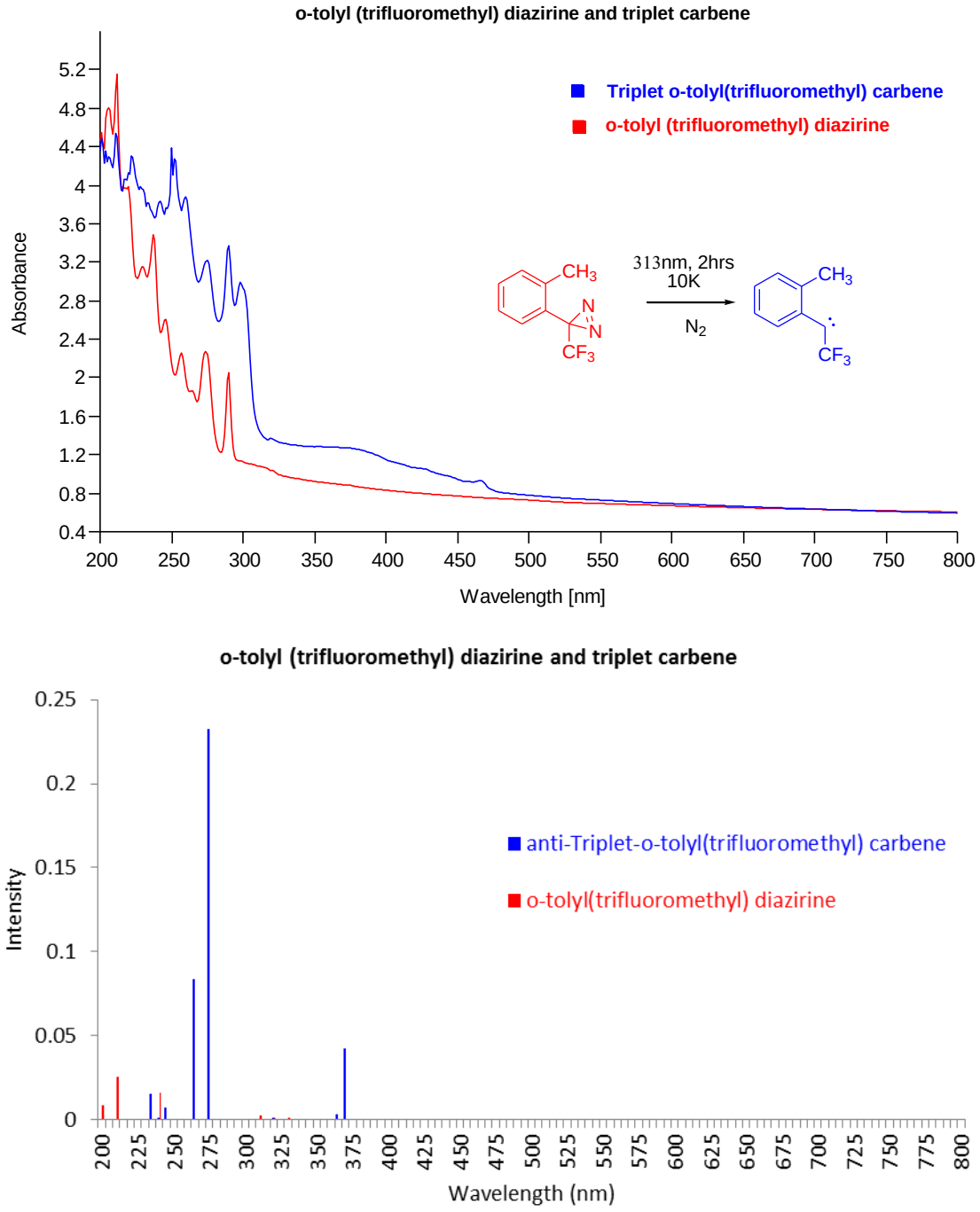

Figure 5-7 Red: calculated and observed UV/vis spectra of o-tolyl (trifluoromethyl) diazirine; Blue: calculated and observed UV/vis spectra of o-tolyl (trifluoromethyl) carbene

As indicated by the DFT calculations, triplet *o*-tolyl (trifluoromethyl) carbene is about 4.13 kcal/mol more stable than the lowest-lying singlet (This value should be 2.13kcal/mol if the overestimated triplet stability is taken into account.) Both IR and UV/vis spectra support that triplet is the ground state which is in accordance with the calculated results. In addition, the experimental IR spectrum matches *anti* conformation better than *syn* isomer. (Figure5-8) Therefore, it is believed that triplet state with an anti-conformation is the most stable state of *o*-tolyl (trifluoromethyl) carbene.

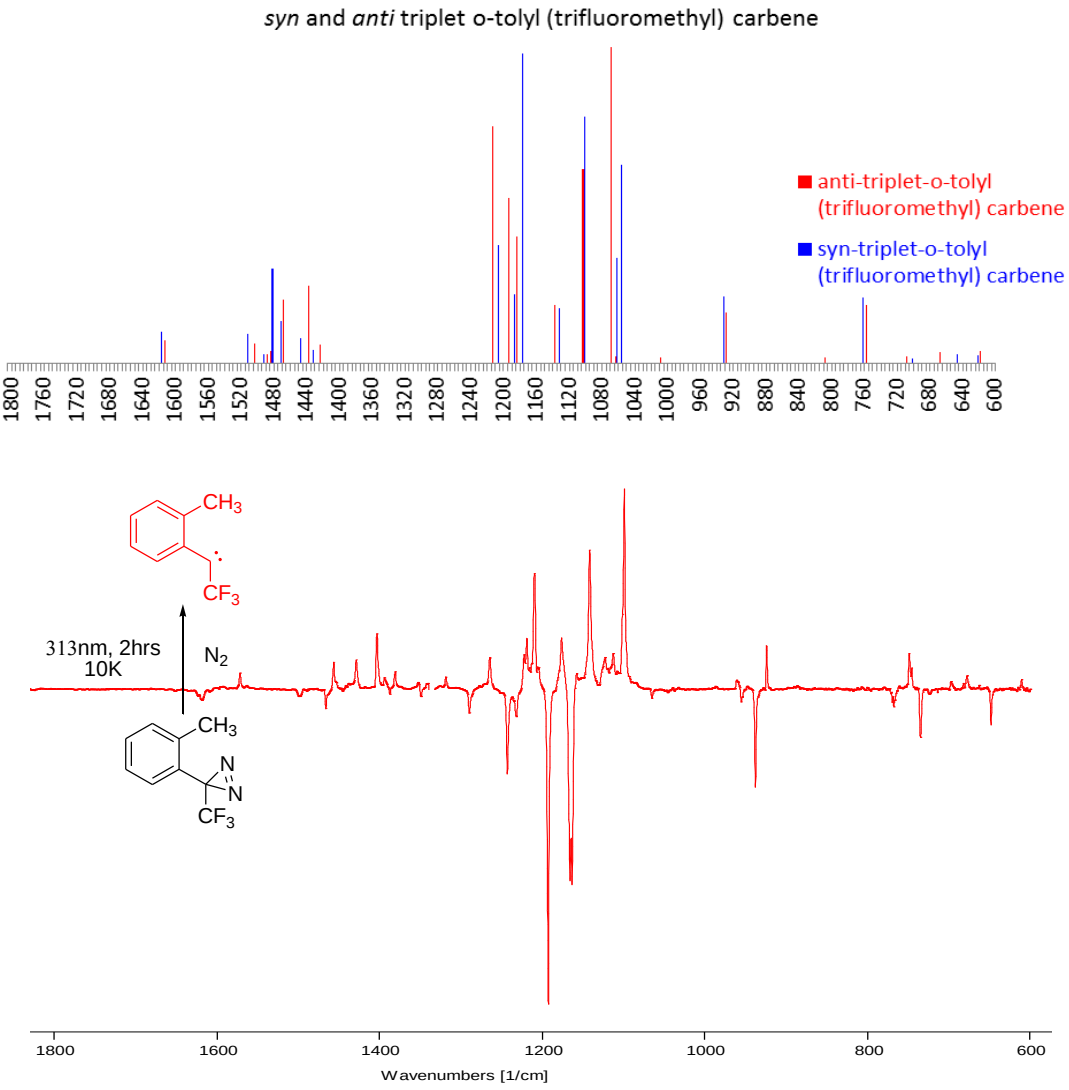

Figure 5-8 Top: calculated IR spectrum of syn (blue) and anti (red)-triplet *o*-tolyl (trifluoromethyl) carbene; Bottome: difference IR spectrum of carbene generation from diazirine precursor

After generation, further irradiation at shorter wavelength (i.e. 313nm, 298nm, 303nm etc.) or even standing in dark at 10K could convert the carbene to a different species. The new species was subsequently known to be trifluoromethyl-*o*-quinomethide based on comparing its IR and UV/vis spectra with DFT frequencies and TD calculations. The quinomethide after 1, 4-H migration is both photochemically and thermally inert under the research conditions. The identification of both carbene and rearranged products is in accordance with the parent *o*-tolyl carbene reported by McMahon and other group member's work. (Figure 5-9) However, in their case only very weak IR spectra of the carbene could be detected.

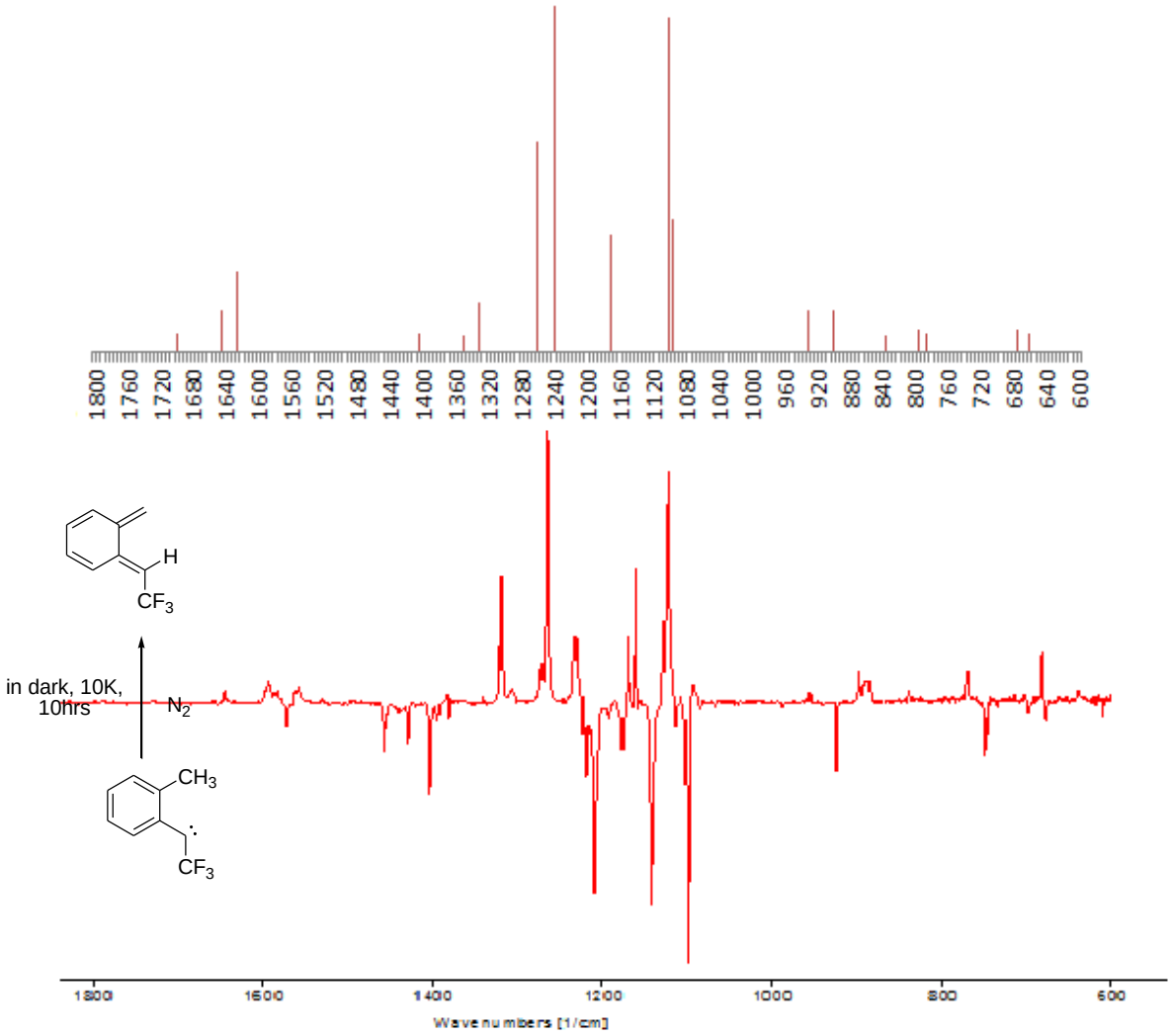

Figure 5-9 Top: Calculated IR spectrum of 2-trifluoromethyl-*o*-quinomethide; Bottom: IR difference spectrum after carbene thermal decay

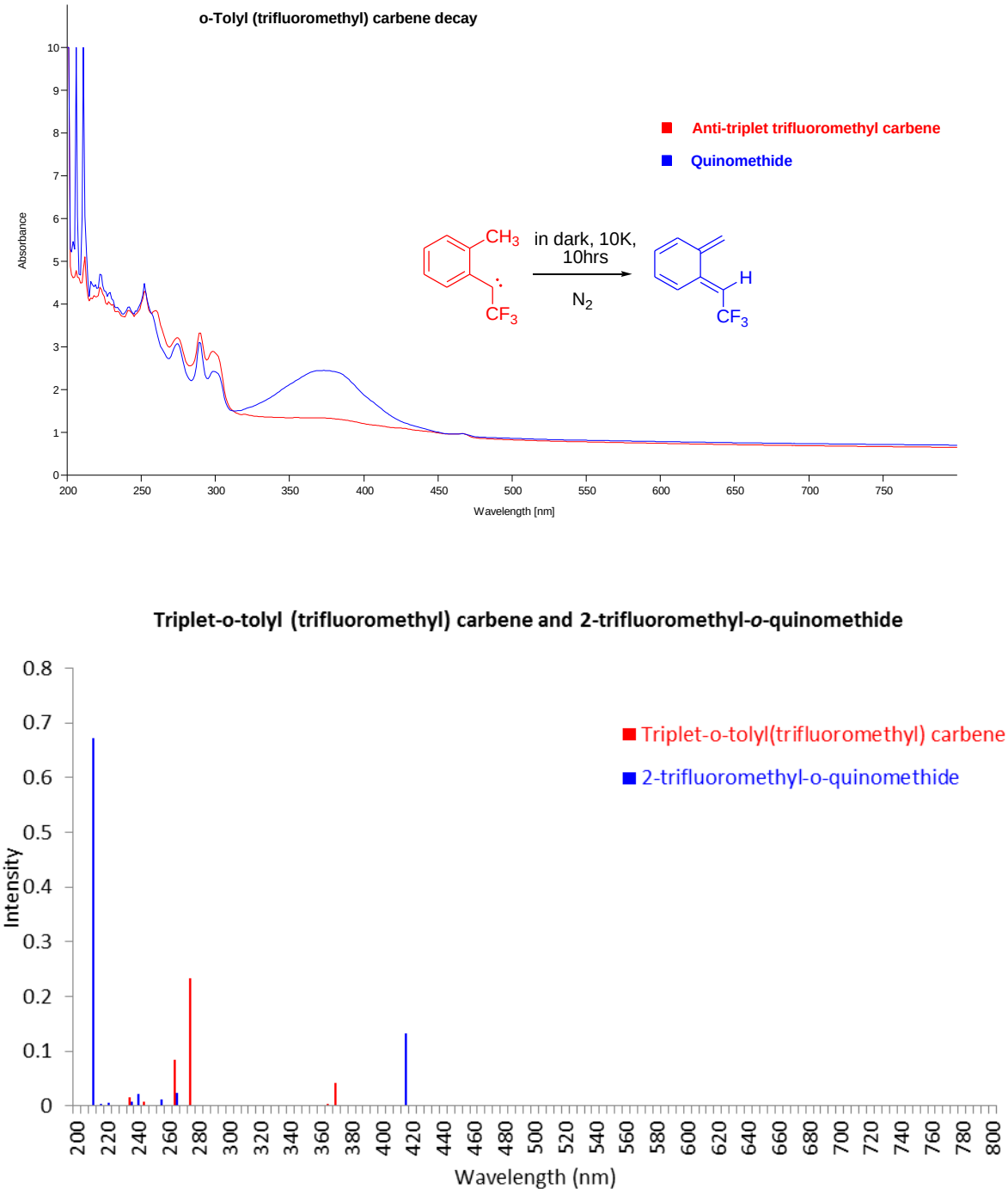

Figure 5-9 Observed (top) and calculated (bottom) UV/vis spectrum of o-tolyl (trifluoromethyl) carbene and 2-triluoromethyl-o-quinomethide

The facile reactivity of *o*-tolyl (trifluoromethyl) carbene at cryogenic temperature was also found in its parent *o*-tolyl carbene by McMahon and Chapman in 1980s, which was proposed to be a quantum mechanical tunneling pathway. To get more intuitive information in its thermal decay, the carbene species was allowed to stand in dark at 10K for 10hrs and the progress was tracked spectroscopically. It was found that those IR bands assigned to carbene disappeared with concomitant growth of quinomethide's peaks. Evidence of reaction is in the time dependent UV/vis spectra, which clearly indicates that the quinomethide (λ_{max}= 373nm) forms and carbene species (λ_{max}= 290nm, 299nm) disappears simultaneously under the research conditions. (Figure 5-10)

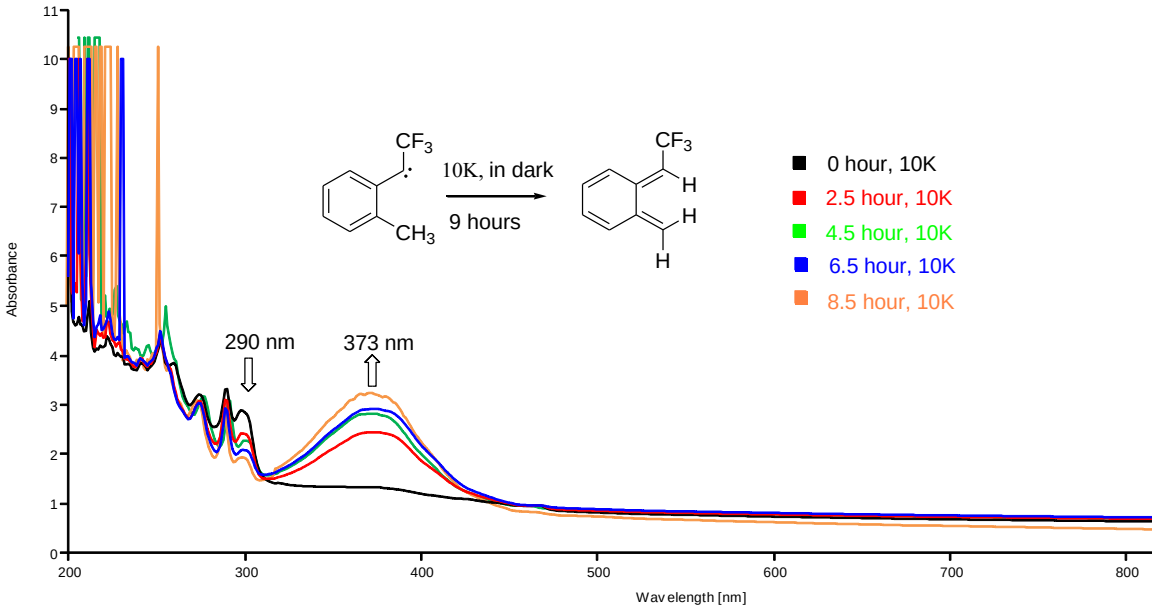

Figure 5-10 UV-vis spectra of time-dependent *o*-tolyl (trifluoromethyl) carbene thermal decay

The reactivity of *o*-tolyl (trifluoromethyl) carbene at low temperatures strongly suggests quantum mechanical tunneling in its thermal decay. However, more precise kinetics measurements are needed to support the assumption. As discussed in previous chapters, "matrix effects" are often found in reaction kinetics of those reactive intermediates involving QMT pathways at cryogenic temperature. Kinetics measurement of the matrix-isolated reactive intermediates decay shows to be exponential in the "fast sites" and non-exponential in the "slow sites". In other words, its first-order plots of ln [intensity] versus time are generally "upwardly curved".

To explore the matrix effect in *o*-tolyl (trifluoromethyl) carbene thermal decay, at 10K , the intensities of the carbene's three characteristic IR bands (1099cm^{-1}, 1141cm^{-1}, and 1209 cm^{-1}) were measured at different reaction times and the "first order" plots of ln [intensity] versus time were obtained.(Figure 5-11(a)) The same experiment was also taken at 23 K, but the first-order plots of ln [intensity] vs. time gave a larger slope at 1209 cm^{-1}. (Figure 5-11 (b)).However, we are unclear if this result was caused by the matrix annealing and IR band broadening at a higher temperature or different sites of the matrix were studied at different times. To get better kinetic measurements, more matrix experiments are needed to generate the carbene as much as possible and monitor the thermal decay in the same site of matrix.

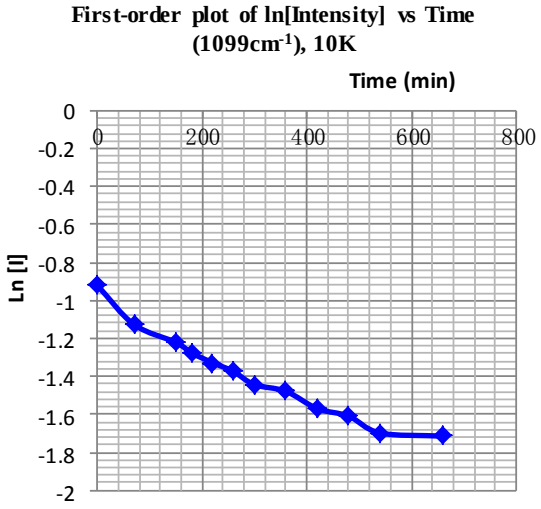

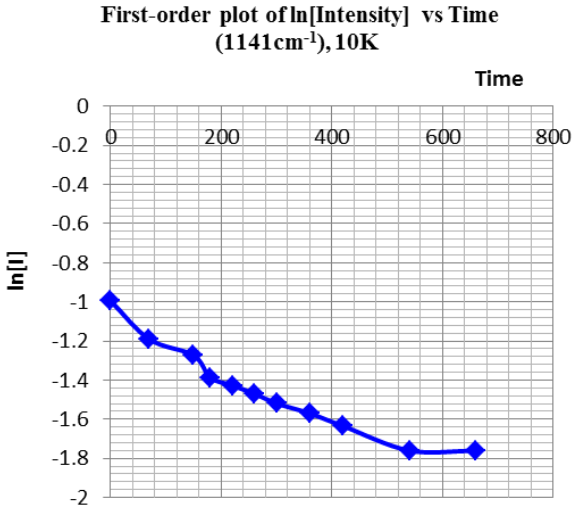

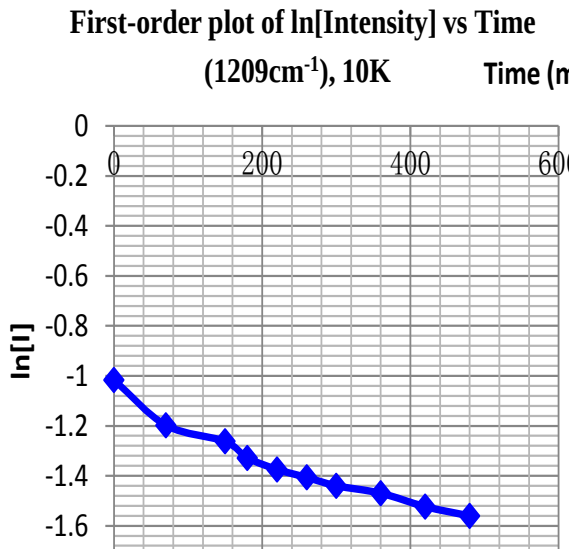
First-order plot of ln[Intensity] vs Time
(1209cm-1), 10K
Time (n
ln[I]
0
-0.2
-0.4
-0.6
-0.8
-1
-1.2
-1.4
-1.6
0
200
400
60

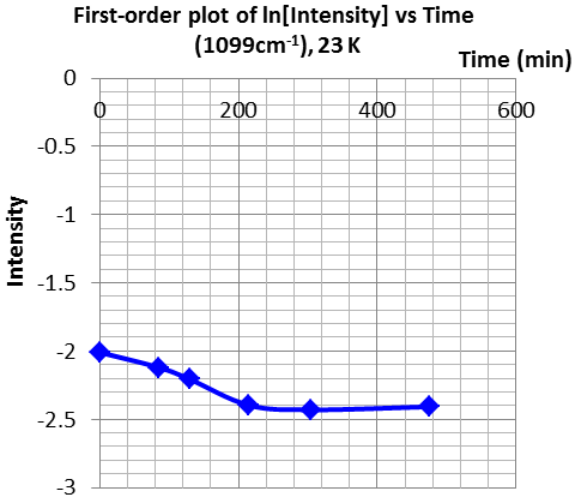
First-order plot of ln[Intensity] vs Time
(1099cm-1), 23 K
Time (min)
Intensity
0
-0.5
-1
-1.5
-2
-2.5
-3
0
200
400
600

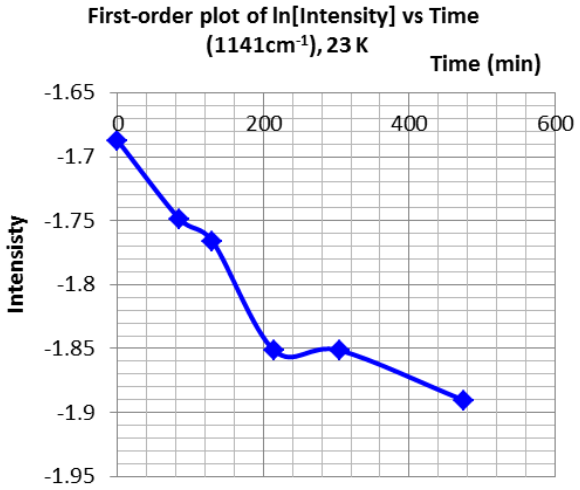
First-order plot of ln[Intensity] vs Time
(1141cm-1), 23 K
Time (min)
Intensisty
-1.65
-1.7
-1.75
-1.8
-1.85
-1.9
-1.95
0
200
400
600

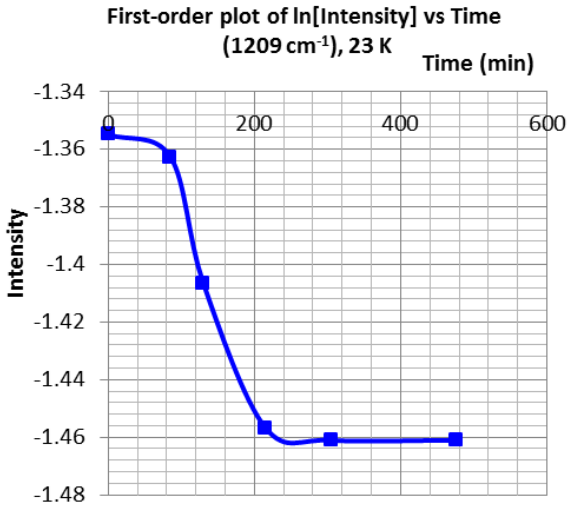

Figure 5-11 *o*-tolyl (trifluoromethyl) carbene thermal decay kinetics:

First-order plots of ln [intensity] vs. time (a) at 10K; (b) at 23K.

All these results showed the matrix effect in carbene decay. As discussed before, one of the most persuasive evidence of quantum mechanical tunneling kinetics is the non-linear Arrhenius plot. To get more evidence of temperature independence in our carbene decay and plot of the Arrhenius relationship, a series of experiments under different temperature are needed. However, when we warmed up the matrix to 30K, a set of new peaks in the IR spectrum, which is different from the quinomethide, grew up and the carbene was quenched in just few hours. It was believed that small amount of oxygen leaked into the gas handling system during sample deposition and was then trapped by carbene species at higher temperature to give carbonyl oxide. In addition, an apparent change was found in its UV/vis spectra, which shows a broad and strong absorption at 357 nm, which was characteristic for carbonyl oxide by comparing with the calculated spectra. After further irradiation at 336nm, the strong absorption at 357nm disappeared and the carbonyl oxide was thought to be converted to dioxirane. This assumption was confirmed by a later oxygen trapping experiment on its isotopic counterpart, methyl-d_3-*o*-tolyl (trifluoromethyl) carbene, (See **5.2** for details). At the same time, its triplet ground state was also reasserted by the reaction with oxygen. Thus, we didn't get any data related to tunneling at 30K.

Limited by research time and instrument technique, we only qualitatively studied the tunneling effect in *o*-tolyl (trifluoromethyl) carbene's 1, 4-hydrogen shift thermal decay. More precise kinetics measurements under different matrix temperatures are needed to obtain enough ln*k* versus 1/T relationships to get the Arrhenius plot, which has been considered as a direct evidence of quantum mechanical tunneling in reactive molecules' decay.

5.2 Trideuteriomethyl-*o*-tolyl (trifluoromethyl) carbene

Kinetic isotope effects are an important tool in studying quantum mechanical tunneling of reactive molecules. The 1,4-deuterium transfer in trideuterated tolyl (trifluoromethyl) carbene is expected to be strongly diminished if this transformation involves a tunneling pathway. Thus, it is worth generating the trideuterated carbene species in a matrix to explore the kinetic isotope effects in its thermal decay.

5.2.1 Synthesis of trideuteriomethyl-*o*-tolyl (trifluoromethyl) diazirine precursor

Following the same procedures of its protio case preparation, trideuteriomethyl-*o*-tolyl (trifluoromethyl) diazirine was synthesized from the corresponding trideuteriomethyl-2-bromotoluene followed by Grignard trifluoromethyl acetylation, oximation, mesylation, ammonation and oxidation. (Scheme 5-2)

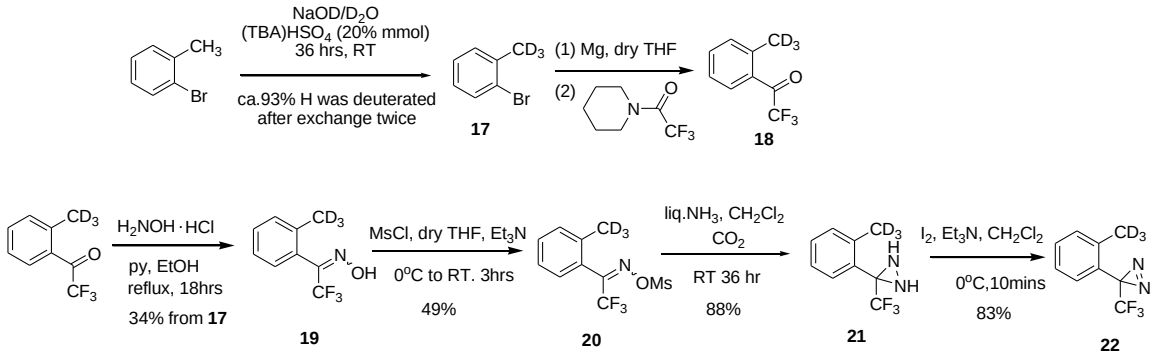

Scheme 5-2 Preparation of trideuteriomethyl-o-tolyl (trifluoromethyl) diazirine precursors

As expected, introducing the trideuteriomethyl group is the most challenging step because (1) the alkyl C-H bonds are too inert to be deuterated under normal conditions; (2) multi-sites deuteration (i.e. aromatic moiety) might be competitive; (3) few reported strategies are available to be scaled up. In our research, the

preparation of trideuteriomethyl-2-bromotoluene was accomplished on a large scale (up to 10 grams) by optimizing Rabinovitz and coworkers' procedure via hydrogen-deuterium (H-D) exchange under strong basic conditions with a phase transfer catalyst (PTC). [33]

The methyl hydrogens in 2-bromotoluene as well as other toluene derivatives are slightly acidic with pKa as low as 30 to 34. Theoretically, proton abstraction on the methyl groups could happen if strong-enough bases were applied. However, H-D exchange in those compounds with very weak acidity is rather difficult. Regular strong bases, such as alkoxides or hydrides, can only partially deprotonate those toluene derivatives having strong electron-withdrawing groups, and are strictly limited to water-free reactions. A practical method to enhance the basicity of regular bases, such as sodium hydroxide, is transferring the basic anions to organic layer by phase-transfer-catalysis. With a source of deuterium and strong base in presence, the methyl groups in toluene derivatives could be deprotonated and then deuterated after repeated H-D exchange processes. A combination of tetrabutylammonium hydrogen sulfate ($(TBA)HSO_4$) along with NaOD in D_2O and hexane were found to deprotonate substituted toluenes effectively and promote the methyl group H-D exchange efficiently. A plausible mechanism of this process is that deuteroxide anions are extracted into the organic phase with the assistance of PTC and they are more basic comparing with those acting at the aqueous-organic interface. After that, small amount of D_2O molecules from NaOD/ D_2O solution are also extracted into organic phase. Due to salting-out and Le Chatellier principles, more deuteroxide anions are subsequently moved into the organic layer. The PTC promoted extraction of base into the organic layer enables the abstraction of hydrogen from toluene derivatives with low acidity.

Practically, the 40%w/w fresh sodium deuteroxide (NaOD) in deuterium oxide (D_2O) solution was made by carefully adding small sodium metal cuts into deuterated water with magnetic bar stirring and inert gas protection. Heating are needed toward the end of addition. Once addition was complete, the pasty solution was obtained without titration. To the fresh made NaOD/D_2O solution, 2-bromotoluene, $(TBA)HSO_4$ and dry hexane were added. Magnetic bar was then replaced with mechanical stirring equipment and the system was stirred vigorously for 2 days. Hexane was added periodically to compensate for the evaporation during the reaction period. After normal dichloromethane/D_2O extraction and silica chromatography purification with hexane, deuteriomethyl 2-bromotoluene after H-D exchange was afforded as light yellow oil. By

comparison with the standard, non-changed aromatic protons with ^{1}H NMR spectroscopy, up to 93% of the methyl hydrogens in starting material were exclusively deuterated after a second exchange procedure. In addition, our deuterated product (**17**) was also confirmed by ^{13}CNMR, GC-MS and IR spectra. Most distinctly, the IR spectrum of 2-bromo toluene after repeated deuterium exchange shows that the stretching vibration of methyl group at 2981cm^{-1}, 2947cm^{-1} and 2850cm^{-1} completely vanished while the corresponding trideutriomethyl bands appears at 2361 cm^{-1}, 2231 cm^{-1} and 2140 cm^{-1}. (Figure 5-12)

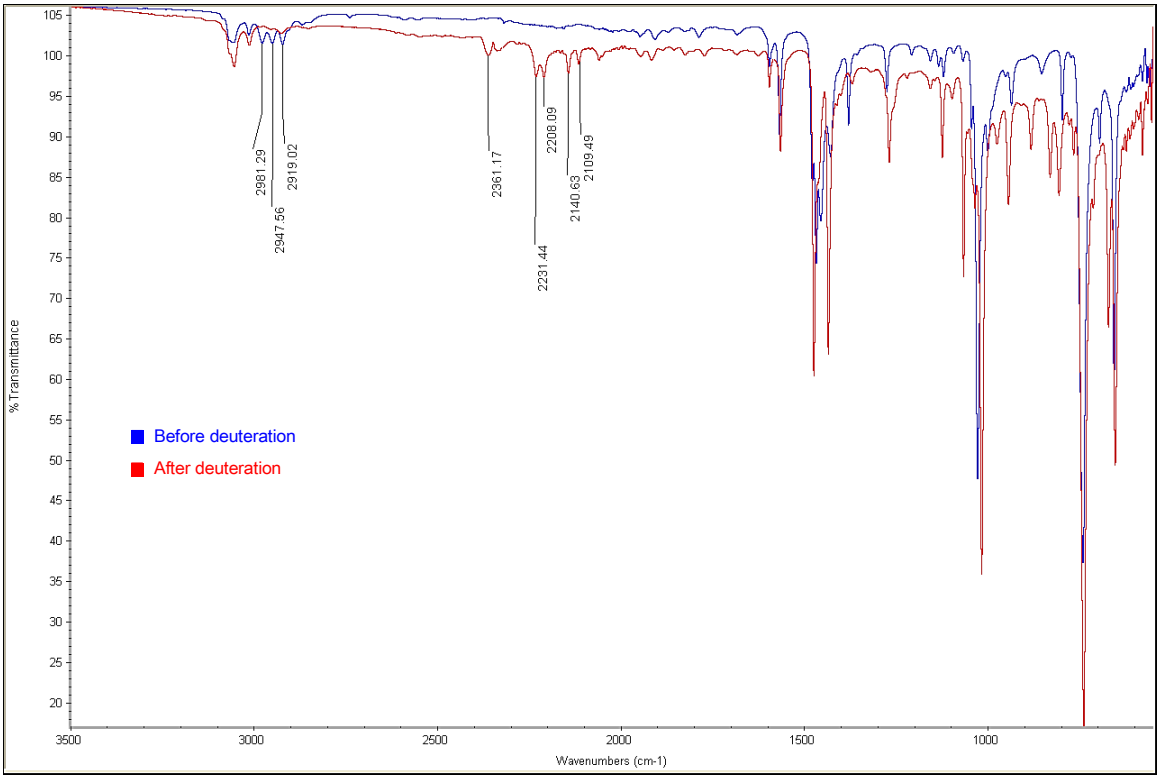

Figure 5-12 Infrared spectra of 2-bromo toluene (blue) and trideuteriomethyl 2-bromo toluene (red)

Considering the inconvenience in preparing NaOD/D_2O pasty solution, several alternative approaches have been tried. Our first thought was inspired by Leitch and Chen's work in the synthesis of trideuteriomethyl toluene by deprotonation with deuterated methyl sulfinyl carbanions and exchange with d_6-dimethylsulfoxide.[34] (Scheme 5-3) They reported about 75% of the methyl groups in toluene could be exclusively deuterated by d_6-DMSO/NaH combination under the condition of heating at 150-160^{o}C for 24

hours. Repeated exchange procedures even raise the trideuteriomethyl content up to 99%. The high deuteration efficiency is so attractive that we were encouraged to try this method on our specific substrates.

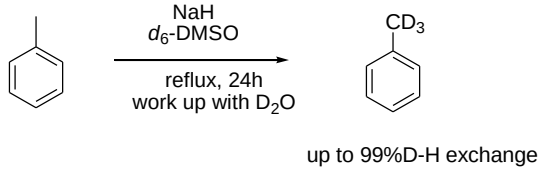

Scheme 5-3 NaH/ d_6-DMSO-mediated D-H exchange reaction of toluene

Activated by neighboring electron-withdrawing groups, the methyl protons in both 2-bromo toluene and *o*-tolyl (trifluoromethyl) acetophenone should be more acidic than those in toluene and more favorable for this transformation. *o*-Tolyl (trifluoromethyl) acetophenone was finally chosen as the substrate for this H-D exchange reaction, because the anion intermediate after deprotonation could be stabilized by the resonance over aromatic ring and carbonyl group and the D-H exchange could be pushed forward to the right. (Scheme 5-4)

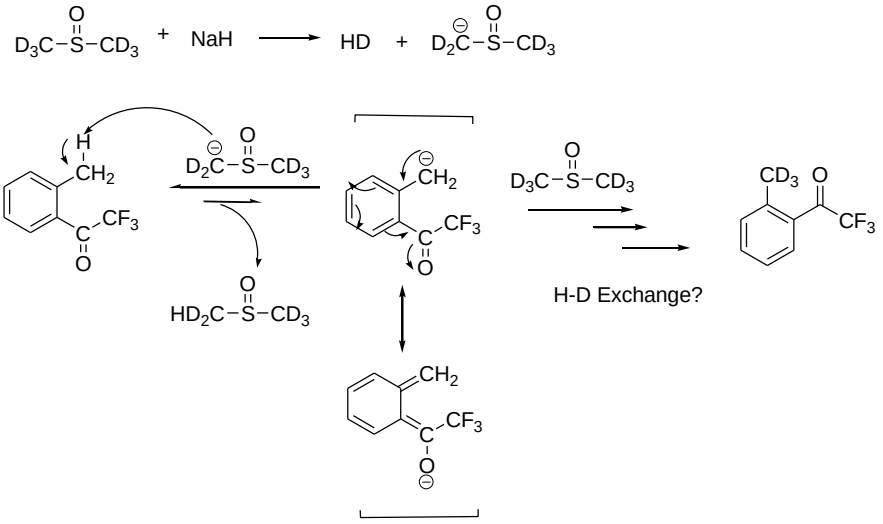

Scheme 5-4 Proposed methyl sulfinyl carbanion mediated D-H exchange in trifluoromethyl ketone

Following the literature procedure, at 50°C, powdered sodium hydride was dissolved in excess dry d_6-dimethyl sulfoxide (d_6-DMSO) under nitrogen with stirring until D_2 gas stopped bubbling. *o*-Tolyl

(trifluoromethyl) acetophenone was then added to the system and stirred for 24hrs at 50°C. After workup with D_2O, no D-H exchanges were observed in the ^{1}HNMR spectrum. The reaction was also carried out at 80 °C for 1hr and then stirred for 4hrs at room temperature. However, no desired proton peaks were found in the ^{1}HNMR spectra and the ketone substrate was believed to be decomposed. The combination of NaH/ d_6-DMSO was proved to be unsuccessful to promote the D-H exchange reaction of methyl moieties in o-tolyl (trifluoromethyl) acetophenone. Although we do not have an answer for sure, possible explanations could be proposed. The methyl sulfinyl carbanions may not be basic enough to initiate D-H exchange of the methyl group under research conditions, thus no expected deuteration happens. (Scheme 5-5)

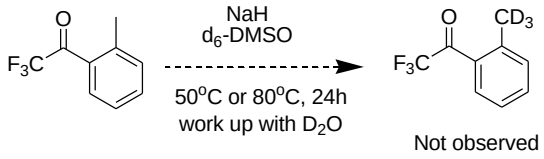

Scheme 5-5 NaH/ d_6-DMSO-mediated D-H exchange reaction of trifluoromethyl ketone

More recently, Sajiki and coworker reported an efficient Pd/C catalyzed H-D exchange reaction on the methyl groups of tolyl derivatives.[35] In D_2O, heterogeneous Pd/C was found to catalyze deuteration at the benzylic site with a small amount of H_2 gas in presence. Although there are several drawbacks in this methodology, such as the difficulties in introducing catalytic amount hydrogen gas (0.7eq) and few examples were provided on gram-scale, it worthed a try based on its mild conditions and high selectivity. To the suspension of substrate and 10 wt% Pd/C in D_2O, H_2 was introduced via a H_2 gas balloon and the system was then stirred at 50°C for 1 or 2 days. Neither 2-bromotoluene nor trifluoromethyl ketone gave expected deuterated compound. Presumably, the ortho-neighboring groups, such as bromo and trifluoromethyl acetyl prohibited this palladium catalysis process. (Scheme 5-6)

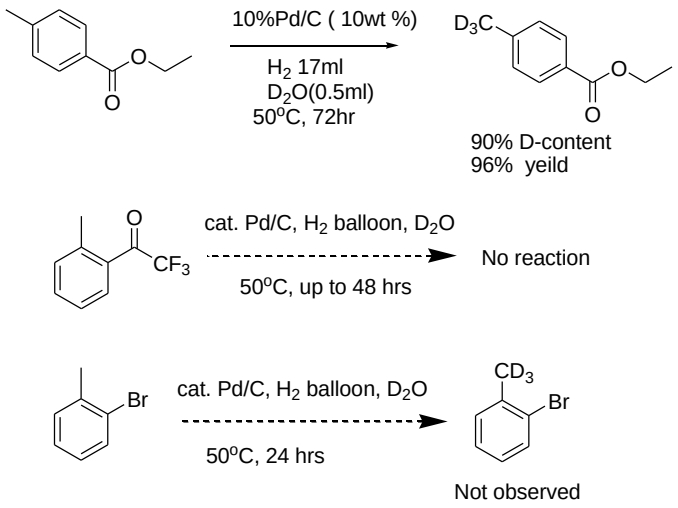

Scheme 5-6 Pd/C catalyzed deuteration at the benzylic site[35]

Additionally, conversion of dibromobenzene to the lithio derivative followed by addition of CD_3I, was also tried to get trideuteriomethyl 2-bromo toluene. The yield were too low to be applicable in our CD_3 substrates preparation. (Scheme 5-7)

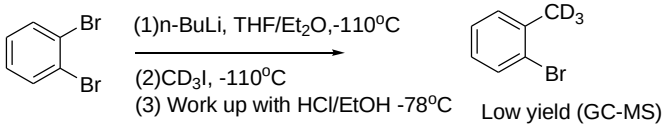

Scheme 5-7 Pd/C catalyzed deuteration at the benzylic site

To find a convenient and efficient way to prepare the CD_3 analogue, several deuteration approach have been tried. However, none of them works better than the PTC hydrogen-deuterium exchange.

5.2.2 Matrix isolation and photochemical/thermal experiments

Once we had the trideuteriomethyl-*o*-tolyl (trifluoromethyl) diazirine in hand, deposition was accomplished by a "pre-mix" method following the same procedure as its protio analogue. The IR spectrum fit calculated results very well. (Figure 5-13) And the UV-vis spectrum matched that of the protio analogue.

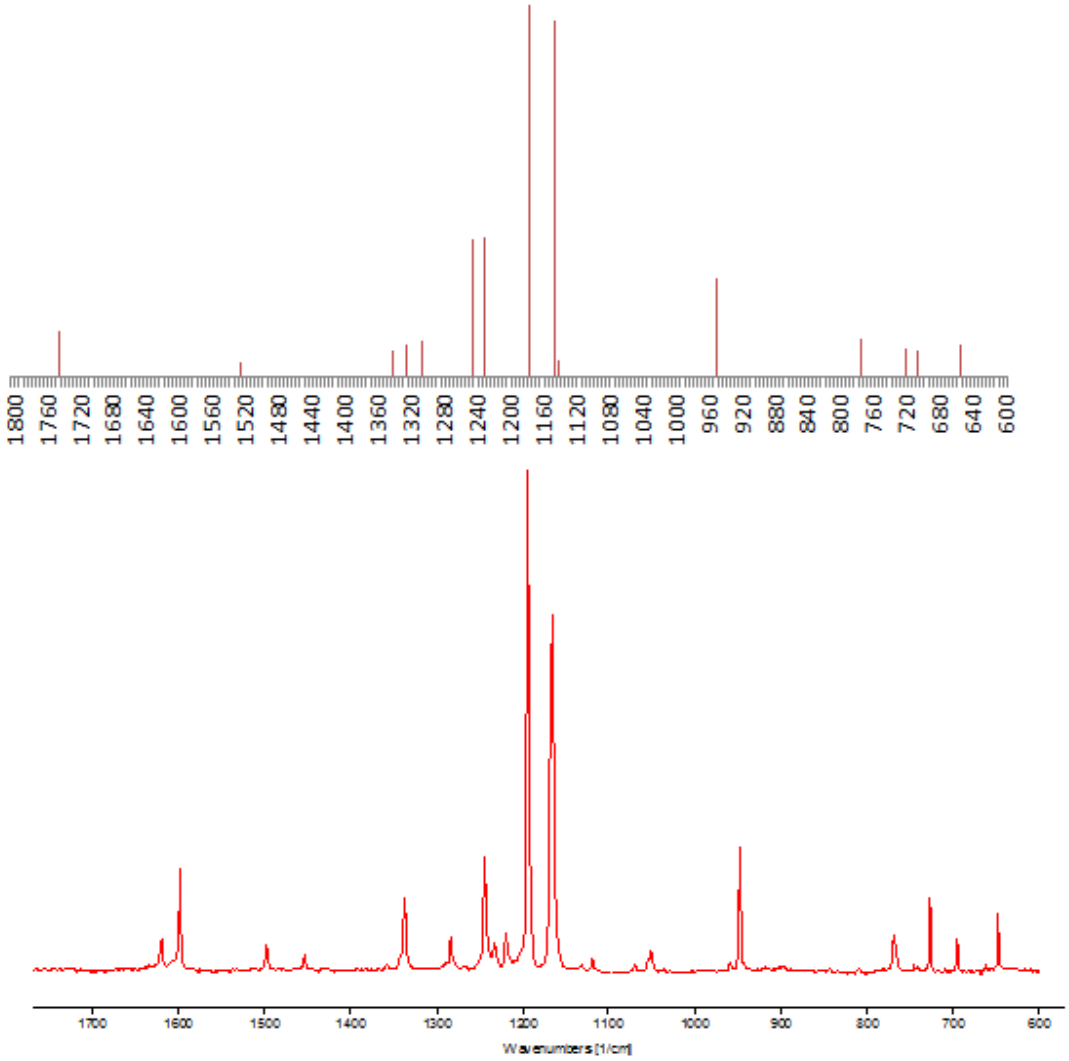

Figure 5-13 Top: Calculated IR spectrum of matrix isolated trideuteriomethyl-*o*-tolyl (trifluoromethyl) diazirine Bottom: Experimental IR spectra of trideuteriomethyl-*o*-tolyl (trifluoromethyl) diazirine

The trideuteriomethyl-*o*-tolyl (trifluoromethyl) carbene was generated photolytically by irradiating the diazirine precursor at 313 nm for 2 hours, followed by 303 nm for 2 hours to cleanly convert most of the diazirine to carbene. (Figure 5-14)

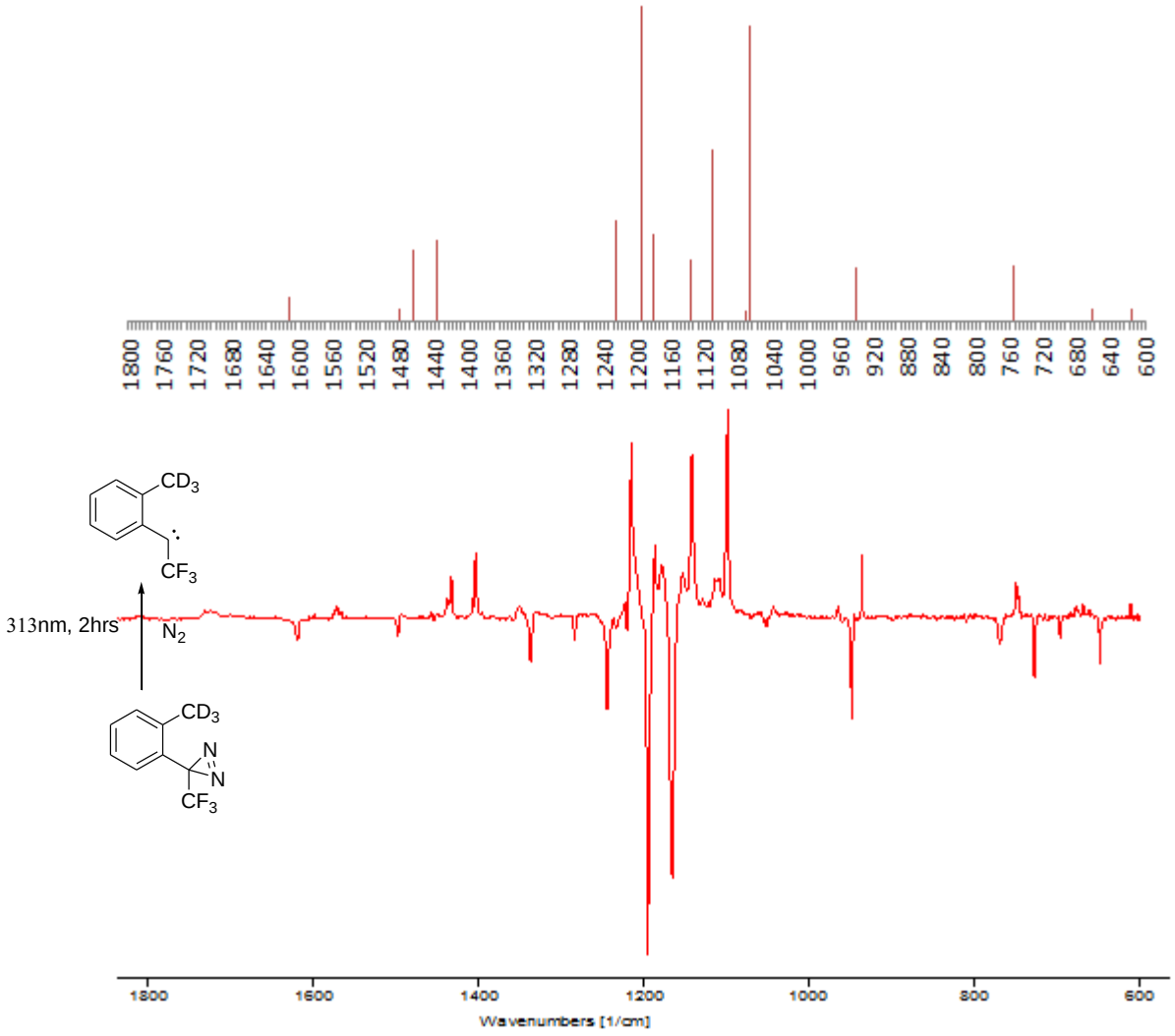

Figure 5-14 Top: calculated IR spectrum of *anti*-triplet trideuteriomethyl-*o*-tolyl (trifluoromethyl) carbene; Bottom: difference IR spectrum of carbene generation from diazirine precursor

Compared with its protio counterpart, deuterated *o*-tolyl (trifluoromethyl) carbene is exceptionally stable under different irradiation conditions. Our photochemical experiments showed that short-term (1 to 2 hours) irradiation at 296 nm, 366 nm, 369 nm, 404 nm, 546 nm or 578 nm led to no pronounced change in the IR spectra. Even after irradiation (>416 nm) with a Xe lamp up to 8 hour, only slight IR change was detected. However, it was found that 366 nm light could slowly induce the 1, 4-deuterium migration photochemically at 10K. After extended irradiation at 366 nm (12 hours), deuterated trifluoromethyl-*o*-tolyl-quinomethide was formed slowly, which was confirmed by comparing with the calculated IR and UV/vis spectra (Figure 5-15)

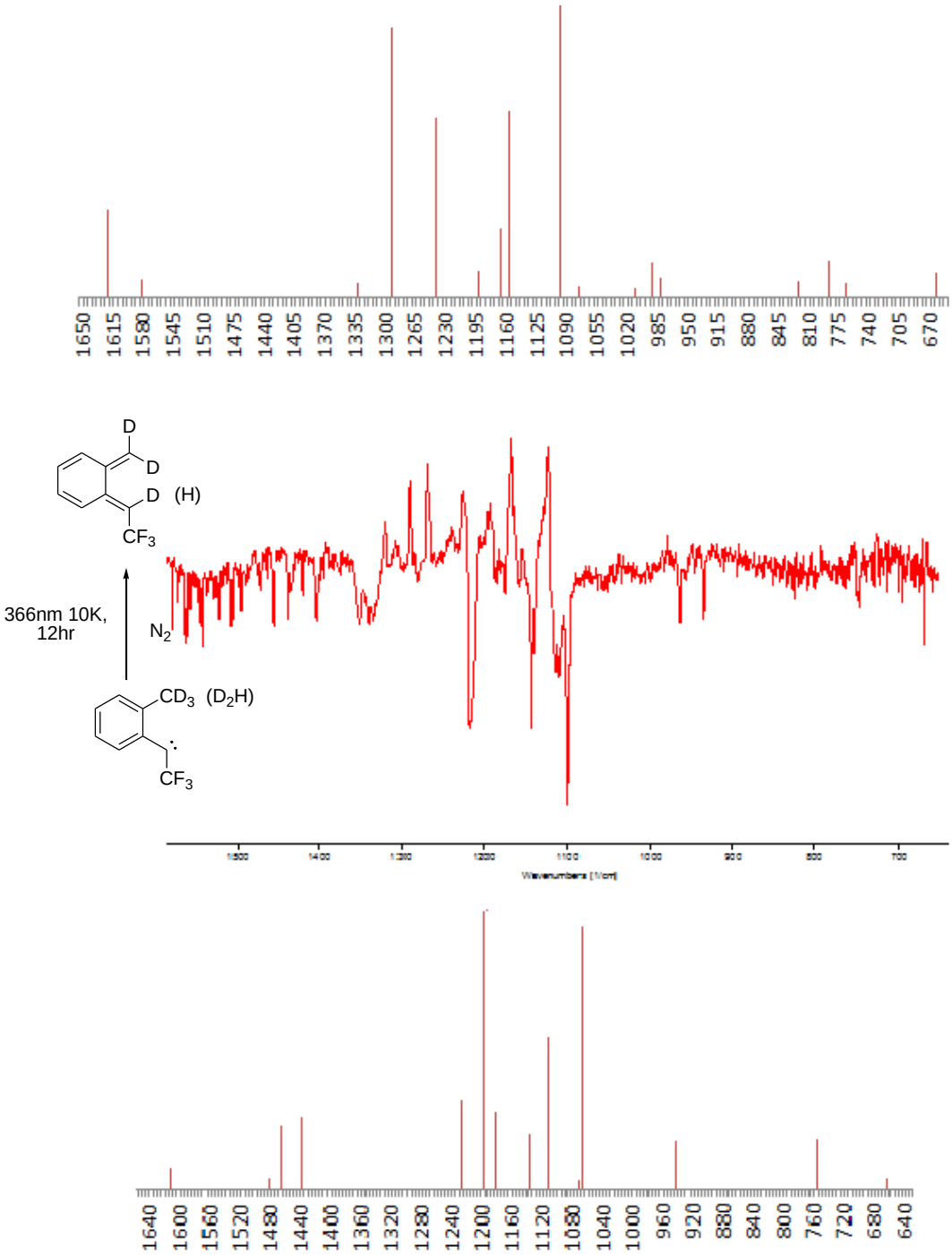

Figure 5-15 Top: calculated IR spectrum of deuterated trifluoromethyl-*o*-tolyl-quinomethide; Middle: difference IR spectrum of carbene decay by irradiation at 366 nm; Bottom: Calculated IR spectra of *anti*-triplet trideuteriomethyl-*o*-tolyl (trifluoromethyl) carbene

As expected, the thermal reactivity in trideuteriomethyl carbene species was significantly diminished by the isotopic effects and the 1, 4-deuterium migration was extremely slow. As we did in the protio case, we also monitored the thermal decay in the dark at 12K over 9hrs by measuring the characteristic IR bands of deuterated carbene species (1098 cm^{-1}, 1141 cm^{-1} and 1214 cm^{-1}). However, the IR bands intensities only showed slight or negligible changes even after staying overnight in the dark.

Even though deuterating the diazirine precursor as best as we could, it is appropriate to emphasize that our deuteriomethyl carbene species is not completely 100% deuterated, which means the remaining protons might also be involved in the photochemically and thermally induced rearrangement. Unless we have made the completely deuterated carbene species, we cannot 100% confidently tell the proton-tunneling from deuterium migration in its thermal decay. However, our data in the isotopic experiment qualitatively suggested the tunneling effects in *o*-tolyl (trifluoromethyl) carbene thermal decay and the $\boldsymbol{k}_H/\boldsymbol{k}_D$ is estimated to be at least 800 based on their first-order plots at 10K and 12K respectively. Again, limited by our research time and experimental techniques, we didn't get more precise measurements and enough $\boldsymbol{k}_H$ and $\boldsymbol{k}_D$ values under various reaction conditions to confirm the tunneling effect quantitatively.

Considering its stability under cryogenic conditions, an oxygen-trapping experiment was carried out to verify the ground spin state multiplicity of trideuteriomethyl *o*-tolyl (trifluoromethyl) carbene. Annealing of a 1% O_2-doped-matrix at 30K was found to convert trideuteriomethyl *o*-tolyl (trifluoromethyl) carbene into corresponding carbonyl oxide after 120mins, which could be photochemically rearranged to dioxirane under irradiation at 366 nm for 1 hour. (Figure 5-17, 5-18 and 5-19)

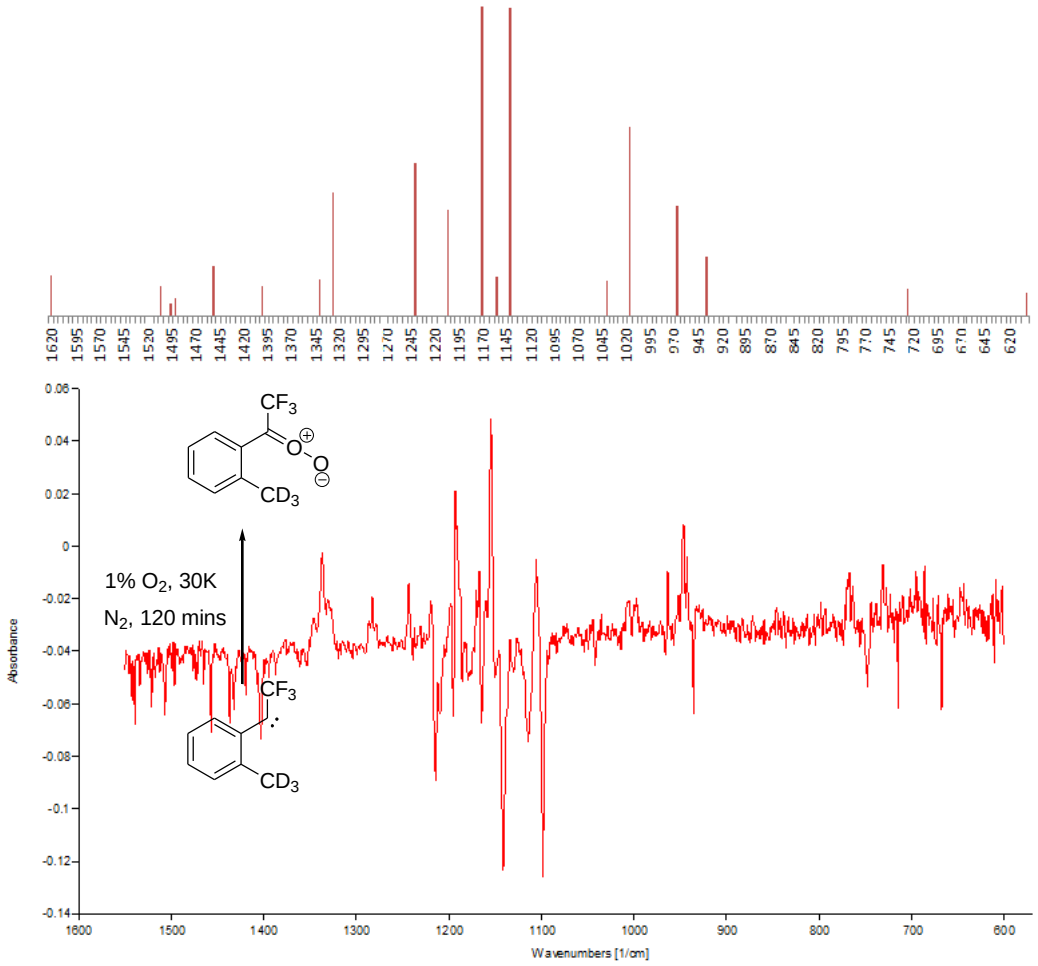

Figure 5-17 Top: Calculated IR spectrum trideuteriomethyl *o*-tolyl (trifluoromethyl) carbonyl oxide

Bottom: Difference IR spectrum after trideuteriomethyl *o*-tolyl (trifluoromethyl) carbene O_2 trap experiment

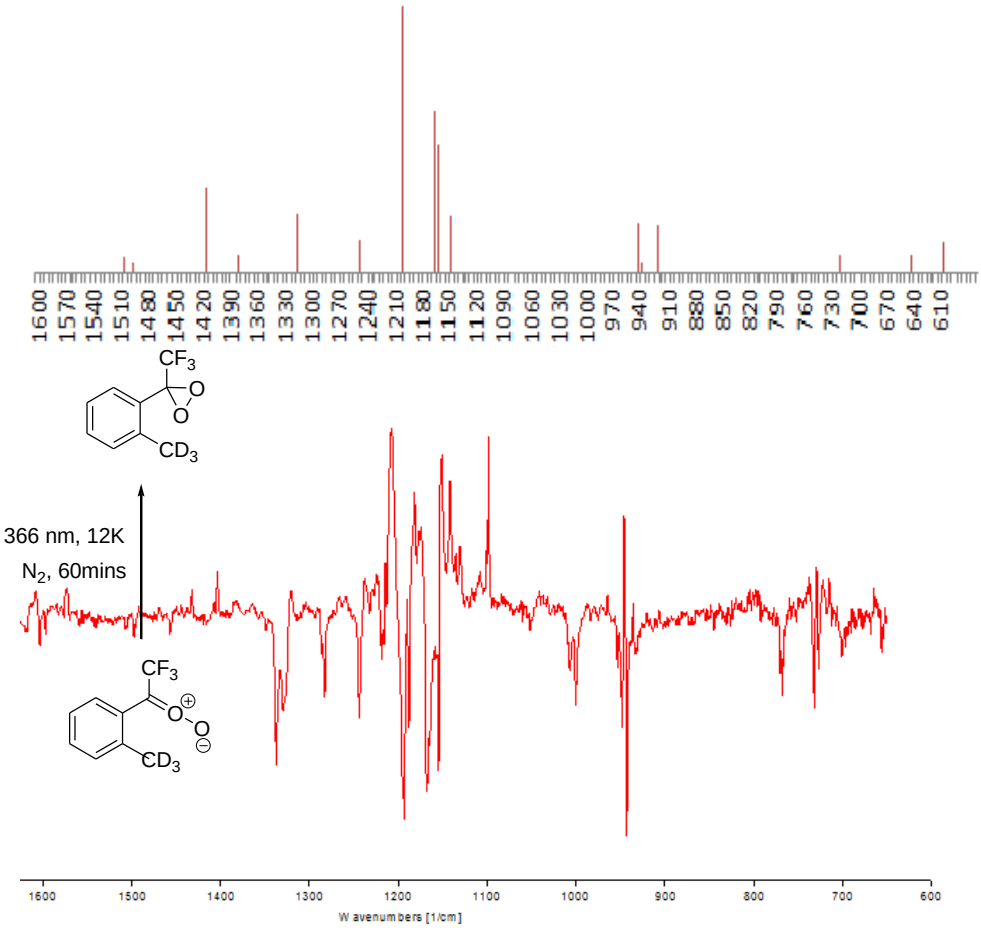

Figure 5-18 Top: Calculated IR spectrum of trideuteriomethyl *o*-tolyl (trifluoromethyl) dioxirane

Bottom: Difference IR spectrum after carbonyl oxide irradiation at 366 nm

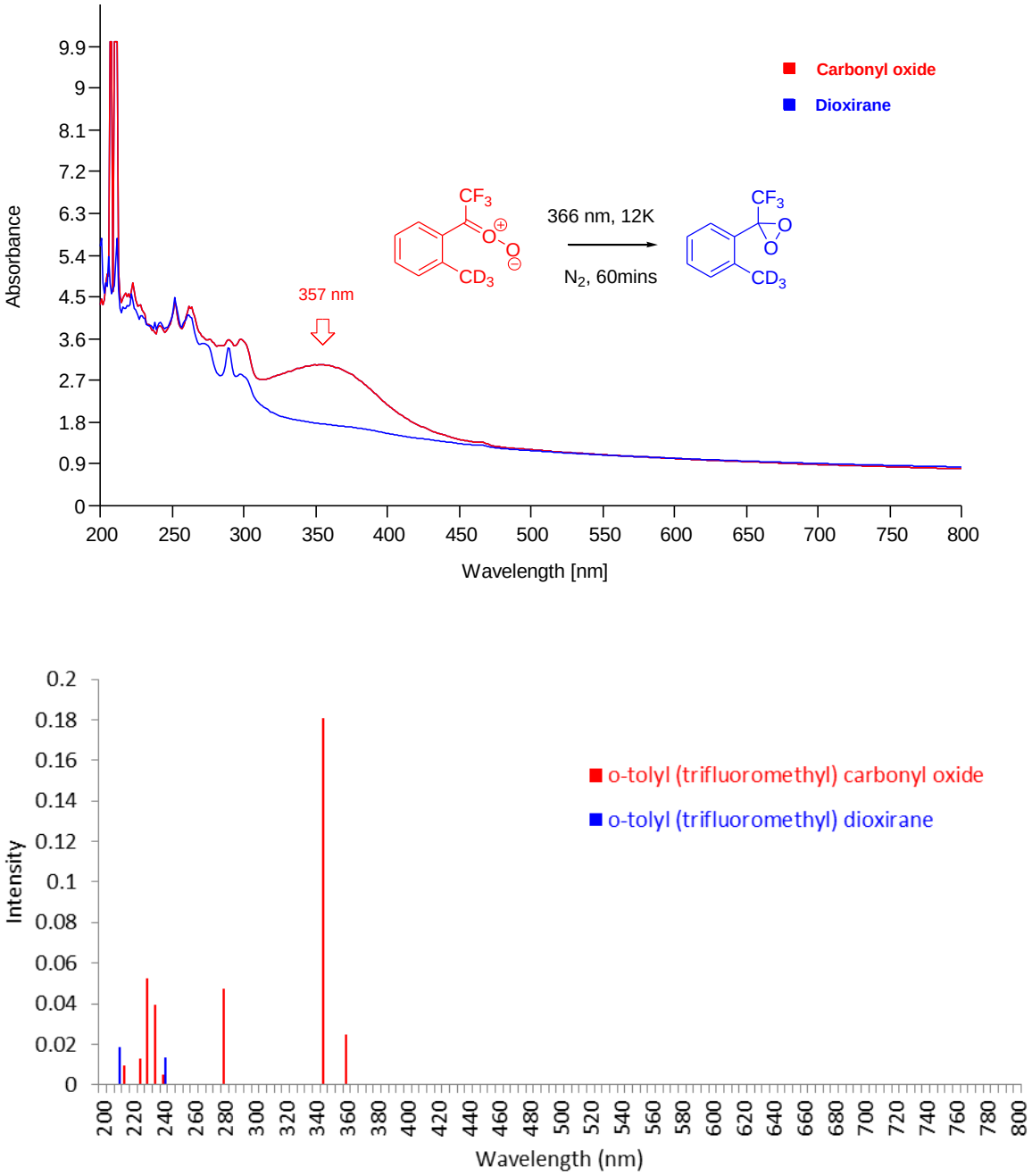

Figure 5-19 Top: Experimental UV/vis spectrum of trideuteriomethyl *o*-tolyl (trifluoromethyl) carbonyl oxide and dioxirane; Bottom: Calculated UV/vis spectrum of trideuteriomethyl *o*-tolyl (trifluoromethyl) carbonyl oxide and dioxirane

In summary, we obtained the deuterated *o*-tolyl (trifluoromethyl) diazirine precursor and generated the corresponding carbene species photolytically. Our preliminary results showed that upon trideuteration of the methyl group, *o*-tolyl (trifluoromethyl) carbene's thermal and photochemical reactivity was significantly inhibited. In comparison with its protio analogue, thermal decay of the trideuterated carbene was found to be extremely slow under tunneling conditions. Our kinetics studies qualitatively support the tunneling effects. In addition, the O_2-trapping experiment confirmed *o*-tolyl (trifluoromethyl) carbene is a ground state triplet.

5.3 *p*-methoxy-*o*-tolyl (trifluoromethyl) carbene

Quantum mechanical tunneling has been studied more in triplet carbenes than in singlets traditionally. Both our research group and others have recognized tunneling effects in singlet carbenes intramolecular reactions, but extensive studies and more examples have only been reported recently. We were wondering if the intramolecular 1, 4-H migrations with tunneling pathways would happen in singlet *o*-tolyl (trifluoromethyl) carbene. However, as far as we know, it would be very challenging to trap the singlet *o*-tolyl (trifluoromethyl) carbene, which has a higher energy than its triplet ground state. As discussed in the previous chapter, although Hund's rule predicts that most simple carbenes prefer high-spin and triplet ground states, appropriate regiochemical substituents could switch their spin states and make the singlet states more favorable than the triplets. Carbenes with lone-pair electron donating groups, such as alkoxy and halogen substituents, can have singlet ground states because of the interaction between lone pair electrons and empty *p* orbital in carbenic center via resonance effects. However, strongly singlet-stablizing groups may slow down tunneling also. Most recently, Sheridan and Song reported *p*-methoxy phenyl (trifluoromethyl) carbene has a singlet ground spin state, which was confirmed by DFT calculations and trapping experiments. We estimated the ground spin state of *o*-tolyl (trifluoromethyl) carbene species may be reversed by introducing a methoxy substituent at the *para* position, based on the same resonance stabilizing effects. (Scheme 5-8)

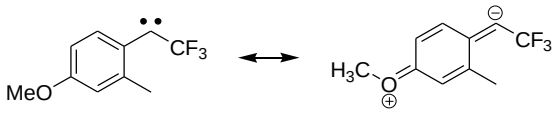

Scheme 5-8 Resonance stabilized singlet *p*-methoxy-*o*-tolyl (trifluoromethyl) carbene

5.3.1 Synthesis of *p*-methoxy-*o*-tolyl (trifluoromethyl) diazirine precursor

Following the established synthesis of *o*-tolyl (trifluoromethyl) diazirines, preparation of *p*-methoxy-*o*-tolyl (trifluoromethyl) diazirine was accomplished by a modified procedure. The precursor synthesis started with 3-methyl anisole, followed by bromination, organolithiation-trifluoroacetylation, oximation, mesylation, ammonation and oxidation. As found in preparation of other diazirines, introducing the trifluoroacetyl group to the aromatic ring is also the limiting step. Combination of n-BuLi/ ethyl trifluoroacetate was found to give more selective and convenient products than other methods, such as Grignard reaction and metallic lithium/*N*-trifluoroacetyl piperidine combination. The purification of mesylated oxime in this *p*-methoxy case was frustrating. Neither column chromatography nor recrystallization afforded perfectly pure compounds. But even the unpurified mesylated oxime could be used directly in following steps and the diazirine was isolated easily by running through a silica gel column in the last step (Scheme 5-9)

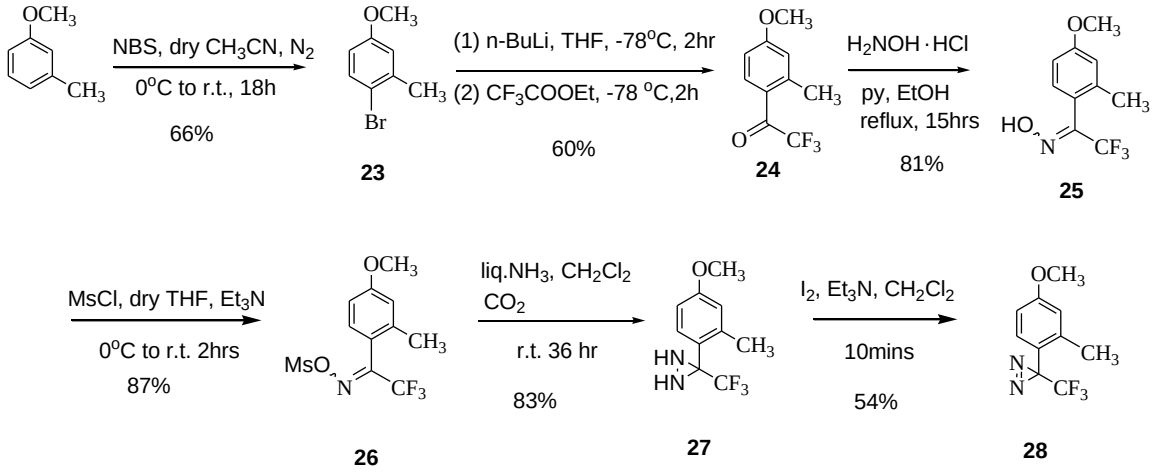

Scheme 5-9 Preparation of *p*-methoxy-*o*-tolyl (trifluoromethyl) diazirine precursor

5.3.2 Computational studies

As we did in the parent *o*-tolyl (trifluoromethyl) carbenes, geometry optimization and DFT calculations at B3LYP/6-31G** level were also carried out on *p*-methoxy-*o*-tolyl (trifluoromethyl) carbene species to obtain the sum of electronic and zero point energies of its four lowest-lying conformers. In agreement with our previous prediction, the *para*-methoxy carbene was found to be a ground state singlet with a small singlet-triplet gap. Relative energy calculation shows that the singlet ground state is only about 0.4kcal/mol lower than the most favorable CF_3-anti-triplet (ca. 2.4 kcal/mol if the overestimated triplet state stabilization was taken into consideration). In contrast, the triplet ground state of *o*-tolyl (trifluoromethyl) carbene was predicted as much as 4.13kcal/mol more stable than the lowest-lying singlet (ca. 2.13 kcal/mol, if the triplet over-stabilization was considered). Considering this narrow singlet-triplet gap, the singlet *para*-methoxy carbene may intersystem cross to its triplet state very easily followed by 1, 4-H abstraction-recombination and give out the rearranged quinomethide. Alternatively, the singlet carbene species may go through a concerted intramolecular 1, 4-H migration via a tunneling pathway and make the same rearranged quinomethide. To distinguish between these two possibilities, experimental evidence is needed.

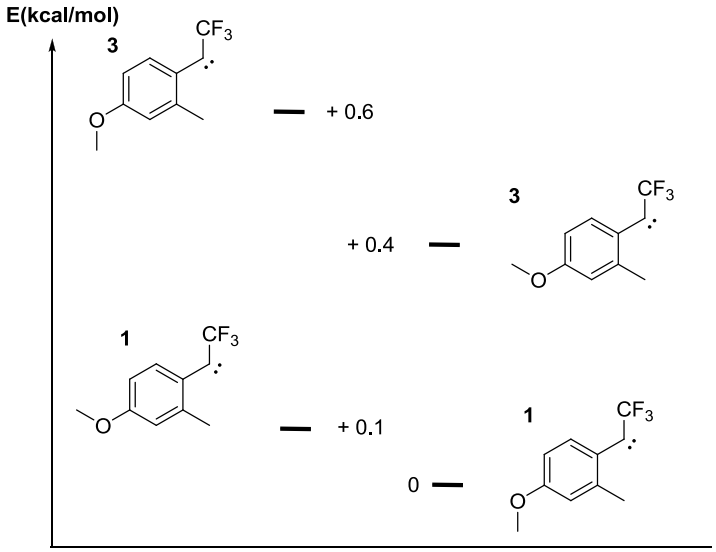

Figure 5-3 Geometries and relative energies of *p*-methoxy-*o*-tolyl (trifluoromethyl) carbenes

In addition to the relative energies, both IR and UV-vis spectra of all *para*-methoxy diazirine precursors, carbenes and possible rearranged products were predicted by frequency and TD DFT calculations at B3LYP/6-31G** level. It was shown that the most stable singlet *p*-methoxy-*o*-tolyl (trifluoromethyl) carbene species has characteristic vibrational frequencies at 1645cm^{-1}, 1365cm^{-1}, 1270cm^{-1}, 1175cm^{-1} and 1130cm^{-1} as well as a distinct UV-vis absorption at 335 nm. These results would be used to compare with the observed data in the following matrix experiments.

5.3.3 Matrix isolation and photochemical/thermal reactions

3-(4-Methoxy-2-methyl-phenyl)-3-trifluoromethyl-diazirine (*p*-methoxy-*o*-tolyl (trifluoromethyl) diazirine) and nitrogen gas were co-deposited into the matrix window at 21K. The matrix isolated diazirine precursor was characterized and confirmed by both IR and UV-vis spectroscopies. Again, the typical diazirines' n-π^* absorption was not observed in its UV-vis spectrum, which could also be rationalized as due to the steric hindrance of *ortho* methyl group. (Figure 5-20)

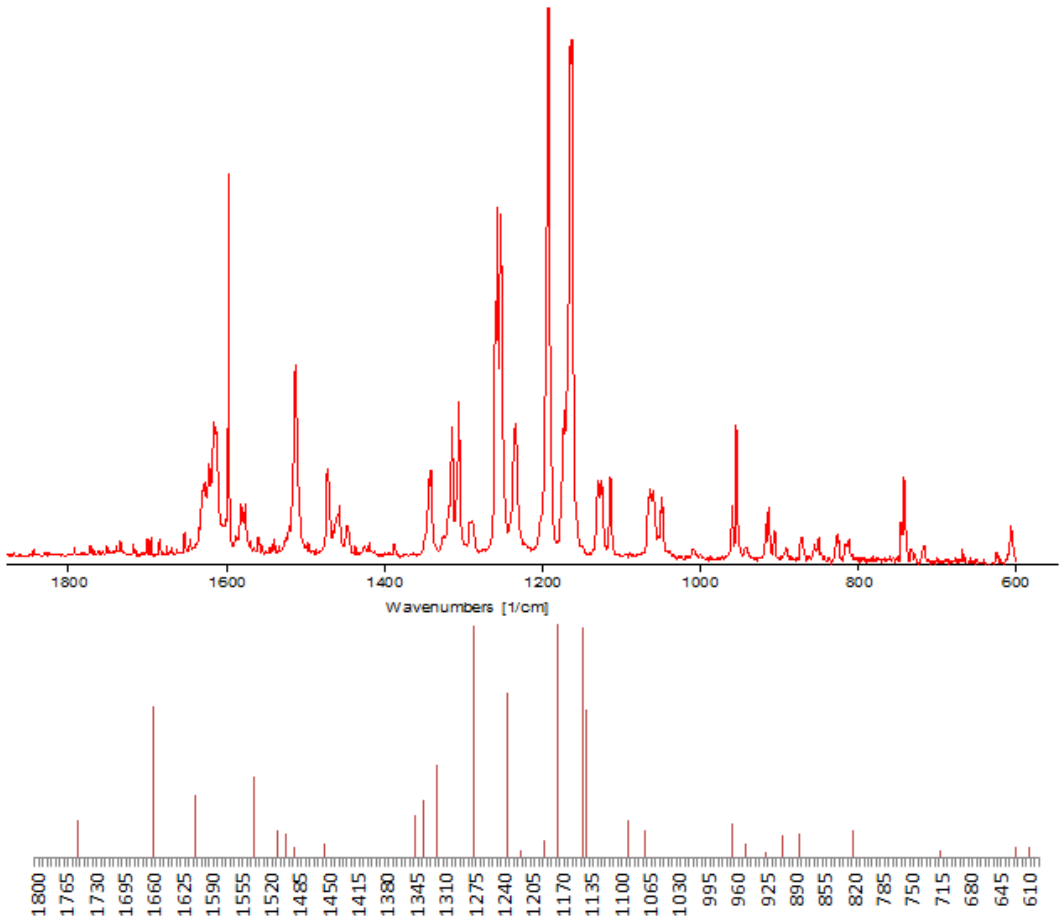

Figure 5-20 Top: Experimental IR spectrum of matrix-isolated *p*-methoxy-*o*-tolyl (trifluoromethyl) diazirine; Bottom: Calculated vibrational frequencies of *p*-methoxy-*o*-tolyl (trifluoromethyl) diazirine

Once the matrix temperature was decreased to its lowest minimum, the diazirine was irradiated at 313 nm for 1hour at 10K and a mixture of diazirine precursor, carbene species and rearranged product were observed in both IR and UV-vis spectra. Prolonged irradiation up to 4 hours converted all of the diazirine and carbene species into the photochemically unreactive product after rearrangement, which was predicted to be quinomethide and then confirmed by comparing with calculated data. To generate the carbene species exclusively without further quenching, a series of wavelengths and irradiation time were carefully tried. However, none of them could generate the carbene species without subsequent rearrangement. In other words, we didn't observe the apparent carbene formation directly in the IR spectrum, which was always contaminated with either diazirine precursor or quinomethide. We believe that, under all the photolytic

conditions we have tried, the singlet *p*-methoxy carbene species is too reactive to stay before characterization and easily to rearrange to the corresponding quinomethide. Again, we didn't get a satisfyingly clean IR spectrum of the singlet *p*-methoxy carbene without contamination by other species. Irradiation with a shorter wavelength light of 280 nm for 30 min was found to generate an intermediate having a distinct singlet carbene UV-vis absorption (λ_{max}=343 nm) together with small amount of quinomethide (λ_{max}=410 nm). Under tunneling conditions, the mixture was let to stay in dark overnight at 10K. The facile intermediate disappearance and quinomethide evolving were monitored spectroscopically. (Figure 5-21 and Figure 5-22) By comparing with calculated results, both IR and UV-vis spectra strongly suggested the intermediate species generated by 280nm irradiation was *p*-methoxy carbene, which could thermally decay to quinomethide via a tunneling pathway. Even though the carbene species was detected by monitoring its thermal decay with spectroscopic tools, however, we didn't find an appropriate condition generate and trap carbene exclusively, without contamination by unreacted diazirine precursors or rearranged quinomethide.

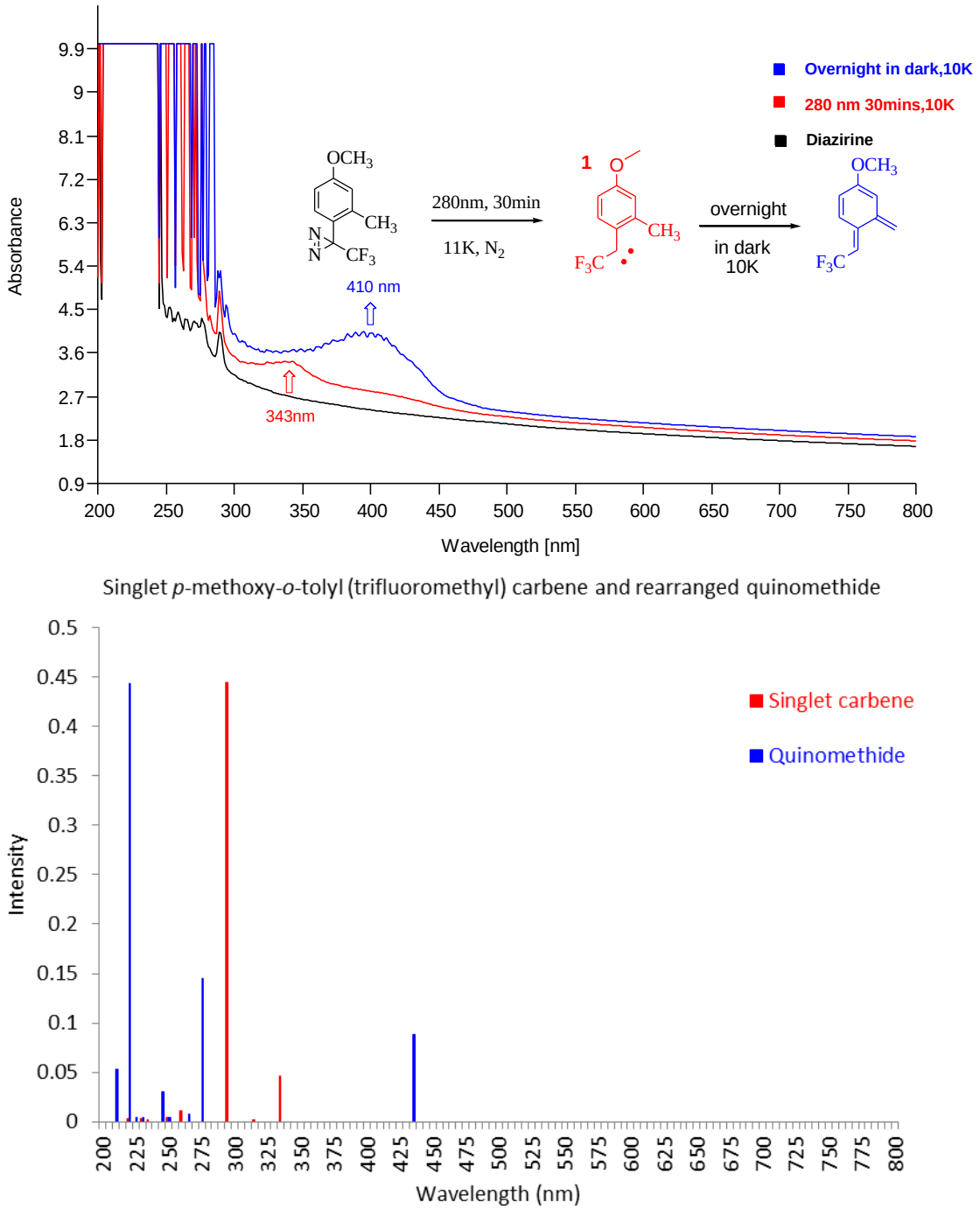

Figure 5-21 Top: observed UV-vis spectra of *p*-methoxy-*o*-tolyl (trifluoromethyl) diazirine (black); carbene species (red) and corresponding quinomethide (blue). Bottom: calculated UV-vis spectra of singlet *p*-methoxy-*o*-tolyl (trifluoromethyl) carbene (red) and quinomethide (blue)

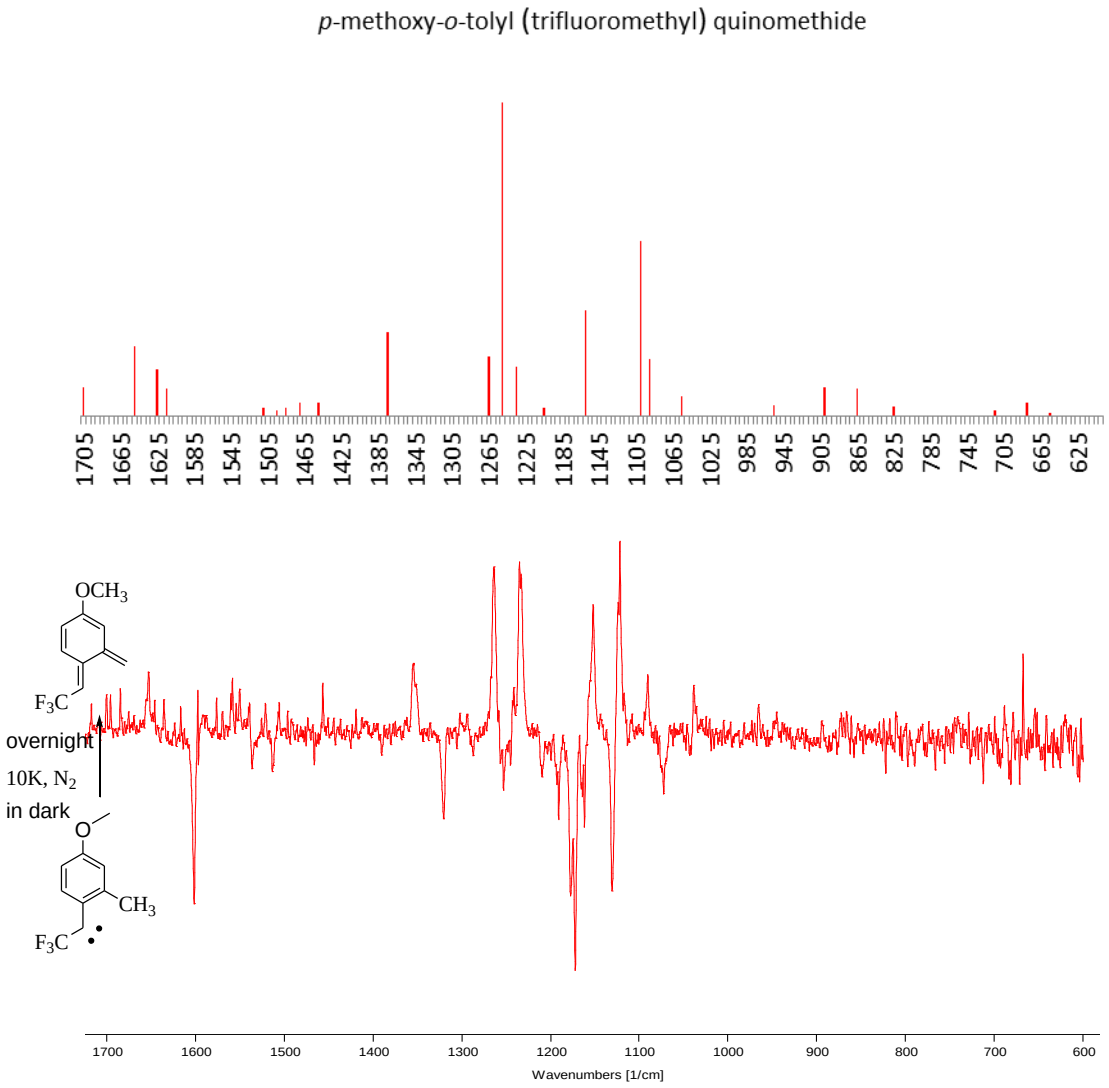

Figure 5-21 Top: calculated IR spectrum of quinomethide; Bottom: experimental IR difference spectrum of carbene thermal decay

To confirm that the intermediate formed after 280 nm light irradiation was indeed *p*-methoxy carbene, light of 341 nm was induced to the matrix right after its generation. As we expected, the characteristic carbene's IR bands at 1601cm^{-1}, 1320cm^{-1}, 1252cm^{-1}, 1175cm^{-1}, 1130cm^{-1} and 1072cm^{-1} disappeared along with the formation of corresponding quinomethide bands after 15mins. The observed IR picture of carbene photochemical reaction shows no variance with that in thermal decay, which fits the singlet state much

better than the lowest-lying triplet state by comparing with the calculated vibrational frequencies. (Figure 5-22)

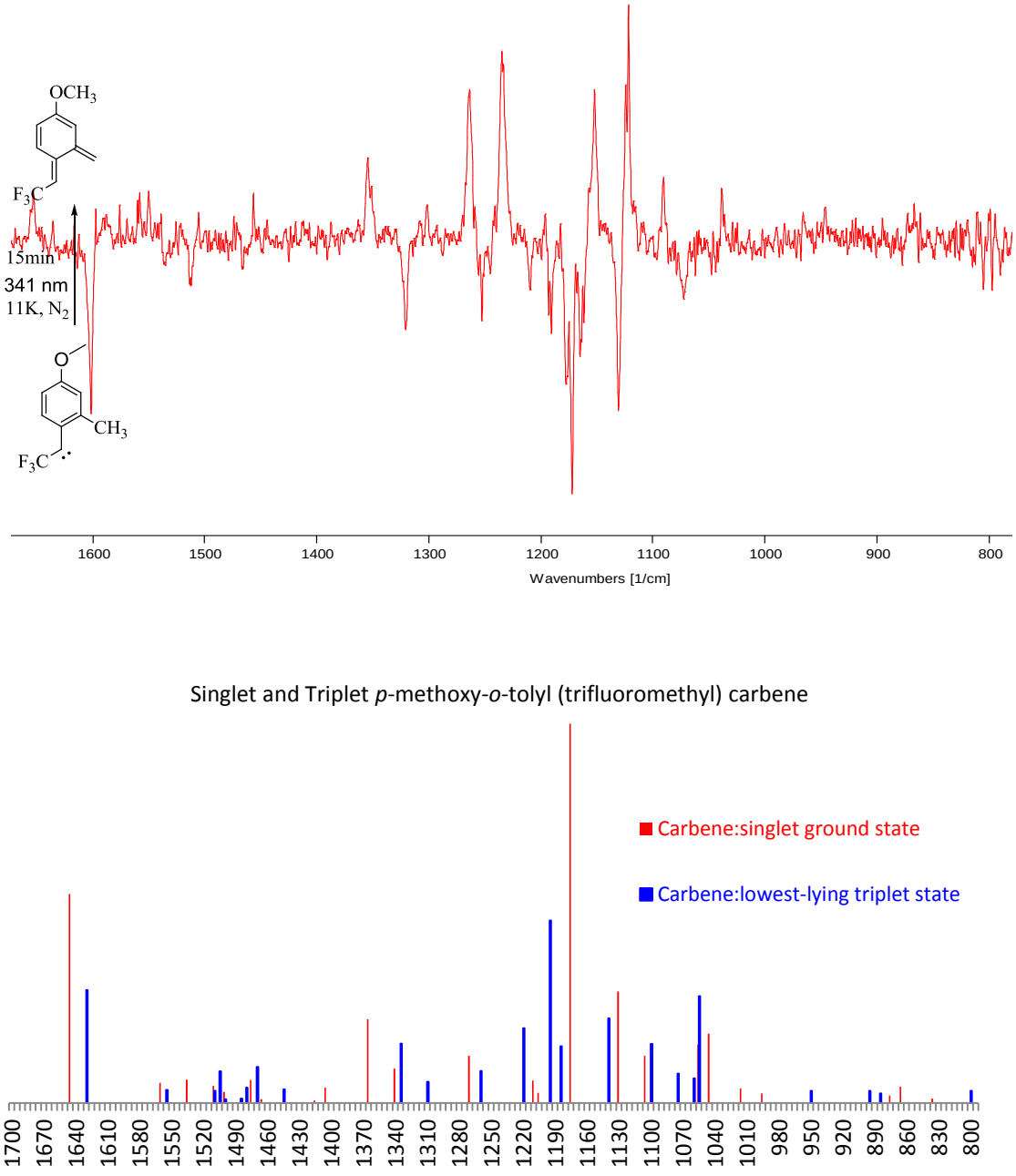

Figure 5-22 Top: IR difference spectrum of *p*-methoxy-*o*-tolyl (trifluoromethyl) carbene photolytic decay; Bottom: calculated IR spectrum of singlet *p*-methoxy-*o*-tolyl (trifluoromethyl) carbene (red) and its lowest-lying triplet state (blue)

To summarize, we synthesized *p*-methoxy-*o*-tolyl (trifluoromethyl) diazirine and generated the corresponding carbene in low temperature nitrogen matrices. DFT calculations predict singlet is the ground state, which is ca. 0.4-2.4kcal/mol lower than lowest triplet. As with the parent triplet *o*-tolyl (trifluoromethyl) carbene, the *p*-methoxy carbene was found to be both photo and thermally labile, but its rearrangement to quinomethide is very fast even at as low as 10K in the dark. Irradiation for 30mins was shown effectively to generate carbene species without too much further rearrangement and the carbene was clearly observed by UV-vis spectroscopy. However, because of the coexistence of either diazirine and/ or quinomethide, it was difficult to observe the carbene species formation directly in IR spectra under all research conditions we have tried. An indirect but compelling evidence of the existence of *p*-methoxy carbene, however, was provided by IR difference spectra during its thermal and photolytic decay, in which IR bands of *p*-methoxy carbene were observed. Both the experimental IR and UV-vis spectra fit calculated results very well suggesting *p*-methoxy carbene is ground state singlet. These results support that the singlet state of these carbenes can undergo direct, concerted 1,4 H migration via tunneling.

6. Conclusions and outlook

o-Tolyl (trifluoromethyl) carbene was chosen as a parent system in this chemistry and generated by irradiating the N_2 matrix-isolated diazirine precursor with 313 nm light at 10K. It was found that the *o*-tolyl (trifluoromethyl) carbene is a ground state triplet, which was confirmed by trapping experiments together with DFT calculations at the B3LYP/6-31G** level. The thermal intramolecular 1, 4-H migrations were observed at temperatures as low as 10K in the dark to form *o*-trifluoromethylquinomethide. The carbene decay process was tracked spectroscopically at 10K and 20K respectively and our preliminary kinetic measurements show that the reaction rates are temperature independent and the "first-order" plots of ln [Intensity] versus time are nonexponetial. A quantum mechanical tunneling (QMT) process instead of a classical energy barrier mechanism was suggested for the triplet *o*-tolyl (trifluoromethyl) carbene decay and was supported by the kinetic isotope effects in trideuteriomethyl-*o*-tolyl(trifluoromethyl)carbene decay. As expected, after deuteration the carbene species is thermally stable in the dark and no evident sign of decay was observed up to 30K. Additionally, it was also found to be photochemically somewhat inert and the rearrangement to quinomethide was exceptionally slow under various irradiation conditions. However, to confirm the QMT effect, more precise kinetic measurements of the carbene decay at a range of different temperatures are needed to obtain the nonlinear Arrhenius plots. It is still unclear whether the rearrangement involves direct intersystem crossing to singlet product.

In addition to its parent system, *p*-methoxy-*o*-tolyl (trifluoromethyl) carbene was also generated and investigated in low temperature N_2 matrices and a similar, but more facile thermal intramolecular 1, 4-H migration was observed under tunneling conditions. In contrast to its triplet parent carbenes, the ground state of *p*-methoxy-*o*-tolyl (trifluoromethyl) carbene was estimated to be singlet by DFT calculations and supported by spectroscopic observations. Because of its evident lability and limited by time, we didn't observe the *p*-methoxy-*o*-tolyl (trifluoromethyl) carbene formation clearly in IR spectra without contamination by diazirine and/or quinomethide. In future work, more careful control of the irradiation wavelength is needed to generate carbene species exclusively. Trapping experiments as well as EPR spectroscopy are also needed to confirm its ground singlet multiplicity. Kinetics study of carbene thermal decay and isotope-labeling experiments will help to verify the tunneling mechanism.

Experimental Section

General Information

All solvents used in precursors' synthesis were purchased from Sigma-Aldrich and dried before use. Reagents obtained from commercial source were used without further purification unless otherwise noted. All reactions were performed in pre-dried glassware and protected with nitrogen gas. Thin-layer chromatography (TLC) was carried out using commercial glass backed silica gel plates with thickness of 250μm. TLC plates were visualized with short wavelength ultra-violet light (254 nm). Flash column chromatography was performed using silica gel F60 (230-400 mesh, Silicycle). ^{1}H, ^{13}C and ^{19}F nuclear magnetic resonance (NMR) spectra were recorded on Varian 400 Hz or 500 Hz instruments with $CDCl_3$ as solvent. Chemical shifts (δ) are reported in parts per million (ppm) relative to $(CH_3)_4Si$ as internal standard (δ = 0.00 for ^{1}H and ^{13}C NMR) and coupling constants (J) are recorded in Hertz (Hz). Mass spectral data were recorded on an Agilent GC-MS instrument. IR and UV/vis spectra were obtained on a Perkin Elmer System 2000 FT-IR spectrometer with 1 cm^{-1} resolution and a Perkin Elmer Lambda 850 UV/Vis spectrophotometer respectively.

Matrix isolation of carbenes and the subsequent photochemistry experiments were performed on a mobile low temperature apparatus and the general description has been published previously.[36] A DE-202 closed cycle helium refrigerator and an APD Cryogenics compressor could make the experimental temperature as low as 10K. The temperature of system was monitored and controlled with a digital temperature controller (Model 9650, Scientific Instruments Inc.) and pressure was measured with a differential pressure gauge (PDR-C-2C, MKS Instruments Inc).

The diazirine precursors could either be premixed with inert gas in a 3 L glass manifold evacuated to ca. 10^{-3} torr before deposition on to a 2.54 cm CSI window or co-deposited with the carrier gas directly from a sample handling inlet.

In a typical "pre-mix" deposition procedure, the purified diazirine was analyzed by ^{1}H NMR before use and then the solvent ($CDCl_3$) was removed under reduced pressure. Considering the three diazirines in this study are volatile at room temperature, the $CDCl_3$ solution of diazirine was cooled with ice bath during water pump concentration and once concentrated to about 0.25ml, the solution was transferred into a pre-dried deposition tube, which was then connected to the gas handling system in the matrix isolation apparatus. Air in the deposition tube could be removed by a so called "freeze-thaw-pump" method, in which the deposition tube was first placed under vacuum while being cooled with liquid nitrogen and then allowed to sit at room temperature for couple of minutes with the vacuum off, and this procedure was repeated three times. Then a cooling bath (about -50 ℃) made with ethanol and liquid nitrogen was used to remove solvent left in the deposition tube. The pressure of the system was monitored carefully. Once no more solvent remains, when there are no sharp jumps in pressure, vacuum was turned off and diazirine was sublimated into the 3L mixing bulb. After the pressure reached about 0.4 torr, the mixing bulb was closed and deposition tube was removed from the system. Inert gas (high purity N_2 in this study) inlet was then connected to the gas handling system and pumped three times to get rid of air. After about 400 torr inert gas was introduced into the mixing bulb (a 0.1% diazirine in nitrogen), the temperature was set to be 21K and the premixed diazirine sample was deposited into the matrix head at a rate of 1 torr/min approximately up to ca. 110 torr.

The diazirine could alternatively be added to matrix head via a "direct-deposition" method. In this way, the system was evacuated to 10^{-3} torr and the mixing bulb was then filled with approximate 400torr nitrogen gas from the gas handling system. The deposition tube with diazirine sample was connected to sample inlet and air and solvent was removed by the same "freeze-thaw-pump" method described above. After the matrix head had been cooled to 21K, both the inert gas line and sample deposition line were opened to deposit and the rate was controlled as approximate 1torr/min up to ca. 100torr. In this study, 3-o-tolyl-3-trifluoromethyl diazirine and the 3-(2-methyl-($\boldsymbol{d}_3$)-phenyl)-3-(trifluoromethyl) diazirine were deposited using the "pre-mix" method and 3-(4-methoxy-2-methyl-phenyl)-3-trifluoromethyl diazirine was deposited with the direct way. After the deposition is complete, heater is turned off and matrix is cooled to lowest temperature (ca. 10K) for subsequent spectroscopic analysis and photochemical experiments.

Photochemistry experiments with light of different wavelengths were conducted by irradiation of the matrices using a Photon Technologies Inc. 01-001 Series monochromator with a HBO 100 W Hg lamp. In the thermal experiments, the temperature of matrix head was regulated with a temperature indicator/controller (Scientific Instruments Inc.). The matrices were then cooled to lowest temperature by turning off the heater before any spectroscopic analysis.

All geometries were fully optimized by analytical gradient methods with the Gaussian03 software package and density functional theory (DFT) calculations were performed on possible structures at the B3LYP 6-31+G** level of theory. Optimized coordinates and the sum of electronic and zero point energies are given in the calculation details. DFT predictions of vibrational frequencies and TD DFT results can be found in the supporting information.

Synthesis of diazirine precursors

N-trifluoroacetyl piperidine) (11)

Piperidine (22.00g, 253mmol), triethylamine (21.32g, 210mmol) and diethyl ether (15mL) were added to a 250mL three neck round bottom flask, which was then cooled to 0 ℃. Trifluoroacetic anhydride (TFAA, 47.92g, 228mmol) was added drop wise and the reaction system was cooled with ice bath periodically so that the temperature didn't go over 10 ℃. After addition of TFAA, the reaction mixture was stirred for an additional 3h below 15 ℃, at which time 1M HCl and 15mL diethyl ether were added to quench any remaining TFAA. After washing with water three times, the organic phase was dried, condensed and the crude product was purified using high vacuum distillation (2 torr / 63 ℃) to afford colorless oil (29.37g, 63%). The proton NMR spectrum is in agreement with reference. ^{1}H NMR (400 MHz, $CDCl_3$) δ: 3.63 – 3.55 (m, 1H), 3.55 – 3.46 (m, 1H), 1.84 – 1.45 (m, 3H). ^{19}F NMR (376 MHz, $CDCl_3$) δ: 69.02 (s).

2, 2, 2-Trifluoro-1-o-tolyl-ethanone (12)

As found in other organomagnesium mediated transformations, the activation of magnesium is essentially important to get reaction started. To achieve this, the magnesium turnings were washed with 1% HCl

solution and acetone, and then dried under vacuum. The dry magnesium was abraded by stirring with magnetic bars overnight in the flasks under nitrogen before use. The activated magnesium turnings (1g, 42mmol), anhydrous diethyl ether (25mL) and 2-bromotoluene (5g, 29.2mmol) were added in a 100ml round bottom flask. The mixture was heated cautiously with warm water to reflux. The exothermic reaction was allowed to proceed for 1h before being cooled in an ice bath. 1-Trifluoroacetyl piperidine (6.98g, 38mmol) was added dropwise over 30mins with stirring at 0 ℃. After addition was complete, ice bath was replaced with cold water (10-15 ℃) and was cooled periodically over the following 2hrs. Then, the reaction was quenched with 1:1 ice and 5% HCl. The quenched mixture was extracted using a diethyl ether and dichloromethane mixture (1:1). The organic layer was washed with 1M HCl and then dried over anhydrous magnesium sulfate. The crude product was then condensed to be dark brown oil, which was then distilled under high vacuum (2 torr / 60 ℃) to afford the desired product and 1-trifluoroacetyl piperidine as a mixture (4.30g). After column chromatography with hexane and ethyl acetate as eluent (4:1), 2, 2, 2-trifluoro-1-o-tolyl-ethanone (R_f: 0.80, 2.1g, 38%) was obtained as a colorless liquid. ^{1}H NMR (400 MHz, $CDCl_3$) δ 7.88 (d, *J* = 8.2 Hz, 1H), 7.53 (t, *J* = 7.5 Hz, 1H), 7.34 (t, *J* = 7.2 Hz, 2H), 2.58 (s, 3H). ^{19}F NMR (376 MHz, $CDCl_3$) δ: -71.39 (s). ^{13}C NMR (101 MHz, $cdcl_3$) δ 182.31 (q, *J* = 34.1 Hz), 142.30 (s), 133.97 (s), 132.60 (s), 130.42 (q, *J* = 3.8 Hz), 129.16 (s), 125.94 (s), 116.45 (q, *J* = 292.7 Hz), 21.78 (s).Note: The product and excess reactant mixture after vacuum distillation could also be used for the next step without further purification.

2, 2, 2-Trifluoro-1-*o*-tolyl-ethanone oxime (**13**)

A mixture of 2, 2, 2-trifluoro-1-o-tolyl-ethanone and *N*-trifluoroacetyl piperidine (4.00g) after vacuum distillation was placed in to a 250 mL round bottom flask equipped with a magnetic bar. To this pyridine (60mL), absolute ethanol (15mL) were added and heated to reflux. Then, hydroxylamine hydrochloride (6.00g) was added in one portion and this mixture was stirred and allowed to reflux for 18h. After pyridine and ethanol were removed under reduced pressure, the crude product was dissolved in diethyl ether and washed with 1M HCl (70mL) three times. The organic phase was neutralized with 1M $NaHCO_3$ followed by washing with brine. The collected organic layer was then dried over anhydrous magnesium sulfate and

solvent was removed under reduced pressure to afford the off white solid as a mixture of two isomers (2.7g, 45.55 % from 2-bromo toluene)**.** ^{1}H NMR (400 MHz, $CDCl_3$) δ: 8.99 (s, 1H), 8.73 (s, 1H), 7.40 – 7.17 (m, 8H), 2.32 (s, 3H), 2.28 (s, 3H). ^{19}F NMR (376 MHz, $CDCl_3$) δ: -64.13 (s), -68.33 (s).

2, 2, 2-Trifluoro-1-*o*-tolyl-ethanone methanesulfonic oxime (14)

At 0 ℃, methanesulfonyl chloride (1.27g, 11mmol, 1.5eq) was added to 2, 2, 2-trifluoro-1-o-tolyl-ethanone oxime (1.5g, 7.4mmol, 1eq) in 15mL dry THF. To this solution was added drop wise a solution of triethylamine (1.5g, 14.8mmol, 2eq) in anhydrous THF (15mL) over a 20 min period, which was stirred at 0 ℃ for additional 20min before the ice bath was removed. The solution was then stirred for 2h at room temperature. When the reaction was complete, THF was removed under reduced pressure and the residue was dissolved in water, and extracted by diethyl ether. The diethyl ether phase was washed with brine and then dried over anhydrous magnesium sulfate. After removal of solvent, the viscous oil was recrystallized with hexane to afford white solid as a mixture of two isomers (1.54g, 77%). ^{1}H NMR (400 MHz, $CDCl_3$) δ: 7.47 – 7.41 (m, 2H), 7.33-7.28 (m, *J* = 7.8, 5.3 Hz, 5H), 7.18 (d, *J* = 7.6 Hz, 1H), 3.25 (s, 3H), 3.24 (s, 3H), 2.37 (s, 3H), 2.29 (s, 3H). ^{19}F NMR (376 MHz, $CDCl_3$) δ: -63.22 (s), -68.30 (s). m.p.: 57.9-58.8 ℃.

3-o-Tolyl-3-trifluoromethyl-diaziridine (15)

To a 30 mL high pressure tube, 2, 2, 2-Trifluoro-1-o-tolyl-ethanone methanesulfonic oxime (0.63, 2.2mmol) and dry dichloromethane (2mL) was added, and the solution was cooled with liquid nitrogen. Liquid ammonia was introduced and the high pressure tube was capped tightly. Liquid nitrogen was then removed and the reaction mixture was stirred gently at room temperature for 36 h, at which point, the high pressure tube was cooled in liquid nitrogen before opening cap and the excess ammonia was allowed to evaporate slowly as the mixture warmed to room temperature. The residue was partitioned between water and dichloromethane, and the organic layer was dried over anhydrous magnesium sulfate. After concentration under reduced pressure, viscous light yellow oil (0.42g, 93%) was collected as a mixture of diaziridine and trace of oxime. ^{1}H NMR (400 MHz, $CDCl_3$) δ: 7.43 (d, *J* = 7.3 Hz, 1H), 7.34 (t, *J* = 7.5 Hz, 1H), 7.23 (t, *J* = 7.1 Hz, 2H), 2.83 (d, *J* = 8.6 Hz, 1H), 2.46 (s, 3H), 2.38 (d, *J* = 8.5 Hz, 1H). ^{19}F NMR (376 MHz, $CDCl_3$) δ: -76.61 (s). Note: The mixture was used for the next reaction without further purification.

3-o-Tolyl-3-trifluoromethyl-diazirine (16)

Triethylamine (0.4g, 4mmol) was added to a mixture of 3-o-tolyl-3-trifluoromethyl-diaziridine with trace oxime (0.42g, 2mmol) in dichloromethane (10mL), and the solution was then cooled to 0 ℃ before iodine (0.6g, 2.4mmol) was added by portions. Reaction process was tracked with TLC (R_f: 0.9, hexane: ethyl acetate: 1:10 on silica). When the reaction was complete, sodium bicarbonate (0.2g, 2.4mmol) and water (10mL) was added and the mixture was extracted with 5mL dichloromethane three times. The resulting organic phase was then washed with water (5mL) twice and dried over anhydrous magnesium sulfate. Dichloromethane was removed under reduced pressure in ice bath and the dark brown residue was purified with column chromatography (hexane) to afford light yellow to pink color oil (R_f: 0.9, 0.22g, 55%). The pure diazirine was kept in deuterated chloroform and was concentrated right before matrix experiments. ^{1}H NMR (400 MHz, $CDCl_3$) δ: 7.56 (d, *J* = 7.7 Hz, 1H), 7.32 – 7.29 (m, 1H), 7.23 – 7.19 (m, 2H), 2.58 (s, 3H). ^{19}F NMR (376 MHz, $CDCl_3$) δ: -68.51 (s). ^{13}C NMR (126 MHz, cdcl$_3$) δ 140.03 (s), 131.30 (s), 130.93 (s), 130.74 (s), 126.80 (s), 126.69 (s), 122.44 (q, *J* = 274.7 Hz), 27.97 (q, *J* = 41.7 Hz), 19.10 (s).

2-Bromo-(methyl-*d*$_3$)-toluene (17)

A 100 mL three neck round bottom flask with D_2O (20mL) was flushed by strong nitrogen stream, to which tiny sodium metal (9g) cubes were added carefully to afford a pasty NaOD/D_2O solution. (Toward the end of the addition, heating is required.) Then, 2-bromotoluene (3.0g), tetrabutylammonium hydrogensulfate (phase-transfer catalyst, 1g, 20mol %) and dry hexane (6mL) was added. When the addition was complete, a mechanic stirrer was added and the reaction mixture was stirred vigorously at room temperature for 20h, followed by addition of deuterium oxide (5mL) and three extractions with dichloromethane. The combined extracts were washed with water, dried over anhydrous $MgSO_4$. After removal of solvent under vacuum, CH_3-deuterated 2-bromotoluene was obtained with catalyst and its decomposition products (1.8g, 60%). After repeating the same procedure, crude product was run through silica column with hexane as the eluent to afford the desired product as light yellow oil (1.2g, 40%, R_f =0.9). Proton NMR spectrum shows the degree of H/D exchanges up to 90% after second time deuteration. ^{1}H NMR (400 MHz, $CDCl_3$) δ: 7.51 (d,

J = 7.5 Hz, 1H), 7.28 – 7.09 (m, 2H), 7.09 – 6.91 (m, 1H). ^{13}C NMR (101 MHz, cdcl$_3$) δ 137.74 (s), 132.31 (s), 130.82 (s), 127.31 (s), 127.21 (s), 124.95 (s), 22.36 – 21.83 (m). MS (EI): m/z 173.0, 175.0 (M^+)

2, 2, 2-Trifluoro-1-(2-methyl-(*d*$_3$)-phenyl) ethanone (18)

Magnesium turnings (2.1g, 83mmol), anhydrous diethyl ether (25ml) and 2-bromo-(methyl-***d*$_3$)-toluene (3.05g, 17.5mmol) were added in a 100ml round bottom flask, and the mixture was heated cautiously with warm water to reflux. The exothermic reaction was allowed to proceed for 1hr before being cooled in an ice bath. *N*-trifluoroacetyl piperidine (5.8g, 32mmol) was added drop wise over 30mins with stirring at 0 ℃. After addition is complete, ice bath was replaced with cold water (10-15 ℃) and was cooled periodically over the following 2hrs. Then, the reaction was quenched with 1:1 ice and 5% HCl. The quenched mixture was extracted using a diethyl ether and dichloromethane mixture (1:1). The organic layer was washed with 1M HCl and then dried over anhydrous magnesium sulfate. The crude product was then condensed to be dark brown oil, which was then distilled under high vacuum (2 torr / 60 ℃) to afford the desired product and 1-trifluoroacetyl piperidine as colorless liquid (5.2g). The mixture could be used for the next step without further purification. ^{1}H NMR (400 MHz, $CDCl_3$) methyl-***d*$_3$**-2, 2, 2-trifluoro-1-o-tolyl-ethanone: δ 7.89 (d, *J* = 8.3 Hz, 1H), 7.55 (t, *J* = 7.6 Hz, 1H), 7.41 – 7.33 (m, 2H); 1-trifluoroacetyl piperidine: δ 3.68 – 3.59 (m, 7H), 3.58 – 3.51 (m, 7H), 1.77 – 1.59 (m, 21H). ^{19}F NMR (376 MHz, $CDCl_3$) methyl-***d*$_3$**-2, 2, 2-trifluoro-1-o-tolyl-ethanone: δ: -68.96 (s), 1-trifluoroacetyl piperidine: δ -71.35 (s). MS (EI): m/z 191,181 (M^+)

2, 2, 2-Trifluoro-1-(2-methyl-(*d*$_3$)-phenyl) ethanone oxime (19)

A mixture of 2, 2, 2-trifluoro-1-(2-methyl-***(d*$_3$*)***-phenyl) ethanone and *N*-trifluoroacetyl piperidine (3.00g) after vacuum distillation was placed in to a 250 mL round bottom flask equipped with a magnetic bar. To this pyridine (50mL), absolute ethanol (15mL) were added and heated to reflux. Then, hydroxylamine hydrochloride (6.00g) was added in one portion and this mixture was stirred and allowed to reflux for 18hrs. After pyridine and ethanol were removed under reduced pressure, crude product was dissolved in diethyl ether and washed with 1M HCl (70mL) three times. The organic phase was neutralized with 1M $NaHCO_3$

followed by washing with brine. The collected organic layer was then dried over anhydrous magnesium sulfate and solvent was removed under reduced pressure to afford light yellow oil as a mixture of two isomers (1.20, 34 % 2 steps from 2-bromo-(methyl-***d*$_3$**)–toluene**).** ^{1}H NMR (500 MHz, $CDCl_3$) δ: 9.38 (s, 1H), 9.13 (s, 1H), 7.39 – 7.33 (m, 2H), 7.28 (dd, *J* = 11.7, 4.2 Hz, 2H), 7.23 – 7.16 (m, 4H). ^{19}F NMR (376 MHz, $CDCl_3$) δ: -64.17 (s), -68.35 (s). MS(EI): m/z 206 (M^+)

2, 2, 2-Trifluoro-1-(2-methyl-*(d$_3$)*-phenyl) ethanone methanesulfonyl oxime (20)

At 0 ℃, methanesulfonyl chloride (1 g, 8.74mmol, 1.5eq) was added to 2, 2, 2-trifluoro-1-(2-methyl-(***d*$_3$**)-phenyl) ethanone oxime (1.2g, 5.8mmol, 1eq) in 15mL dry THF. To the reaction mixture was added dropwise a solution of triethylamine (1.18g, 11.7mmol, 2eq) in anhydrous THF (15mL) over a 20 min period, which was stirred at 0 ℃ for additional 20min before ice bath was removed. The solution was then stirred for 2 more hours at room temperature. When the reaction was complete, THF was removed under reduced pressure and the residue was dissolved in water, and extracted with diethyl ether. The organic phase was washed with brine and then dried over anhydrous magnesium sulfate. After removal of solvent, the crud product was recrystallized with hexane to afford off-white solid as a mixture of two isomers (0.80g, 49%). ^{1}H NMR (400 MHz, $CDCl_3$) δ: 7.47 – 7.41 (m, 2H), 7.33 – 7.29 (m, 5H), 7.19-7.17 (d, *J* = 7.6 Hz, 1H), 3.24 (s, 2H), 3.23 (s, 3H). ^{19}F NMR (376 MHz, $CDCl_3$) δ: -63.23 (s), -68.31 (s). MS(EI): m/z 205 (M^+)

3-(2-Methyl-(*d*$_3$)-phenyl)-3-(trifluoromethyl) diaziridine (21)

2,2,2-Trifluoro-1-(2-methyl-***(d*$_3$*)***-phenyl) ethanone methanesulfonyl oxime (0.34g) and dry dichloromethane (2mL) was added to a 30 ml high pressure tube, and the solution was cooled with liquid nitrogen. Liquid ammonia was introduced and the high pressure tube was capped tightly. Liquid nitrogen was then removed and the reaction mixture was stirred gently at room temperature for 36 h, at which point, the high pressure tube was cooled in liquid nitrogen before opening cap, the liquid nitrogen was removed and the excess ammonia was allowed to evaporate slowly. The residue was partitioned between water and dichloromethane, and the organic layer was dried over anhydrous magnesium sulfate. After concentration under reduced pressure, viscous light yellow oil was collected and recrystallized with dry hexane to afford pure diaziridine as white solid (0.22g, 88%). ^{1}H NMR (500 MHz, $CDCl_3$) δ: 7.44 (d, *J* = 7.6 Hz, 1H), 7.34

(t, *J* = 7.5 Hz, 1H), 7.23 (d, *J* = 7.7 Hz, 2H), 2.81 (d, *J* = 8.9 Hz, 1H), 2.34 (d, *J* = 8.3 Hz, 1H). ^{19}F NMR (376 MHz, $CDCl_3$) δ: -68.15 (s), -76.63 (s).

3-(2-Methyl-(d_3)-phenyl)-3-(trifluoromethyl) diazirine (22)

Triethylamine (0.30g, 2.93mmol) was added to 3-(2-methyl-(***d*$_3$)-phenyl)-3-(trifluoromethyl) diaziridine (0.30g, 1.46mmol) in dichloromethane (12mL), and the solution was then cooled down to 0 ℃ before iodine (0.55g, 2.19mmol) was added by portions. Reaction process was tracked with TLC (R_f: 0.9, hexane on silica). When the reaction was complete, sodium hydroxide (0.06g, 1.46mmol) and water (10ml) were added and the mixture was extracted three times with 5ml dichloromethane. The resulting organic phase was then washed with water (5mL) twice and dried over anhydrous magnesium sulfate. Dichloromethane was removed under reduced pressure in ice bath and the dark brown residue was purified with column chromatography (hexane) to afford light yellow to pink color oil (R_f: 0.9, 0.25g, 83%). The pure diazirine was kept in deuterated chloroform and was concentrated right before matrix experiments. ^{1}H NMR (400 MHz, $CDCl_3$) δ: 7.56 (d, *J* = 7.7 Hz, 1H), 7.32 (t, *J* = 7.5 Hz, 1H), 7.23 -7.20(m, *J* = 8.7, 2.3 Hz, 2H). ^{19}F NMR (376 MHz, $CDCl_3$) δ: -68.47 (s). ^{13}C NMR (126 MHz, cdcl$_3$) δ 139.89 (s), 131.26 (s), 130.89 (s), 130.71 (s), 126.79 (s), 126.68 (s), 122.40 (q, *J* = 274.7 Hz), 27.94 (q, *J* = 41.7 Hz), 18.31 (dt, *J* = 39.0, 19.5 Hz).

1-Bromo-4-methoxy-2-methylbenzene (23)

A solution of N-bromosuccinimide (NBS, 8.90g, 50mmol) in 50 mL anhydrous acetonitrile was added to a 0 ℃ solution of 3-methylanisole (6.11g, 50mmol) in 40mL dry acetonitrile in one portion. The reaction mixture was allowed to come to room temperature and stirred overnight. Reaction was tracked by TLC (R_f: 0.20, hexanes on silica) and quenched with water after 18hrs. Hexane was added and the aqueous phase was extracted with three times with hexane. Organic phase was dried over magnesium sulfate and concentrated under reduced pressure. A clear oil-like liquid was obtained (6.67g, 66%) and the proton NMR spectrum is in agreement with reference. ^{1}HNMR (400 MHz, $CDCl_3$) δ: 7.23 (d, J = 8.7 Hz, 1H), 6.63 (d, J = 3.0 Hz, 1H), 6.45 (dd, J = 8.7, 3.0 Hz, 1H), 3.59 (s, 3H), 2.21 (s, 3H).

2, 2, 2-Trifluoro-1-(4-methoxy-2-methyl-phenyl)-ethanone (24)

12.8 mL n-BuLi in hexane (1.60 M, 20.47mmol, 1.50 eq) was slowly added into a solution of 1-bromo-4-methoxy-2-methylbenzene (2.74g, 13.65mmol, 1.00eq) in 45 ml anhydrous THF at -100℃ . The reaction mixture was allowed to stir for 2h at -100℃ before a solution of ethyl trifluoroacetate (2.52g, 17.75mmol, 1.30eq) in 20 mL THF was added over a period of 0.5 h. After the reaction mixture was stirred for an additional 2h, a solution of concentrated HCl (4.5mL) in methanol (10mL) was added to quench the reaction, followed with 25 mL diethyl ether. The mixture was washed with water twice and organic phase was dried by magnesium sulfate and concentrated under vacuum. 1.77g Clear oil (60%) was obtained after running silica column with hexane and ethyl acetate as eluent (4:1, R_f: 0.60). ^{1}H NMR (500 MHz, $CDCl_3$) δ 7.90 (d, *J* = 7.5 Hz, 1H), 6.84 – 6.80 (m, 2H), 3.88 (s, 3H), 2.60 (s, 3H). ^{19}F NMR (376 MHz, $CDCl_3$) δ: -70.41 (s). ^{13}C NMR (126 MHz, $cdcl_3$) δ 180.13 (q, *J* = 33.1 Hz), 164.00 (s), 146.52 (s), 133.90 (q, *J* = 4.2 Hz), 121.68 (s), 118.39 (s), 116.93 (q, *J* = 293.0 Hz), 111.16 (s), 55.53 (s), 22.89 (s). MS (EI): m/z 218.0 (M^+).

2, 2, 2-Trifluoro-1-(4-methoxy-2-methyl-phenyl)-ethanone oxime (25)

Hydroxylamine hydrochloride (5.23g, 75mmol) was added to a solution of 2, 2, 2-trifluoro-1-(4-methoxy-2-methyl-phenyl)-ethanone (5.47g, 25mmol) in absolute ethanol (65mL) and dry pyridine (12mL). The reaction mixture was refluxed for 12h. After ethanol and pyridine were removed under reduced pressure, the remaining residue was dissolved in diethyl ether (50ml) and washed with 1M hydrochloride three times. The organic layer was washed with water and dried over magnesium sulfate. After removing diethyl ether, light yellow oil (4.74g, 81%) was obtained as two isomers. ^{1}H NMR (400 MHz, $CDCl_3$) δ: 8.73 (s, 1H), 8.48 (s, 1H), 7.16 (d, J = 8.3 Hz, 1H), 7.12 (d, J = 8.4 Hz, 1H), 6.85 – 6.79 (m, 2H), 6.78 – 6.73 (m, 2H), 3.82 (s, 6H), 2.30 (s, 3H), 2.25 (s, 3H). ^{19}F NMR (376 MHz, $CDCl_3$) δ: -68.32 (s).

2, 2, 2-Trifluoro-1-(4-methoxy-2-methyl-phenyl)-ethanone methanesulfonyl oxime (26)

At 0℃, methanesulfonyl chloride (0.52g, 4.5mmol,1.5eq) was added to 2, 2, 2-trifluoro-1-(4-methoxy-2-methyl-phenyl)-ethanone oxime (0.70g, 3mmol, 1eq) in 15ml dry THF. To this solution was added drop

wise a solution of triethylamine (0.49g, 4.5mmol, 1.6eq) in anhydrous THF (8mL) over a 15min period, at which point the ice bath was removed and the solution was stirred for 1hr at room temperature. When the reaction was complete, THF was removed under reduced pressure and the residue was dissolved in water, and extracted by diethyl ether. The diethyl ether layer was washed with brine and then dried over anhydrous magnesium sulfate. After removal of solvent, the viscous oil was recrystallized with hexane to afford light yellow solid as a mixture of two isomers (0.82g, 87.0%).^{1}H NMR (400 MHz, $CDCl_3$) δ 7.11 (d, *J* = 8.3 Hz, 1H), 6.84 – 6.80 (m, 2H), 3.83 (s, 3H), 3.24 (s, 3H), 2.25 (s, 3H).^{19}F NMR (376 MHz, $CDCl_3$) δ: -68.34 (s).

3-(4-Methoxy-2-methyl-phenyl)-3-trifluoromethyl-diaziridine (27)

To a 30 ml high pressure tube, 2, 2, 2-trifluoro-1-(4-methoxy-2-methyl-phenyl)-ethanone mesylate oxime (2.43g, 7.81mmol) and dry dichloromethane (2mL) was added, and the solution was cooled with liquid nitrogen for 5mins. Liquid ammonia (8.00mL) was introduced and the high pressure tube was capped tightly. Liquid nitrogen was removed and the reaction mixture was stirred gently at room temperature for 36 h, at which point, the high pressure tube was cooled in liquid nitrogen, the tube opened and let warm and the excess ammonia was allowed to evaporate slowly. The residue was partitioned between water and dichloromethane, and the organic layer was dried over anhydrous magnesium sulfate. After concentration under reduced pressure, viscous light yellow oil (1.51g, 83%) was collected as a mixture of diaziridine and oxime. The mixture was used for the next reaction without purification. ^{1}H NMR (400 MHz, $CDCl_3$) δ 7.35 (d, *J* = 8.2 Hz, 1H), 6.78 – 6.73 (m, 2H), 3.80 (s, 3H), 2.78 (d, *J* = 8.6 Hz, 1H), 2.44 (s, 3H), 2.31 (d, *J* = 9.3 Hz, 1H). Diaziridine: ^{19}F NMR (376 MHz, $CDCl_3$) δ -76.75 (s).

3-(4-Methoxy-2-methyl-phenyl)-3-trifluoromethyl-diazirine (28)

Triethylamine (0.29g, 2.84mmol) was added to a mixture of 3-(4-methoxy-2-methyl-phenyl)-3-trifluoromethyl-diaziridine with trace oxime (0.33g, 1.42mmol) in dichloromethane (15mL), and the solution was then cooled down to 0 ℃ with ice bath. Iodine (0.432g, 1.7mmol) was added to the solution by portions. Reaction process was tracked with TLC (R_f: 0.85, hexane: ethyl acetate: 1:10 on silica). When the reaction was complete, sodium hydroxide (0.06g, 1.42mmol) and water (10mL) were added and the

mixture was extracted with 5mL dichloromethane three times. The organic phase was washed with water (5mL) twice and dried over anhydrous magnesium sulfate. Dichloromethane was removed under reduced pressure in ice bath and the dark brown residue was purified with column chromatography (hexane: ethyl acetate: 1:10) to afford light yellow to pink color liquid (R_f: 0.85, 0.15g, 45%). The pure diazirine was kept in deuterated chloroform and was concentrated right before matrix experiments. ^{1}H NMR (400 MHz, $CDCl_3$) δ: 7.47 (d, *J* = 8.3 Hz, 1H), 6.73 (ddd, *J* = 6.6, 2.7, 1.7 Hz, 2H), 3.78 (s, 3H), 2.55 (s, 3H). ^{19}F NMR (376 MHz, $CDCl_3$) δ: -68.60 (s). ^{13}C NMR (101 MHz, $cdcl_3$) δ 161.01 (s), 141.74 (s), 132.31 (s), 122.36 (q, *J* = 274.6 Hz), 118.66 (s), 116.37 (s), 112.11 (s), 55.18 (s), 27.43 (q, *J* = 41.6 Hz), 19.26 (s).

References

1.McMahon, R. J.; Chapman, O. L., Direct spectroscopic observation of intramolecular hydrogen shifts in carbenes. *Journal of the American Chemical Society* **1987,** *109* (3), 683-692.

2.Tomioka, H.; Enyo, T.; Nakane, N., Photolysis of 3-(2-Formylphenyl)-3-chlorodiazirine in an Ar Matrix at Low Temperature. *The Journal of Organic Chemistry* **2004,** *69* (10), 3538-3545.

3.von E. Doering, W.; Hoffmann, A. K., The Addition of Dichlorocarbene to Olefins. *Journal of the American Chemical Society* **1954,** *76* (23), 6162-6165.

4.Schaefer, H. F., Methylene: A Paradigm for Computational Quantum Chemistry. *Science* **1986,** *231* (4742), 1100-1107.

5.Foster, J. M.; Boys, S. F., Quantum Variational Calculations for a Range of CH_2 Configurations. *Reviews of Modern Physics* **1960,** *32* (2), 305-307.

6.Herzberg, G., The Bakerian Lecture. The Spectra and Structures of Free Methyl and Free Methylene. *Proceedings of the Royal Society of London. Series A. Mathematical and Physical Sciences* **1961,** *262* (1310), 291-317.

7.Pople, J. A.; Segal, G. A., Approximate Self-Consistent Molecular Orbital Theory. III. CNDO Results for AB_2 and AB_3 Systems. *The Journal of Chemical Physics* **1966,** *44* (9), 3289-3296.

8.Bender, C. F.; Schaefer, H. F., New theoretical evidence for the nonlinearity of the triplet ground state of methylene. *Journal of the American Chemical Society* **1970,** *92* (16), 4984-4985.

9.Bernheim, R. A.; Bernard, H. W.; Wang, P. S.; Wood, L. S.; Skell, P. S., ^{13}C Hyperfine Interaction in CD_2. *The Journal of Chemical Physics* **1971,** *54* (7), 3223-3225.

10.Wasserman, E.; Yager, W. A.; Kuck, V. J., EPR of CH_2: a substiantially bent and partially rotating ground state triplet. *Chemical Physics Letters* **1970,** *7* (4), 409-413.

11.Herzberg, G.; Johns, J. W. C., On the Structure of CH_2 in its Triplet Ground State. *The Journal of Chemical Physics* **1971,** *54* (5), 2276-2278.

12.Bunker, P. R.; Jensen, P., A refined potential surface for the X-tilde $^3B_1$ electronic state of methylene CH_2. *The Journal of Chemical Physics* **1983,** *79* (3), 1224-1228.

13.Hayden, C. C.; Neumark, D. M.; Shobatake, K.; Sparks, R. K.; Lee, Y. T., Methylene singlet--triplet energy splitting by molecular beam photodissociation of ketene. *The Journal of Chemical Physics* **1982,** *76* (7), 3607-3613.

14.Sheridan, R. S.; Moss, R. A.; Wilk, B. K.; Shen, S.; Wlostowski, M.; Kesselmayer, M. A.; Subramanian, R.; Kmiecik-Lawrynowicz, G.; Krogh-Jespersen, K., Direct observational studies of a singlet alkylcarbene: methylmethoxycarbene, a remarkably selective nucleophile. *Journal of the American Chemical Society* **1988,** *110* (22), 7563-7564.

15.Ho, G. J.; Krogh-Jespersen, K.; Moss, R. A.; Shen, S.; Sheridan, R. S.; Subramanian, R., Kinetics of a carbene rearrangement: the 1,2-carbon migration of cyclopropylchlorocarbene. *Journal of the American Chemical Society* **1989,** *111* (17), 6875-6877.

16.Wang, J.; Sheridan, R. S., A Singlet Aryl-CF_3 Carbene: 2-Benzothienyl(trifluoromethyl)carbene and Interconversion with a Strained Cyclic Allene. *Organic Letters* **2007,** *9* (16), 3177-3180.

17.Song, M. G.; Sheridan, R. S., Regiochemical Substituent Switching of Spin States in Aryl(trifluoromethyl)carbenes. *Journal of the American Chemical Society* **2011,** *133* (49), 19688-19690.

18.Paulsen, S. R., 3.3-Dialkyl-diazacyclopropen-(1). *Angewandte Chemie* **1960,** *72* (21), 781-782.

19.Korshunova, G. A.; Sumbatyan, N. V.; Topin, A. N.; Mtchedlidze, M. T., Photoactivatable reagents based on aryl(trifluoromethyl) diazirines: Synthesis and application for studying nucleic acid-protein interactions. *Molecular Biology* **2000,** *34* (6), 823-839.

20.Skell, P. S.; Woodworth, R. C., Structure of carbene, CH_2. *Journal of the American Chemical Society* **1956,** *78* (17), 4496-4497.

21.Wentrup, C., Reactive Molecules. *John Wiley & Sons: New York,* **1984**, 2.

22.(a) Eric Whittle, D. A. D., George C. Pimentel, Matrix Isolation Method for the Experimental Study of Unstable Species. *The Journal of Chemical Physics* **1954,** *22* (11), 1; (b) Matzinger, S.; Bally, T., Spectroscopic Characterization of Matrix-Isolated Phenylcarbene and Cycloheptatetraene†. *The Journal of Physical Chemistry A* **2000,** *104* (16), 3544-3552.

23.Zuev, P. S.; Sheridan, R. S., Low-Temperature Hydrogenation of Triplet Carbenes and Diradicaloid BiscarbenesElectronic State Selectivity. *Journal of the American Chemical Society* **2001,** *123* (49), 12434-12435.

24.Gerbig, D.; Reisenauer, H. P.; Wu, C.-H.; Ley, D.; Allen, W. D.; Schreiner, P. R., Phenylhydroxycarbene. *Journal of the American Chemical Society* **2010,** *132* (21), 7273-7275.

25.Matthew S. Platz, R. A. M., Maitland Jones, Jr., Reviews of Reactive Intermediate Chemistry. *John Wiley & Sons, Inc.* **2007**.

26.Bell, R. P., *The tunnel effect in chemistry, Chapman and Hall, New York* **1980**.

27.Zuev, P. S.; Sheridan, R. S.; Albu, T. V.; Truhlar, D. G.; Hrovat, D. A.; Borden, W. T., Carbon tunneling from a single quantum state. *Science* **2003,** *299* (5608), 867-870.

28.Song, M.-G.; Sheridan, R. S., Effects of CF3 groups and charged substituents on singlet carbene stabilities–a density functional theory study. *Journal of Physical Organic Chemistry* **2011,** *24* (10), 889-893.

29.(a) Chapman, O. L.; Johnson, J. W.; McMahon, R. J.; West, P. R., Rearrangements of the isomeric tolylmethylenes. *Journal of the American Chemical Society* **1988,** *110* (2), 501-509; (b) Brunner, J.; Senn, H.; Richards, F., 3-Trifluoromethyl-3-phenyldiazirine. A new carbene generating group for photolabeling reagents. *J. Biol. Chem.* **1980,** *255* (8), 3313-3318.

30.Dubinsky, L.; Krom, B. P.; Meijler, M. M., Diazirine based photoaffinity labeling. *Bioorganic & Medicinal Chemistry* **2012,** *20* (2), 554-570.

31.Hatanaka, Y.; Hashimoto, M.; Kurihara, H.; Nakayama, H.; Kanaoka, Y., NOVEL FAMILY OF AROMATIC DIAZIRINES FOR PHOTOAFFINITY-LABELING. *Journal of Organic Chemistry* **1994,** *59* (2), 383-387.

32.Ross, S. P., Matrix Isolation of ortho and para-tolyl(trifluoromethyl)carbenes. *B.S. Thesis of The University of Nevada, Reno* **2011**.

33.Feldman, D.; Halpern, M.; Rabinovitz, M., Hydrogen-deuterium exchange of weak carbon acids under phase-transfer catalysis conditions. *Journal Name: J. Org. Chem.; (United States); Journal Volume: 50:10* **1985**, Medium: X; Size: Pages: 1746-1749.

34.Chen, T. S.; Wolinska-Mocydlarz, J.; Leitch, L. C., Synthesis of deuteriomethyl aromatic hydrocarbons by exchange with dimethylsulfoxide-d6. *Journal of Labelled Compounds* **1970,** *6* (3), 285-288.

35.Kurita, T.; Hattori, K.; Seki, S.; Mizumoto, T.; Aoki, F.; Yamada, Y.; Ikawa, K.; Maegawa, T.; Monguchi, Y.; Sajiki, H., Efficient and Convenient Heterogeneous Palladium-Catalyzed Regioselective Deuteration at the Benzylic Position. *Chemistry – A European Journal* **2008,** *14* (2), 664-673.

36.Rempala, P.; S. Sheridan, R., Matrix isolation and photochemistry of 1- and 2-naphthylchlorocarbene. *Journal of the Chemical Society, Perkin Transactions 2* **1999,** (11), 2257-2265.

Appendix A: Calculation Details

Optimized coordinates and the sum of electronic and zero point energies were give below.

Singlet-*o*-tolylmethylene 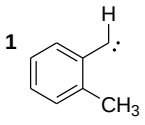

Standard orientation:

Center Number	Atomic Number	Atomic Type	Coordinates (Angstroms) X	Y	Z
1	6	0	2.004454	0.316061	0.004007
2	6	0	1.662112	-1.044759	-0.016624
3	6	0	0.326153	-1.450738	-0.015019
4	6	0	-0.717184	-0.517392	-0.004027
5	6	0	-0.392175	0.884079	0.012267
6	6	0	0.987471	1.256618	0.033756
7	6	0	-1.444133	1.853305	-0.068308
8	6	0	-2.145057	-0.989269	0.020566
9	1	0	3.046996	0.619665	0.006125
10	1	0	2.447310	-1.796386	-0.032882
11	1	0	0.092426	-2.512078	-0.029933
12	1	0	1.226349	2.316722	0.059888
13	1	0	-0.975039	2.850383	0.056744
14	1	0	-2.467160	-1.161562	1.055647
15	1	0	-2.253976	-1.935344	-0.518731
16	1	0	-2.806745	-0.228837	-0.396560

Zero-point correction= 0.129980 (Hartree/Particle)
Sum of electronic and zero-point Energies= -309.434945

3 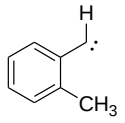

Triplet-*o*-tolylmethylene

Standard orientation:

Center Number	Atomic Number	Atomic Type	Coordinates (Angstroms) X	Y	Z
1	6	0	1.987648	0.374627	-0.000001
2	6	0	1.710976	-0.999978	-0.000003
3	6	0	0.379628	-1.441825	0.000003
4	6	0	-0.690834	-0.552248	0.000003
5	6	0	-0.418966	0.861104	-0.000009
6	6	0	0.947944	1.292352	0.000002
7	6	0	-1.448399	1.798225	0.000014
8	6	0	-2.116405	-1.040108	-0.000002
9	1	0	3.015909	0.725146	-0.000003
10	1	0	2.521935	-1.721963	0.000006
11	1	0	0.173390	-2.509398	0.000004
12	1	0	1.158787	2.357850	0.000008
13	1	0	-1.499022	2.879786	-0.000042
14	1	0	-2.660316	-0.675759	0.879896
15	1	0	-2.159904	-2.132892	-0.000055
16	1	0	-2.660327	-0.675672	-0.879858

Zero-point correction= 0.129434 (Hartree/Particle)
Sum of electronic and zero-point Energies= -309.443432

3 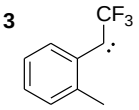

***anti*-Triplet-o-tolyl (trifluoromethyl) carbene**

Standard orientation:

Center Number	Atomic Number	Atomic Type	Coordinates (Angstroms) X	Y	Z
1	6	0	2.072689	-1.828118	-0.000612
2	6	0	0.771670	-1.349708	-0.011124
3	6	0	0.513869	0.058306	-0.011086
4	6	0	1.623783	0.971235	-0.002729
5	6	0	2.913828	0.448834	0.006723
6	6	0	3.150900	-0.932724	0.008275
7	6	0	1.377995	2.457697	-0.003265
8	6	0	-0.793360	0.543722	-0.021013
9	6	0	-2.149597	-0.010463	0.000234
10	9	0	-3.080963	0.961379	-0.151782
11	9	0	-2.438622	-0.656561	1.169430
12	9	0	-2.361302	-0.925282	-0.994255
13	1	0	2.250873	-2.899258	-0.000342
14	1	0	-0.064650	-2.040231	-0.021733
15	1	0	3.756719	1.134911	0.013408
16	1	0	4.170388	-1.306005	0.015764
17	1	0	0.806076	2.765783	-0.886590
18	1	0	2.320448	3.011507	0.001714
19	1	0	0.797470	2.764783	0.874825

Zero-point correction= 0.135045 (Hartree/Particle)

Sum of electronic and zero-point Energies= -646.498718

TD calculations

Excitation energies and oscillator strengths:

```
 Excited State   1:   ?Spin  -A      2.9616 eV  418.64 nm  f=0.0068
     45A -> 46A        0.31562
     45A -> 47A       -0.11905
     43B -> 44B        0.18899
     43B -> 45B        0.94736

 Excited State   2:   ?Spin  -A      3.0735 eV  403.40 nm  f=0.0001
     42B -> 44B       -0.23324
```

```
    43B -> 44B        0.95457
    43B -> 45B       -0.18701

Excited State   3:   ?Spin  -A      3.4088 eV  363.72 nm  f=0.0068
    44A -> 46A       -0.13896
    45A -> 46A        0.13946
    45A -> 47A        0.48168
    42B -> 44B        0.64162
    42B -> 45B        0.60504
    43B -> 44B        0.14709
    43B -> 46B        0.15874

Excited State   4:   ?Spin  -A      3.4245 eV  362.05 nm  f=0.0033
    44A -> 46A        0.10794
    45A -> 46A       -0.11097
    45A -> 47A       -0.35899
    39B -> 44B        0.10931
    42B -> 44B        0.72488
    42B -> 45B       -0.56933
    43B -> 44B        0.18037
    43B -> 46B       -0.12130

Excited State   5:   ?Spin  -A      4.0948 eV  302.78 nm  f=0.0334
    44A -> 46A        0.20762
    44A -> 47A        0.12276
    45A -> 46A        0.88986
    45A -> 47A       -0.12966
    42B -> 46B        0.14102
    43B -> 45B       -0.23503
    43B -> 46B       -0.21183
    43B -> 47B       -0.10989

Excited State   6:   ?Spin  -A      4.3336 eV  286.10 nm  f=0.0200
    44A -> 46A        0.73130
    44A -> 47A       -0.14384
    45A -> 46A       -0.21503
    39B -> 45B       -0.12135
    42B -> 45B        0.28083
    42B -> 46B       -0.11629
    42B -> 47B        0.10040
    43B -> 46B       -0.65083

Excited State   7:   ?Spin  -A      4.8335 eV  256.51 nm  f=0.2563
    45A -> 47A        0.73898
    40B -> 44B        0.10790
    41B -> 44B        0.17436
```

42B -> 45B -0.42791
42B -> 47B -0.12172
43B -> 46B -0.28825

Excited State 8: ?Spin -A 5.1834 eV 239.19 nm f=0.0031
45A -> 48A 0.98941

Excited State 9: ?Spin -A 5.4669 eV 226.79 nm f=0.0003
41B -> 44B 0.23552
41B -> 45B 0.96037

Frequency Calculations:

Frequency (cm^{-1})	Intensity	Frequency (cm^{-1})	Intensity
1613	22	1137	54
1572	1	1109	180
1499	19	1067	293
1485	9	1061	7
1483	12	1004	6
1465	59	986	2
1434	72	927	47
1420	18	806	5
1333	1	757	54
1212	219	705	7
1189	153	664	11
1182	118	616	12

3

***syn*-Triplet-o-tolyl (trifluoromethyl) carbene** 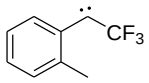

Standard orientation:

Center Number	Atomic Number	Atomic Type	Coordinates (Angstroms) X	Y	Z
1	6	0	2.913674	-1.348644	0.000001
2	6	0	1.544787	-1.555796	-0.000188
3	6	0	0.624966	-0.458311	-0.000193
4	6	0	1.151524	0.884915	-0.000067
5	6	0	2.536445	1.045824	0.000134
6	6	0	3.418804	-0.041384	0.000190
7	6	0	0.247219	2.090197	-0.000191
8	6	0	-0.732449	-0.775540	-0.000337
9	6	0	-2.096263	-0.255764	0.000000
10	9	0	-2.382751	0.516172	-1.092449
11	9	0	-2.382191	0.516213	1.092651
12	9	0	-2.995178	-1.272810	0.000273
13	1	0	3.589022	-2.198735	0.000001
14	1	0	1.141357	-2.563254	-0.000330
15	1	0	2.938698	2.055532	0.000237
16	1	0	4.490519	0.132335	0.000378
17	1	0	-0.403941	2.107143	-0.880595
18	1	0	0.836830	3.010287	-0.000489
19	1	0	-0.403646	2.107529	0.880429

Zero-point correction= 0.135066 (Hartree/Particle)

Sum of electronic and zero-point Energies= -646.495689

TD calculations

Excitation energies and oscillator strengths:

```
Excited State   1:   ?Spin  -A      2.9578 eV  419.18 nm  f=0.0062
    45A -> 46A        0.31784
    45A -> 47A       -0.12302
    43B -> 44B        0.96505
Excited State   2:   ?Spin  -A      3.2204 eV  385.00 nm  f=0.0000
    42B -> 45B       -0.18462
```

```
    43B -> 45B        0.98373
Excited State   3:   ?Spin  -A      3.4225 eV  362.26 nm  f=0.0076
    44A -> 46A       -0.18095
    45A -> 46A        0.21006
    45A -> 47A        0.61204
    42B -> 44B        0.81331
    42B -> 47B        0.10975
    43B -> 46B        0.20156
Excited State   4:   ?Spin  -A      3.5830 eV  346.03 nm  f=0.0004
    39B -> 45B        0.14813
    42B -> 45B        0.97850
    43B -> 45B        0.18405
Excited State   5:   ?Spin  -A      4.0888 eV  303.23 nm  f=0.0352
    44A -> 46A        0.13719
    44A -> 47A        0.13577
    45A -> 46A        0.89988
    45A -> 47A       -0.16384
    42B -> 46B        0.14885
    43B -> 44B       -0.24352
    43B -> 46B       -0.13496
    43B -> 47B        0.10444
Excited State   6:   ?Spin  -A      4.3153 eV  287.32 nm  f=0.0182
    44A -> 46A        0.74370
    44A -> 47A       -0.15009
    45A -> 46A       -0.11908
    39B -> 44B       -0.11843
    42B -> 44B        0.28383
    42B -> 47B       -0.10111
    43B -> 46B       -0.66989
Excited State   7:   ?Spin  -A      4.8248 eV  256.97 nm  f=0.2748
    45A -> 47A        0.72795
    41B -> 45B        0.15344
    42B -> 44B       -0.45638
    42B -> 47B        0.11551
    43B -> 46B       -0.29135
Excited State   8:   ?Spin  -A      5.1404 eV  241.19 nm  f=0.0026
    45A -> 48A        0.98784

Excited State   9:   ?Spin  -A      5.5142 eV  224.85 nm  f=0.0000
    41B -> 44B        0.99454
```

Frequency Calculations:

Frequency (cm^{-1})	Intensity	Frequency (cm^{-1})	Intensity
1616	30	1057	184
1569	1	1009	2
1509	28	931	62
1491	6	804	4
1480	88	758	61
1471	39	701	5
1443	24	645	9
1428	13	620	8
1323	4		
1207	110		
1186	64		
1174	287		
1129	51		
1100	228		
1062	7		
1059	98		

1

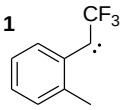

***anti*-Singlet-o-tolyl (trifluoromethyl) carbene**

Standard orientation:

Center Number	Atomic Number	Atomic Type	Coordinates (Angstroms) X	Y	Z
1	6	0	-1.804817	-1.892052	0.001949
2	6	0	-0.565086	-1.282653	0.001561
3	6	0	-0.428272	0.147362	0.021619
4	6	0	-1.633053	0.947233	0.011886
5	6	0	-2.872509	0.299068	-0.011110
6	6	0	-2.960345	-1.092974	-0.010833
7	6	0	-1.582494	2.448668	-0.013368
8	6	0	0.798221	0.846282	0.121594
9	6	0	2.064569	0.055132	-0.001277
10	9	0	3.153468	0.847028	-0.150043
11	9	0	2.125033	-0.823286	-1.058300
12	9	0	2.264366	-0.669278	1.143066
13	1	0	-1.888228	-2.974307	0.006070
14	1	0	0.327827	-1.894962	0.010700
15	1	0	-3.783109	0.891270	-0.020382
16	1	0	-3.939395	-1.565103	-0.018222
17	1	0	-0.689136	2.816266	0.493006
18	1	0	-2.484946	2.875056	0.433944
19	1	0	-1.526109	2.805219	-1.049748

Zero-point correction= 0.135443 (Hartree/Particle)

Sum of electronic and zero-point Energies= -646.492139

TD calculations

Excitation energies and oscillator strengths:

Excited State	1:	Singlet-A	1.0981 eV	1129.10 nm	f=0.0014
44 -> 45		0.58197			
Excited State	2:	Singlet-A	3.3342 eV	371.86 nm	f=0.0413
42 -> 46		0.11881			
43 -> 45		0.65269			
Excited State	3:	Singlet-A	4.1487 eV	298.85 nm	f=0.0024

```
     44 -> 46         0.70139

Excited State   4:   Singlet-A      4.4485 eV  278.71 nm  f=0.2264
     42 -> 45         0.57609
     43 -> 46        -0.11097
     44 -> 47         0.22793

Excited State   5:   Singlet-A      4.7229 eV  262.52 nm  f=0.0502
     41 -> 45         0.18298
     42 -> 45        -0.15298
     44 -> 47         0.63313

Excited State   6:   Singlet-A      4.9900 eV  248.46 nm  f=0.0304
     41 -> 45         0.66397
     42 -> 45         0.11386
     44 -> 47        -0.13744

Excited State   7:   Singlet-A      5.4320 eV  228.25 nm  f=0.0061
     44 -> 48         0.69178

Excited State   8:   Singlet-A      5.4671 eV  226.78 nm  f=0.0021
     40 -> 45         0.68852

Excited State   9:   Singlet-A      5.8174 eV  213.12 nm  f=0.0112
     44 -> 49         0.68979
```

Frequency Calculations:

Frequency (cm^{-1})	Intensity	Frequency (cm^{-1})	Intensity
1641	108	1060	173
1586	19	1050	112
1509	7	1019	6
1495	41	1001	2
1478	36	989	9
1460	16	902	17
1412	8	885	3
1397	14	808	3
1349	31	787	33
1302	4	768	7
1225	21	715	11
1197	6	663	8
1176	639	615	14
1143	42		
1114	180		
1070	17		

1

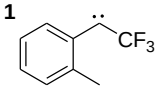

***syn*-Singlet-*o*-tolyl (trifluoromethyl) carbene**

Standard orientation:

Center Number	Atomic Number	Atomic Type	Coordinates (Angstroms) X	Y	Z
1	6	0	2.858249	-1.314766	0.044554
2	6	0	1.521177	-1.536729	-0.251643
3	6	0	0.544875	-0.484918	-0.250403
4	6	0	1.018330	0.877285	-0.081388
5	6	0	2.380230	1.068102	0.147048
6	6	0	3.283728	0.000208	0.242312
7	6	0	0.144874	2.097144	-0.218734
8	6	0	-0.756582	-1.029452	-0.377779
9	6	0	-1.982690	-0.289073	0.047615
10	9	0	-2.371554	0.551990	-0.958010
11	9	0	-1.898644	0.448614	1.205419
12	9	0	-3.021441	-1.133139	0.265981
13	1	0	3.562471	-2.139329	0.085029
14	1	0	1.150140	-2.533930	-0.459377
15	1	0	2.754370	2.081878	0.259659
16	1	0	4.330998	0.208961	0.444327
17	1	0	-0.465117	2.056208	-1.124004
18	1	0	0.762149	2.997829	-0.260309
19	1	0	-0.543406	2.194390	0.624682

Zero-point correction= 0.135764 (Hartree/Particle)

Sum of electronic and zero-point Energies= -646.484011

TD calculations

Excitation energies and oscillator strengths:

Excited State 1: Singlet-A 1.0917 eV 1135.72 nm f=0.0025
44 -> 45 0.57253

Excited State 2: Singlet-A 3.3116 eV 374.39 nm f=0.0335
42 -> 46 0.10539
43 -> 45 0.65752

Excited State 3: Singlet-A 4.1188 eV 301.02 nm f=0.0119
42 -> 45 -0.19419
44 -> 46 0.66244

Excited State 4: Singlet-A 4.4315 eV 279.78 nm f=0.1409
42 -> 45 0.49529
44 -> 46 0.20279
44 -> 47 -0.37053

Excited State 5: Singlet-A 4.6787 eV 265.00 nm f=0.1404
41 -> 45 -0.14075
42 -> 45 0.28269
44 -> 47 0.56622

Excited State 6: Singlet-A 5.1239 eV 241.97 nm f=0.0226
41 -> 45 0.67131

Excited State 7: Singlet-A 5.3795 eV 230.47 nm f=0.0076
44 -> 48 0.68676

Excited State 8: Singlet-A 5.4527 eV 227.38 nm f=0.0070
40 -> 45 0.68479

Excited State 9: Singlet-A 5.7736 eV 214.74 nm f=0.0079
44 -> 49 0.69690

Frequency Calculations:

Frequency (cm^{-1})	Intensity	Frequency (cm^{-1})	Intensity
1632	96	1057	101
1585	7	1050	168
1510	14	1015	11
1492	22	993	1
1488	42	912	23
1462	20	889	1
1424	6	812	4
1402	9	785	43
1330	54	728	3
1292	5	709	12
1214	9	657	5
1191	9	628	9
1173	463		
1129	98		
1108	221		
1073	21		

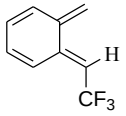

Singlet-2-trifluoromethyl-o-quinomethide

Standard orientation:

Center Number	Atomic Number	Atomic Type	Coordinates (Angstroms) X	Y	Z
1	6	0	2.948351	0.327384	-0.240465
2	6	0	3.035190	-1.021206	-0.162403
3	6	0	1.857386	-1.812996	0.134488
4	6	0	0.631755	-1.244511	0.252232
5	6	0	0.444380	0.188978	0.050343
6	6	0	1.684176	1.023062	-0.008705
7	6	0	1.685058	2.358249	0.220847
8	6	0	-0.779557	0.751146	-0.138425
9	6	0	-2.081198	0.026336	-0.049199
10	9	0	-2.232627	-0.936441	-1.005407
11	9	0	-3.115898	0.891582	-0.202996
12	9	0	-2.275486	-0.607127	1.144243
13	1	0	3.832234	0.934843	-0.413679
14	1	0	3.989615	-1.521488	-0.294682
15	1	0	1.962972	-2.888543	0.242910
16	1	0	-0.238024	-1.862913	0.437239
17	1	0	0.794398	2.900990	0.517082
18	1	0	2.604125	2.930834	0.143061
19	1	0	-0.882470	1.795507	-0.406771

Zero-point correction= 0.136971 (Hartree/Particle)
Sum of electronic and zero-point Energies= -646.552533
TD calculations

Excitation energies and oscillator strengths:

Excited State 1: Singlet-A 2.9868 eV 415.11 nm f=0.1315
43 -> 45 0.10672
44 -> 45 0.59636

Excited State 2: Singlet-A 4.6442 eV 266.97 nm f=0.0225
42 -> 45 0.19520
43 -> 45 0.49668
44 -> 46 -0.43823

```
Excited State   3:   Singlet-A      4.8339 eV  256.49 nm  f=0.0118
     42 -> 45         0.48421
     43 -> 45        -0.24536
     44 -> 46        -0.11624
     44 -> 47        -0.34383
     44 -> 48         0.26237

Excited State   4:   Singlet-A      5.1564 eV  240.45 nm  f=0.0223
     41 -> 45         0.11388
     42 -> 45         0.15320
     43 -> 45         0.32356
     44 -> 46         0.47619
     44 -> 47        -0.21883

Excited State   5:   Singlet-A      5.2776 eV  234.93 nm  f=0.0081
     44 -> 47         0.45716
     44 -> 48         0.51003

Excited State   6:   Singlet-A      5.5436 eV  223.65 nm  f=0.0015
     44 -> 48         0.10322
     44 -> 49         0.68463

Excited State   7:   Singlet-A      5.6879 eV  217.98 nm  f=0.0045
     41 -> 45         0.68416

Excited State   8:   Singlet-A      5.8138 eV  213.26 nm  f=0.0032
     44 -> 50         0.69972

Excited State   9:   Singlet-A      5.9791 eV  207.36 nm  f=0.6724
     42 -> 45         0.33081
     44 -> 47         0.28922
     44 -> 48        -0.34710
     44 -> 49         0.13844
     44 -> 55         0.14571
     44 -> 57        -0.11629
```

Frequency Calculations:

Frequency (cm^{-1})	Intensity	Frequency (cm^{-1})	Intensity
1700	18	969	6
1644	39	929	38
1625	73	899	38
1593	7	849	2
1456	12	837	15
1407	18	794	20
1350	15	786	17
1330	45	716	3
1261	191	675	20
1242	318	657	17
1190	8		
1171	107		
1099	303		
1094	121		
1014	2		
998	2		

Singlet-(trideuteriomethyl)-*o*-tolyl (trifluoromethyl) carbonyl oxide

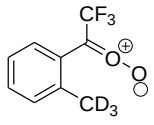

Standard orientation:

Center Number	Atomic Number	Atomic Type	Coordinates (Angstroms) X	Y	Z
1	6	0	2.855089	1.074516	0.683452
2	6	0	3.417845	-0.165846	0.374059
3	6	0	2.622851	-1.179703	-0.162278
4	6	0	1.250175	-1.010495	-0.379534
5	6	0	0.682607	0.248523	-0.043610
6	6	0	1.501714	1.287750	0.453632
7	6	0	-0.745388	0.538442	-0.142177
8	6	0	-1.867452	-0.377618	0.355924
9	9	0	-2.420630	-1.095754	-0.651020
10	9	0	-2.855394	0.331489	0.928299
11	9	0	-1.400703	-1.248735	1.274217
12	8	0	-1.255851	1.635452	-0.565544
13	8	0	-0.484701	2.631345	-1.066558
14	6	0	0.468488	-2.140766	-1.008953
15	1	0	3.467588	1.875979	1.083561
16	1	0	4.478352	-0.339885	0.531115
17	1	0	3.078013	-2.128502	-0.431789
18	1	0	1.061430	2.256055	0.654277
19	1	0	1.153790	-2.850373	-1.478880
20	1	0	-0.220986	-1.786058	-1.779410
21	1	0	-0.118798	-2.693417	-0.268612

Zero-point correction= 0.135276 (Hartree/Particle)
Sum of electronic and zero-point Energies= -796.902090

TD calculations

Excitation energies and oscillator strengths:

Excited State 1: Singlet-A 2.2488 eV 551.33 nm f=0.0006
50 -> 53 -0.11747
51 -> 53 0.51926
52 -> 53 -0.41836

Excited State 2: Singlet-A 3.4575 eV 358.59 nm f=0.0247

```
     50 -> 53         0.65261
     51 -> 53         0.18900

Excited State   3:   Singlet-A      3.5859 eV  345.75 nm  f=0.1808
     49 -> 53        -0.17442
     50 -> 53        -0.15458
     51 -> 53         0.32429
     52 -> 53         0.44455

Excited State   4:   Singlet-A      4.3888 eV  282.50 nm  f=0.0472
     49 -> 53         0.60511
     52 -> 54        -0.18326
     52 -> 55        -0.13178

Excited State   5:   Singlet-A      5.1516 eV  240.67 nm  f=0.0050
     50 -> 55         0.12802
     51 -> 54         0.49045
     51 -> 55         0.14648
     52 -> 54         0.20422
     52 -> 55        -0.40492

Excited State   6:   Singlet-A      5.2359 eV  236.80 nm  f=0.0394
     50 -> 54         0.15773
     50 -> 55         0.14077
     51 -> 54        -0.28392
     51 -> 55        -0.16090
     52 -> 54         0.55760

Excited State   7:   Singlet-A      5.4190 eV  228.79 nm  f=0.0523
     49 -> 54         0.10881
     50 -> 54        -0.20319
     51 -> 54         0.35648
     51 -> 55        -0.14552
     52 -> 54         0.16137
     52 -> 55         0.47133

Excited State   8:   Singlet-A      5.5235 eV  224.47 nm  f=0.0127
     50 -> 54        -0.15482
     50 -> 55        -0.15210
     51 -> 54        -0.10835
     51 -> 55         0.60145
     52 -> 54         0.16502
     52 -> 55         0.10808

Excited State   9:   Singlet-A      5.7944 eV  213.97 nm  f=0.0097
     45 -> 53         0.11371
```

47 -> 53 0.31552
48 -> 53 0.58818

Frequency Calculations:

Frequency (cm^{-1})	Intensity	Frequency (cm^{-1})	Intensity	Frequency (cm^{-1})	Intensity
1622	32	1339	29	1037	28
1582	6	1323	95	1015	145
1505	24	1238	118	964	85
1497	10	1207	82	937	46
1491	14	1172	238	931	4.8
1447	39	1154	31	879	3
1427	2	1142	237	725	21
1399	23	1057	3	600	18

Singlet-(trideuteriomethyl)-*o*-tolyl (trifluoromethyl) dioxirane

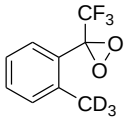

Standard orientation:

Center Number	Atomic Number	Atomic Type	Coordinates (Angstroms) X	Y	Z
1	6	0	-2.566701	-1.634629	0.056207
2	6	0	-3.362700	-0.541811	-0.290085
3	6	0	-2.808122	0.738175	-0.345134
4	6	0	-1.454016	0.968611	-0.064259
5	6	0	-0.664241	-0.147132	0.282178
6	6	0	-1.217271	-1.432392	0.341994
7	6	0	0.794363	-0.006277	0.602416
8	6	0	1.787306	-0.226816	-0.561255
9	9	0	3.057551	-0.021618	-0.195828
10	9	0	1.506853	0.607157	-1.589380
11	9	0	1.679108	-1.495392	-1.017594
12	6	0	-0.897274	2.373515	-0.120491
13	8	0	1.209583	0.953256	1.520314
14	8	0	1.270226	-0.525974	1.806750
15	1	0	-2.989293	-2.633018	0.107518
16	1	0	-4.415988	-0.682748	-0.514336
17	1	0	-3.437610	1.583433	-0.609562
18	1	0	-0.589893	-2.273805	0.620388
19	1	0	-0.536462	2.698766	0.861053
20	1	0	-1.668502	3.076830	-0.444243
21	1	0	-0.060397	2.453500	-0.821549

Zero-point correction= 0.135513 (Hartree/Particle)
Sum of electronic and zero-point Energies= -796.937404

TD calculations

Excitation energies and oscillator strengths:

Excited State 1: Singlet-A 4.1414 eV 299.38 nm f=0.0005
50 -> 53 0.64747
51 -> 53 -0.11855

Excited State 2: Singlet-A 4.4984 eV 275.62 nm f=0.0001
51 -> 53 0.16653

```
     52 -> 53         0.68474

Excited State   3:   Singlet-A      4.7281 eV  262.23 nm  f=0.0002
     50 -> 53         0.12875
     51 -> 53         0.67285
     52 -> 53        -0.15975

Excited State   4:   Singlet-A      5.2030 eV  238.29 nm  f=0.0135
     51 -> 54        -0.15944
     51 -> 55         0.40016
     52 -> 54         0.54544
     52 -> 55         0.15771

Excited State   5:   Singlet-A      5.8674 eV  211.31 nm  f=0.0184
     51 -> 54         0.47056
     52 -> 54         0.18763
     52 -> 55        -0.42781

Excited State   6:   Singlet-A      6.0339 eV  205.48 nm  f=0.0005
     46 -> 53         0.22531
     49 -> 53         0.64269

Excited State   7:   Singlet-A      6.3488 eV  195.29 nm  f=0.0061
     50 -> 54         0.69161

Excited State   8:   Singlet-A      6.4502 eV  192.22 nm  f=0.0032
     52 -> 56         0.70059

Excited State   9:   Singlet-A      6.5649 eV  188.86 nm  f=0.1525
     51 -> 54         0.21660
     51 -> 57         0.16057
     52 -> 55         0.23962
     52 -> 57         0.55187
     52 -> 58         0.11830
```

Frequency Calculations:

Frequency (cm^{-1})	Intensity	Frequency (cm^{-1})	Intensity
1636	7	979	6
1603	2	943	45
1504	16	935	11
1493	10	921	43
1479	6	872	4
1416	76	866	5
1379	18	838	3
1339	6	745	2
1313	52	723	17
1246	29	698	3
1203	247	642	17
1163	115	605	27
1158	116		
1145	51		
1061	4		
1032	3		

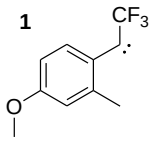

Singlet-CF_3-*anti*-OCH_3-*syn*-p-methoxy-o-tolyl(trifluoromethyl)carbene

Standard orientation:

Center Number	Atomic Number	Atomic Type	Coordinates (Angstroms) X	Y	Z
1	6	0	1.269070	-1.510797	0.000275
2	6	0	-0.032294	-1.084136	-0.000299
3	6	0	-0.388232	0.315940	-0.001238
4	6	0	0.700958	1.271441	-0.001009
5	6	0	2.020292	0.822373	-0.000498
6	6	0	2.311573	-0.550725	0.000063
7	8	0	3.554694	-1.059010	0.000533
8	6	0	0.450051	2.755641	-0.000029
9	6	0	-1.694544	0.833915	-0.002461
10	6	0	-2.821704	-0.148956	-0.000211
11	9	0	-4.039307	0.450453	-0.002657
12	9	0	-2.820503	-0.959400	1.109898
13	9	0	-2.820819	-0.967657	-1.104434
14	6	0	4.686518	-0.180818	-0.000004
15	1	0	1.532813	-2.563100	0.000845
16	1	0	-0.823361	-1.823748	-0.000309
17	1	0	2.822798	1.551118	-0.000392
18	1	0	-0.619205	2.961926	-0.011669
19	1	0	0.920751	3.219493	-0.874908
20	1	0	0.898191	3.213721	0.889766
21	1	0	4.693346	0.446066	-0.897651
22	1	0	5.558695	-0.833584	-0.000193
23	1	0	4.693952	0.446352	0.897445

Zero-point correction= 0.168077 (Hartree/Particle)

Sum of electronic and zero-point Energies = -760.997971

TD calculations

Excitation energies and oscillator strengths:

Excited State 1: Singlet-A 1.2286 eV 1009.12 nm f=0.0011
52 -> 53 0.59974

```
This state for optimization and/or second-order correction.
Copying the excited state density for this state as the 1-particle RhoCI density.

Excited State   2:   Singlet-A      3.7024 eV  334.87 nm  f=0.0457
     50 -> 53         0.55276
     51 -> 53        -0.35287
     52 -> 54        -0.11361

Excited State   3:   Singlet-A      3.9052 eV  317.48 nm  f=0.0023
     52 -> 54         0.69456

Excited State   4:   Singlet-A      4.1881 eV  296.04 nm  f=0.4447
     50 -> 53         0.34637
     50 -> 54         0.10444
     51 -> 53         0.49728

Excited State   5:   Singlet-A      4.7194 eV  262.71 nm  f=0.0115
     52 -> 56         0.68096

Excited State   6:   Singlet-A      4.9323 eV  251.37 nm  f=0.0037
     52 -> 55         0.69565
     52 -> 58        -0.10240

Excited State   7:   Singlet-A      5.2973 eV  234.05 nm  f=0.0022
     47 -> 53        -0.17276
     48 -> 53         0.63602
     49 -> 53         0.22290

Excited State   8:   Singlet-A      5.4529 eV  227.37 nm  f=0.0036
     52 -> 57         0.68826

Excited State   9:   Singlet-A      5.5852 eV  221.99 nm  f=0.0030
     47 -> 53         0.10648
     48 -> 53         0.11763
     49 -> 53        -0.25265
     52 -> 55         0.10258
     52 -> 58         0.59083
     52 -> 62         0.11090
```

Frequency Calculations:

Frequency (cm^{-1})	Intensity	Frequency (cm^{-1})	Intensity
1646	474	1175	860
1560	46	1128	253
1535	53	1104	107
1510	38	1056	132
1502	11	1056	22
1500	25	1044	157
1484	4	1014	33
1474	52	993	22
1463	9	876	17
1415	6	867	37
1405	35	834	10
1366	190	716	5
1341	78	670	4
1272	107		
1212	51		
1205	23		

Singlet-CF_3-*anti*-OCH_3-*anti*-p-methoxy-o-tolyl(trifluoromethyl)carbene 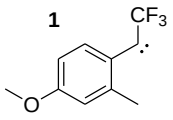

Standard orientation:

Center Number	Atomic Number	Atomic Type	Coordinates (Angstroms) X	Y	Z
1	6	0	1.516530	-1.123074	0.000167
2	6	0	0.159686	-0.882931	0.000163
3	6	0	-0.397442	0.441213	0.000069
4	6	0	0.537945	1.553365	0.000019
5	6	0	1.898417	1.300355	-0.000005
6	6	0	2.397414	-0.017812	0.000052
7	8	0	3.735789	-0.125884	0.000003
8	6	0	0.048076	2.975878	-0.000032
9	6	0	-1.766787	0.757337	0.000063
10	6	0	-2.733907	-0.384410	-0.000041
11	9	0	-4.027222	0.024348	-0.000266
12	9	0	-2.610693	-1.192388	-1.106707
13	9	0	-2.610950	-1.192130	1.106816
14	6	0	4.350121	-1.420870	-0.000165
15	1	0	1.890737	-2.139390	0.000268
16	1	0	-0.514396	-1.730611	0.000272
17	1	0	2.619834	2.111117	-0.000074
18	1	0	-0.582593	3.168146	0.871901
19	1	0	-0.581376	3.168513	-0.872761
20	1	0	0.888617	3.674808	0.000667
21	1	0	5.422799	-1.230840	-0.000426
22	1	0	4.074542	-1.983708	-0.897802
23	1	0	4.074984	-1.983726	0.897598

Zero-point correction= 0.168217 (Hartree/Particle)

Sum of electronic and zero-point Energies= -760.997921

TD Calculations:

Excitation energies and oscillator strengths:

Excited State 1: Singlet-A 1.2242 eV 1012.78 nm f=0.0009

```
     52 -> 53         0.59980
This state for optimization and/or second-order correction.
Copying the excited state density for this state as the 1-particle RhoCI density.

Excited State   2:   Singlet-A      3.6652 eV  338.27 nm  f=0.0409
     50 -> 53         0.56708
     51 -> 53         0.34876

Excited State   3:   Singlet-A      3.8246 eV  324.17 nm  f=0.0000
     52 -> 54         0.70469

Excited State   4:   Singlet-A      4.2074 eV  294.68 nm  f=0.4512
     50 -> 53        -0.32541
     50 -> 54         0.10915
     51 -> 53         0.50944

Excited State   5:   Singlet-A      4.7438 eV  261.36 nm  f=0.0025
     52 -> 56         0.68483

Excited State   6:   Singlet-A      4.9875 eV  248.59 nm  f=0.0103
     52 -> 55         0.69675

Excited State   7:   Singlet-A      5.2473 eV  236.28 nm  f=0.0004
     47 -> 53        -0.11158
     49 -> 53         0.68700

Excited State   8:   Singlet-A      5.3990 eV  229.64 nm  f=0.0020
     52 -> 57         0.67717
     52 -> 58         0.12022

Excited State   9:   Singlet-A      5.6270 eV  220.34 nm  f=0.0223
     48 -> 53        -0.22929
     50 -> 56         0.11067
     51 -> 54        -0.38627
     52 -> 57        -0.15883
     52 -> 58         0.46463
     52 -> 62         0.10988
```

Frequency Calculations:

Frequency (cm^{-1})	Intensity	Frequency (cm^{-1})	Intensity
1647	497	1142	274
1566	75	1106	88
1521	18	1068	60
1507	34	1058	80
1501	73	1043	209
1482	2	1009	19
1472	11	984	18
1470	10	943	11
1420	35	885	29
1415	45	820	17
1358	30	729	2
1345	218	663	8
1270	120		
1226	37		
1194	13		
1173	824		

3

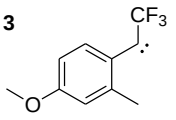

Triplet-CF_3-*anti*-OCH_3-*anti*-p-methoxy-o-tolyl(trifluoromethyl)carbene

Standard orientation:

Center Number	Atomic Number	Atomic Type	Coordinates (Angstroms) X	Y	Z
1	6	0	1.676884	-1.133323	-0.000540
2	6	0	0.298556	-0.969314	-0.001093
3	6	0	-0.299743	0.327135	-0.000996
4	6	0	0.566717	1.478200	-0.000380
5	6	0	1.936524	1.288427	0.000122
6	6	0	2.507180	-0.000866	0.000033
7	8	0	3.866292	-0.038557	0.000550
8	6	0	4.520754	-1.305015	0.000431
9	6	0	-0.028321	2.862300	-0.000054
10	6	0	-1.683349	0.483713	-0.001568
11	6	0	-2.863125	-0.378864	0.000103
12	9	0	-4.007381	0.347976	-0.003568
13	9	0	-2.919037	-1.209919	-1.087575
14	9	0	-2.921375	-1.202418	1.093304
15	1	0	2.089562	-2.134934	-0.000569
16	1	0	-0.339692	-1.846454	-0.001578
17	1	0	2.609112	2.140870	0.000655
18	1	0	5.588487	-1.084890	0.000814
19	1	0	4.267044	-1.882724	-0.896343
20	1	0	4.266502	-1.883173	0.896765
21	1	0	-0.663059	3.018042	0.880307
22	1	0	-0.662349	3.018775	-0.880791
23	1	0	0.751733	3.627836	0.000553

Zero-point correction= 0.167585 (Hartree/Particle)

Sum of electronic and zero-point Energies = -760.997446

TD Calculations:

Excitation energies and oscillator strengths:

Excited State 1: ?Spin -A 2.8895 eV 429.08 nm f=0.0004

```
    49B -> 52B        0.19207
    50B -> 52B        0.48552
    51B -> 52B        0.86384
This state for optimization and/or second-order correction.
Copying the excited state density for this state as the 1-particle RhoCI density.

Excited State   2:   ?Spin  -A      3.1120 eV  398.40 nm  f=0.0077
    53A -> 54A       -0.62489
    53A -> 55A       -0.22241
    50B -> 53B       -0.27888
    51B -> 53B        0.74410

Excited State   3:   ?Spin  -A      3.2723 eV  378.89 nm  f=0.0001
    50B -> 52B        0.86797
    51B -> 52B       -0.49158

Excited State   4:   ?Spin  -A      3.3058 eV  375.05 nm  f=0.0299
    53A -> 54A        0.26331
    53A -> 55A       -0.53246
    50B -> 53B        0.76275
    51B -> 53B        0.35714

Excited State   5:   ?Spin  -A      3.6677 eV  338.04 nm  f=0.0422
    52A -> 55A       -0.13530
    53A -> 54A        0.71258
    50B -> 53B       -0.46779
    50B -> 54B       -0.11839
    51B -> 53B        0.40797
    51B -> 54B       -0.15807

Excited State   6:   ?Spin  -A      4.0771 eV  304.10 nm  f=0.0739
    50A -> 54A        0.10975
    52A -> 54A        0.75058
    53A -> 55A        0.30053
    49B -> 53B       -0.16562
    50B -> 53B        0.20507
    50B -> 54B        0.45686
    50B -> 57B        0.10925
    51B -> 53B        0.20741
    51B -> 54B       -0.40121

Excited State   7:   ?Spin  -A      4.6291 eV  267.83 nm  f=0.0024
    53A -> 56A        0.97928
    53A -> 57A        0.10155
    53A -> 58A        0.11801
```

Excited State 8: ?Spin -A 4.6424 eV 267.07 nm f=0.2845
52A -> 54A -0.20994
53A -> 55A 0.71868
50B -> 53B 0.22162
50B -> 54B -0.28029
51B -> 53B 0.26849
51B -> 54B 0.35471

Excited State 9: ?Spin -A 4.9762 eV 249.15 nm f=0.0015
53A -> 56A -0.10671
53A -> 57A 0.97555

Frequency Calculations:

Frequency (cm^{-1})	Intensity	Frequency (cm^{-1})	Intensity
1631	256	1139	191
1556	30	1102	134
1511	28	1073	66
1506	72	1057	55
1498	9	1053	243
1484	10	1009	5
1480	35	951	28
1468	82	895	28
1446	30	886	22
1420	5	799	28
1333	135	768	4
1308	48	722	11
1260	73	665	11
1217	169		
1194	411		
1185	131		

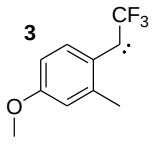

Triplet-CF_3-*anti*-OCH_3-*syn*-p-methoxy-o-tolyl(trifluoromethyl)carbene

Standard orientation:

Center Number	Atomic Number	Atomic Type	Coordinates (Angstroms) X	Y	Z
1	6	0	-1.446727	-1.534329	-0.007162
2	6	0	-0.112727	-1.188190	-0.013774
3	6	0	0.297252	0.186243	-0.012589
4	6	0	-0.719323	1.198198	-0.005742
5	6	0	-2.060667	0.822456	0.000017
6	6	0	-2.436358	-0.531546	-0.000588
7	8	0	-3.722247	-0.973440	0.004591
8	6	0	-0.327401	2.653210	-0.003742
9	6	0	1.645041	0.535420	-0.020960
10	6	0	2.934249	-0.152939	0.002101
11	9	0	3.962828	0.718807	-0.142186
12	9	0	3.059136	-1.083073	-0.995911
13	9	0	3.157559	-0.834658	1.168327
14	6	0	-4.782671	-0.021175	0.010513
15	1	0	-1.756766	-2.574061	-0.007831
16	1	0	0.643727	-1.965304	-0.021563
17	1	0	-2.814912	1.601112	0.005455
18	1	0	0.282338	2.896123	0.874572
19	1	0	-1.207345	3.301922	0.001960
20	1	0	0.274616	2.900978	-0.885981
21	1	0	-5.703009	-0.605540	0.012823
22	1	0	-4.753582	0.611062	-0.884910
23	1	0	-4.746817	0.607452	0.908231

Zero-point correction= 0.167599 (Hartree/Particle)

Sum of electronic and zero-point Energies= -760.997138

TD Calculations:

Excitation energies and oscillator strengths:

```
Excited State   1:   ?Spin  -A      2.8266 eV  438.63 nm  f=0.0004
    49B -> 52B        0.18822
    50B -> 52B        0.23471
    51B -> 52B        0.96378
This state for optimization and/or second-order correction.
Copying the excited state density for this state as the 1-particle RhoCI density.

Excited State   2:   ?Spin  -A      3.1022 eV  399.67 nm  f=0.0201
    53A -> 54A        0.39529
    53A -> 55A       -0.38366
    50B -> 53B       -0.22986
    51B -> 53B        0.84759

Excited State   3:   ?Spin  -A      3.2795 eV  378.05 nm  f=0.0186
    53A -> 54A       -0.50722
    53A -> 55A       -0.42331
    50B -> 52B       -0.10631
    50B -> 53B        0.74374
    51B -> 53B        0.26189

Excited State   4:   ?Spin  -A      3.3772 eV  367.13 nm  f=0.0001
    50B -> 52B        0.96155
    51B -> 52B       -0.24406

Excited State   5:   ?Spin  -A      3.7353 eV  331.92 nm  f=0.0408
    52A -> 55A        0.12508
    53A -> 54A        0.73579
    53A -> 55A       -0.11340
    50B -> 53B        0.52215
    51B -> 53B       -0.23171
    51B -> 54B       -0.22781

Excited State   6:   ?Spin  -A      4.1675 eV  297.50 nm  f=0.1204
    52A -> 54A        0.71208
    53A -> 55A       -0.40176
    49B -> 53B        0.18218
    50B -> 53B       -0.24607
    50B -> 54B        0.44401
    51B -> 53B       -0.22289
    51B -> 54B       -0.29519
    51B -> 56B        0.14386

Excited State   7:   ?Spin  -A      4.5634 eV  271.69 nm  f=0.0033
    53A -> 56A        0.98111
    53A -> 58A       -0.12668
```

Excited State 8: ?Spin -A 4.6507 eV 266.59 nm f=0.2598
52A -> 54A 0.30970
53A -> 55A 0.66513
50B -> 53B 0.16382
50B -> 54B 0.37319
51B -> 53B 0.26863
51B -> 54B -0.35659

Excited State 9: ?Spin -A 5.0551 eV 245.26 nm f=0.0005
53A -> 56A 0.12583
53A -> 58A 0.97516
53A -> 62A -0.10548

Frequency Calculations:

Frequency (cm^{-1})	Intensity	Frequency (cm^{-1})	Intensity
1629	258	1130	158
1555	15	1100	188
1509	56	1065	25
1508	47	1056	276
1499	9	1051	22
1494	27	1014	15
1483	18	960	3
1482	9	958	18
1469	77	904	49
1434	8	862	25
1341	204	817	24
1317	3	767	2
1260	53	710	5
1210	65	670	8
1199	426		
1188	272		

Triplet-CF_3-*syn*-OCH_3-*anti*-p-methoxy-o-tolyl(trifluoromethyl)carbene 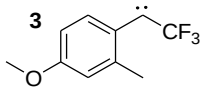

Standard orientation:

Center Number	Atomic Number	Atomic Type	Coordinates (Angstroms) X	Y	Z
1	6	0	2.148097	-1.211595	-0.008240
2	6	0	0.784815	-1.463231	-0.016133
3	6	0	-0.186004	-0.415604	-0.015623
4	6	0	0.293694	0.949123	-0.008309
5	6	0	1.660884	1.171029	0.000152
6	6	0	2.596741	0.118593	0.000495
7	8	0	3.902860	0.496007	0.009322
8	6	0	-0.658989	2.116624	-0.009993
9	6	0	-1.527756	-0.786754	-0.026166
10	6	0	4.911046	-0.512038	0.010580
11	6	0	-2.907566	-0.323582	0.003058
12	9	0	-3.249440	0.453393	-1.072897
13	9	0	-3.767102	-1.376076	0.003184
14	9	0	-3.211448	0.424028	1.110764
15	1	0	2.842316	-2.042991	-0.008486
16	1	0	0.431815	-2.489352	-0.022456
17	1	0	2.044810	2.186747	0.006240
18	1	0	-1.308654	2.103093	-0.891439
19	1	0	-0.109761	3.061128	-0.009056
20	1	0	-1.311984	2.103537	0.868997
21	1	0	5.861526	0.021703	0.018367
22	1	0	4.839471	-1.143655	0.903968
23	1	0	4.849708	-1.135739	-0.889109

Zero-point correction= 0.167620 (Hartree/Particle)

Sum of electronic and zero-point Energies= -760.994364

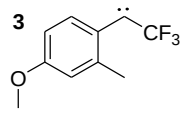

Triplet-CF_3-*syn*-OCH_3-*syn*-p-methoxy-o-tolyl(trifluoromethyl)carbene

Standard orientation:

Center Number	Atomic Number	Atomic Type	Coordinates (Angstroms) X	Y	Z
1	6	0	1.971258	-1.672275	-0.000032
2	6	0	0.596828	-1.747428	-0.000039
3	6	0	-0.228247	-0.573779	-0.000045
4	6	0	0.427019	0.708326	-0.000057
5	6	0	1.821719	0.754811	-0.000051
6	6	0	2.601267	-0.412251	-0.000034
7	8	0	3.960621	-0.431268	-0.000037
8	6	0	-0.359218	1.994273	-0.000087
9	6	0	-1.607198	-0.763292	-0.000054
10	6	0	4.672042	0.803954	0.000144
11	6	0	-2.912534	-0.119048	0.000028
12	9	0	-3.129643	0.680644	1.092170
13	9	0	-3.129775	0.680658	-1.092085
14	9	0	-3.906407	-1.044970	0.000080
15	1	0	2.585530	-2.566396	-0.000021
16	1	0	0.109319	-2.716831	-0.000036
17	1	0	2.297924	1.728645	-0.000070
18	1	0	-1.006526	2.069961	-0.880167
19	1	0	0.311513	2.857178	-0.000131
20	1	0	-1.006485	2.070023	0.880019
21	1	0	5.728525	0.534982	0.000264
22	1	0	4.444899	1.392865	0.896744
23	1	0	4.445141	1.392988	-0.896438

Zero-point correction= 0.167576 (Hartree/Particle)

Sum of electronic and zero-point Energies= -760.994284

Singlet-CF_3-*syn*-OCH_3-*anti*-p-methoxy-o-tolyl(trifluoromethyl)carbene 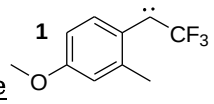

Standard orientation:

Center Number	Atomic Number	Atomic Type	Coordinates (Angstroms) X	Y	Z
1	6	0	2.130339	-1.229985	-0.000157
2	6	0	0.776898	-1.500646	-0.000086
3	6	0	-0.253852	-0.497575	-0.000147
4	6	0	0.197066	0.894891	-0.000074
5	6	0	1.556670	1.148846	-0.000028
6	6	0	2.524879	0.119803	-0.000159
7	8	0	3.800851	0.537681	0.000035
8	6	0	-0.724222	2.085889	0.000031
9	6	0	-1.529292	-1.095666	-0.000013
10	6	0	4.862338	-0.425424	0.000119
11	6	0	-2.807161	-0.330853	-0.000044
12	9	0	-2.974455	0.458343	-1.112634
13	9	0	-3.889200	-1.155937	-0.000486
14	9	0	-2.974324	0.457254	1.113398
15	1	0	2.853034	-2.036276	-0.000123
16	1	0	0.425832	-2.526457	-0.000012
17	1	0	1.925043	2.169947	0.000088
18	1	0	-1.375259	2.085573	-0.876831
19	1	0	-0.144026	3.011395	0.000305
20	1	0	-1.375510	2.085211	0.876717
21	1	0	5.782188	0.158150	0.000243
22	1	0	4.820767	-1.050840	0.897686
23	1	0	4.820956	-1.050760	-0.897511

Zero-point correction= 0.168652 (Hartree/Particle)

Sum of electronic and zero-point Energies= -760.989854

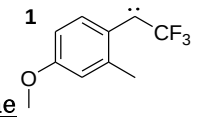

Singlet-CF_3-*syn*-OCH_3-*syn*-p-methoxy-o-tolyl(trifluoromethyl)carbene

Standard orientation:

Center Number	Atomic Number	Atomic Type	Coordinates (Angstroms) X	Y	Z
1	6	0	-1.954918	1.696801	-0.000201
2	6	0	-0.584652	1.787783	-0.000377
3	6	0	0.301610	0.648293	-0.000330
4	6	0	-0.334977	-0.663879	-0.000263
5	6	0	-1.723477	-0.738289	-0.000017
6	6	0	-2.536929	0.414601	0.000049
7	8	0	-3.879301	0.382066	0.000228
8	6	0	0.414306	-1.969813	-0.000462
9	6	0	1.649215	1.056625	-0.000123
10	6	0	-4.572078	-0.872209	0.000301
11	6	0	2.809319	0.124176	0.000121
12	9	0	2.867424	-0.680616	1.113775
13	9	0	2.868004	-0.680930	-1.113266
14	9	0	3.994721	0.791809	0.000285
15	1	0	-2.596851	2.570717	-0.000215
16	1	0	-0.096850	2.755900	-0.000497
17	1	0	-2.187199	-1.717530	0.000092
18	1	0	1.060331	-2.057238	-0.876525
19	1	0	-0.284841	-2.809350	-0.000766
20	1	0	1.060048	-2.057657	0.875781
21	1	0	-5.630909	-0.615870	0.000331
22	1	0	-4.332556	-1.451159	0.898075
23	1	0	-4.332626	-1.451237	-0.897441

Zero-point correction = 0.168547 (Hartree/Particle)

Sum of electronic and zero-point Energies = -760.989214

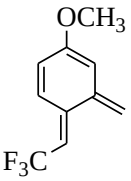

Singlet-p-methoxy-o-tolyl(trifluoromethyl)quinomethide

Standard orientation:

Center Number	Atomic Number	Atomic Type	Coordinates (Angstroms) X	Y	Z
1	6	0	-1.305576	-1.416103	0.314258
2	6	0	-0.012006	-1.028189	0.362398
3	6	0	0.370101	0.358222	0.103926
4	6	0	-0.738918	1.361543	0.073228
5	6	0	-2.100749	0.860378	-0.084994
6	6	0	-2.370060	-0.465453	0.039558
7	6	0	-0.517230	2.688029	0.244864
8	6	0	1.651516	0.723739	-0.161066
9	6	0	2.836548	-0.182155	-0.104931
10	9	0	3.978283	0.519388	-0.320953
11	9	0	2.806023	-1.174467	-1.042085
12	9	0	2.987497	-0.814244	1.095403
13	8	0	-3.596060	-1.051008	-0.040625
14	6	0	-4.719788	-0.217232	-0.305286
15	1	0	-1.588988	-2.453842	0.458342
16	1	0	0.764107	-1.763693	0.535148
17	1	0	-2.886974	1.592131	-0.227006
18	1	0	-1.337630	3.397051	0.195550
19	1	0	0.464001	3.091466	0.465652
20	1	0	1.893325	1.733448	-0.469282
21	1	0	-5.582632	-0.882241	-0.346685
22	1	0	-4.860152	0.519431	0.495293
23	1	0	-4.605832	0.301555	-1.265028

Zero-point correction= 0.169501 (Hartree/Particle)

Sum of electronic and zero-point Energies= -761.052122

TD Calculations:

Excitation energies and oscillator strengths:

Excited State 1: Singlet-A 2.8536 eV 434.48 nm f=0.0886

```
     52 -> 53         0.60549
This state for optimization and/or second-order correction.
Copying the excited state density for this state as the 1-particle RhoCI density.

Excited State   2:   Singlet-A      4.4825 eV  276.60 nm  f=0.1453
     51 -> 53         0.60691
     52 -> 54         0.12954
     52 -> 56         0.24877

Excited State   3:   Singlet-A      4.6749 eV  265.21 nm  f=0.0077
     50 -> 53         0.44419
     52 -> 54         0.50894
     52 -> 56        -0.16166

Excited State   4:   Singlet-A      4.9588 eV  250.03 nm  f=0.0040
     52 -> 55         0.67275
     52 -> 57         0.11308

Excited State   5:   Singlet-A      5.0622 eV  244.92 nm  f=0.0298
     50 -> 53         0.43984
     52 -> 54        -0.41445
     52 -> 55         0.13968
     52 -> 56        -0.14087

Excited State   6:   Singlet-A      5.4091 eV  229.21 nm  f=0.0039
     52 -> 55        -0.10550
     52 -> 57         0.68018

Excited State   7:   Singlet-A      5.4897 eV  225.85 nm  f=0.0045
     52 -> 56         0.15181
     52 -> 58         0.67547

Excited State   8:   Singlet-A      5.6093 eV  221.03 nm  f=0.4431
     48 -> 53        -0.21801
     50 -> 53         0.14664
     51 -> 53        -0.16515
     51 -> 54        -0.12225
     52 -> 56         0.51280
     52 -> 58        -0.12213
     52 -> 59        -0.11923
     52 -> 60         0.12261

Excited State   9:   Singlet-A      5.8398 eV  212.31 nm  f=0.0531
     48 -> 53        -0.10031
     52 -> 59         0.67071
```

Frequency Calculations:

Frequency (cm^{-1})	Intensity	Frequency (cm^{-1})	Intensity
1704	50	1100	304
1651	120	1092	99
1623	81	1055	34
1616	47	955	19
1508	15	901	48
1495	10	866	47
1486	13	840	16
1468	23	826	16
1451	22	814	3
1374	144	716	9
1325	5	679	24
1267	104	656	6
1252	544		
1234	85		
1205	14		
1161	183		

Appendix B: NMR Specta of substrates

(See next page)

1-Bromo-4-methoxy-2-methylbenzene-1H

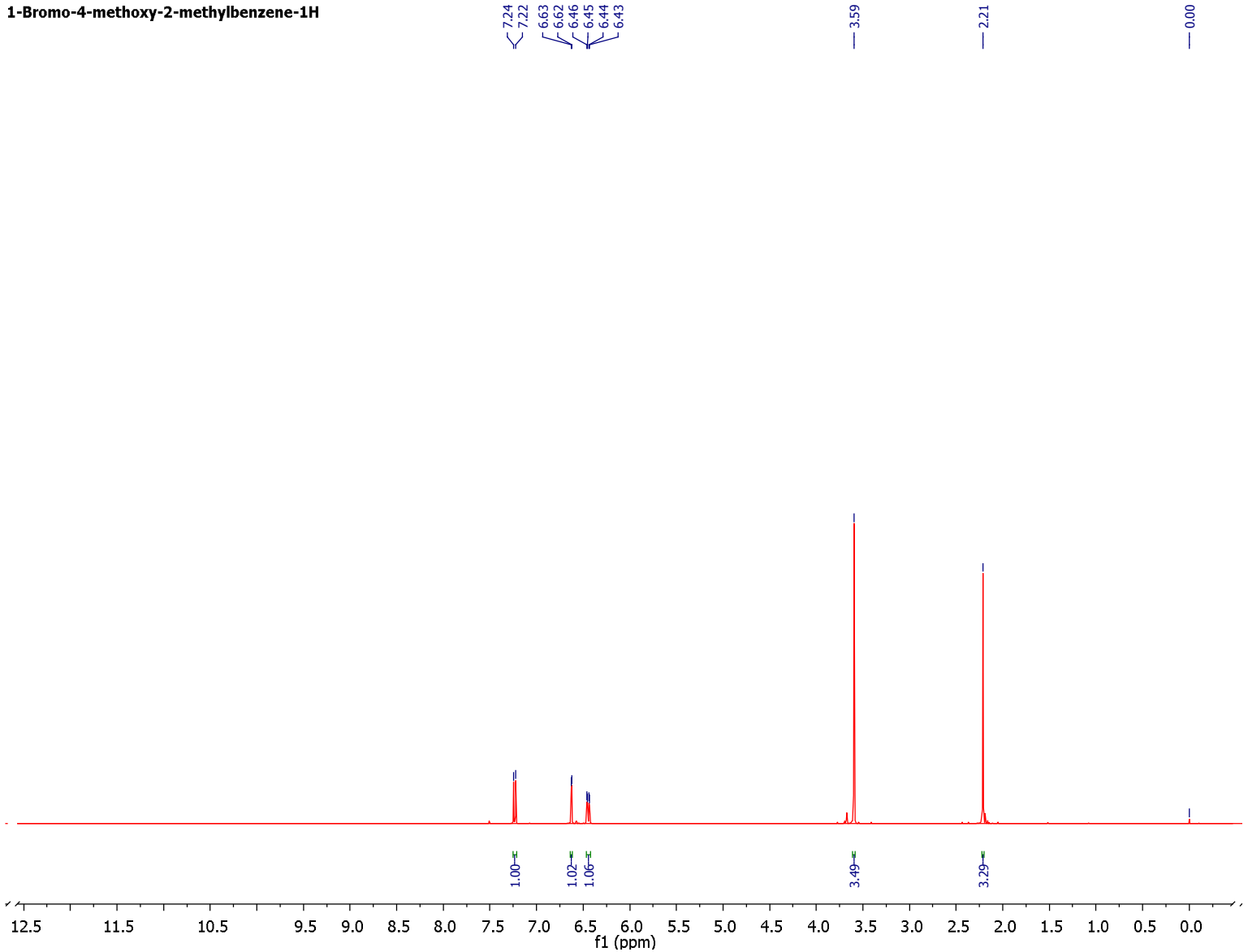

2, 2, 2-Trifluoro-1-(4-methoxy-2-methyl-phenyl)-ethanone-1H

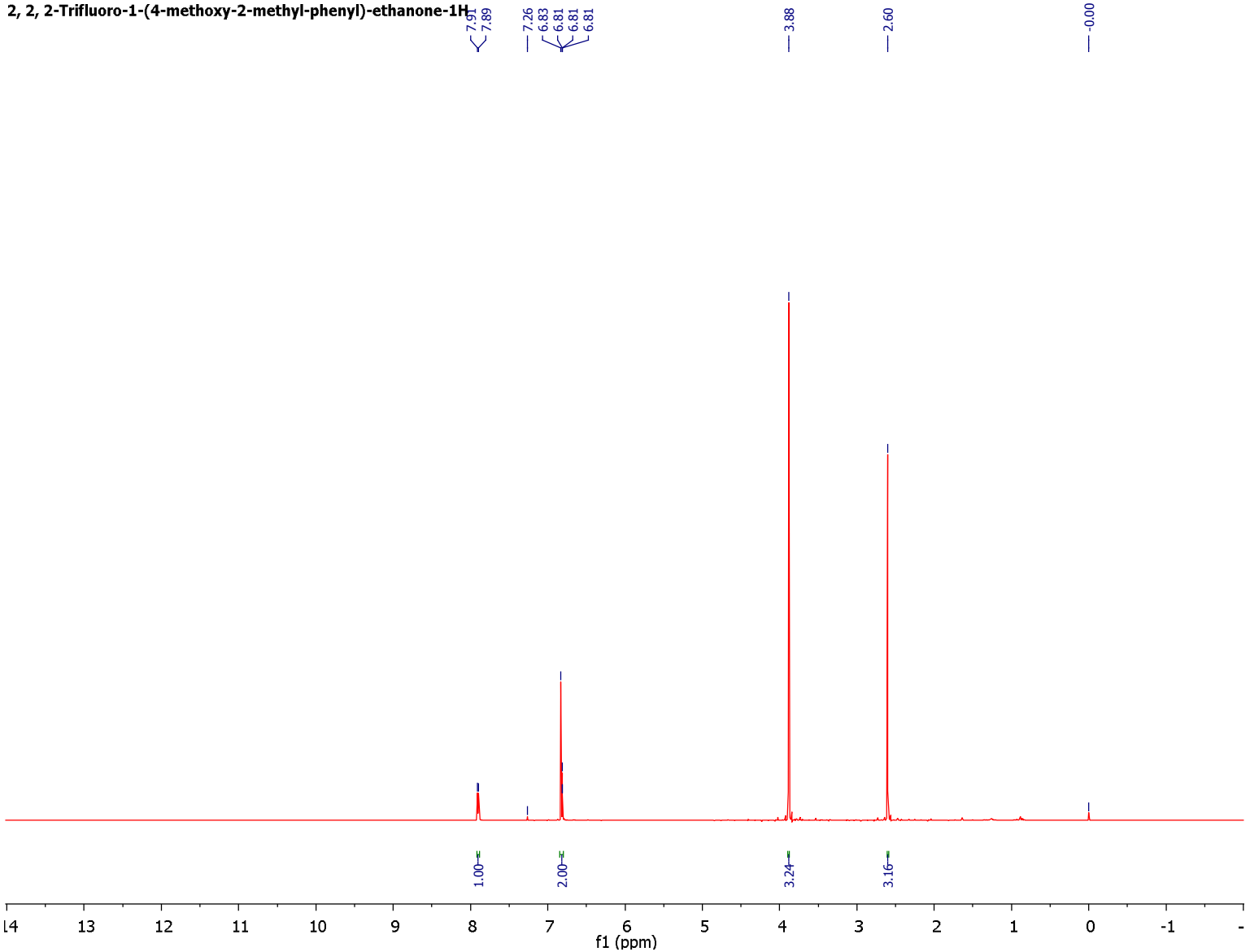

2, 2, 2-Trifluoro-1-(4-methoxy-2-methyl-phenyl)-ethanone-19F

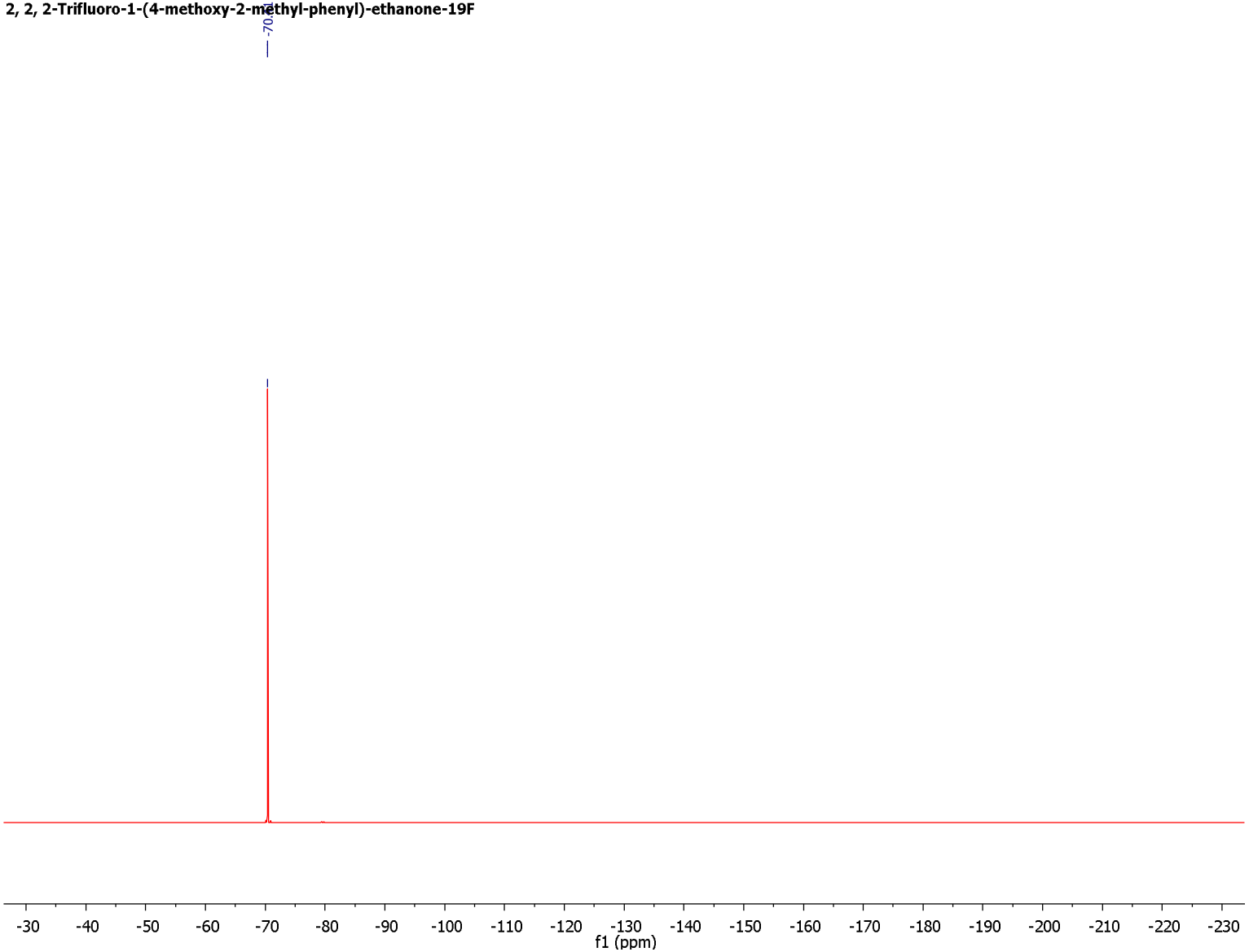

2, 2, 2-Trifluoro-1-(4-methoxy-2-methyl-phenyl)-ethanone-13C

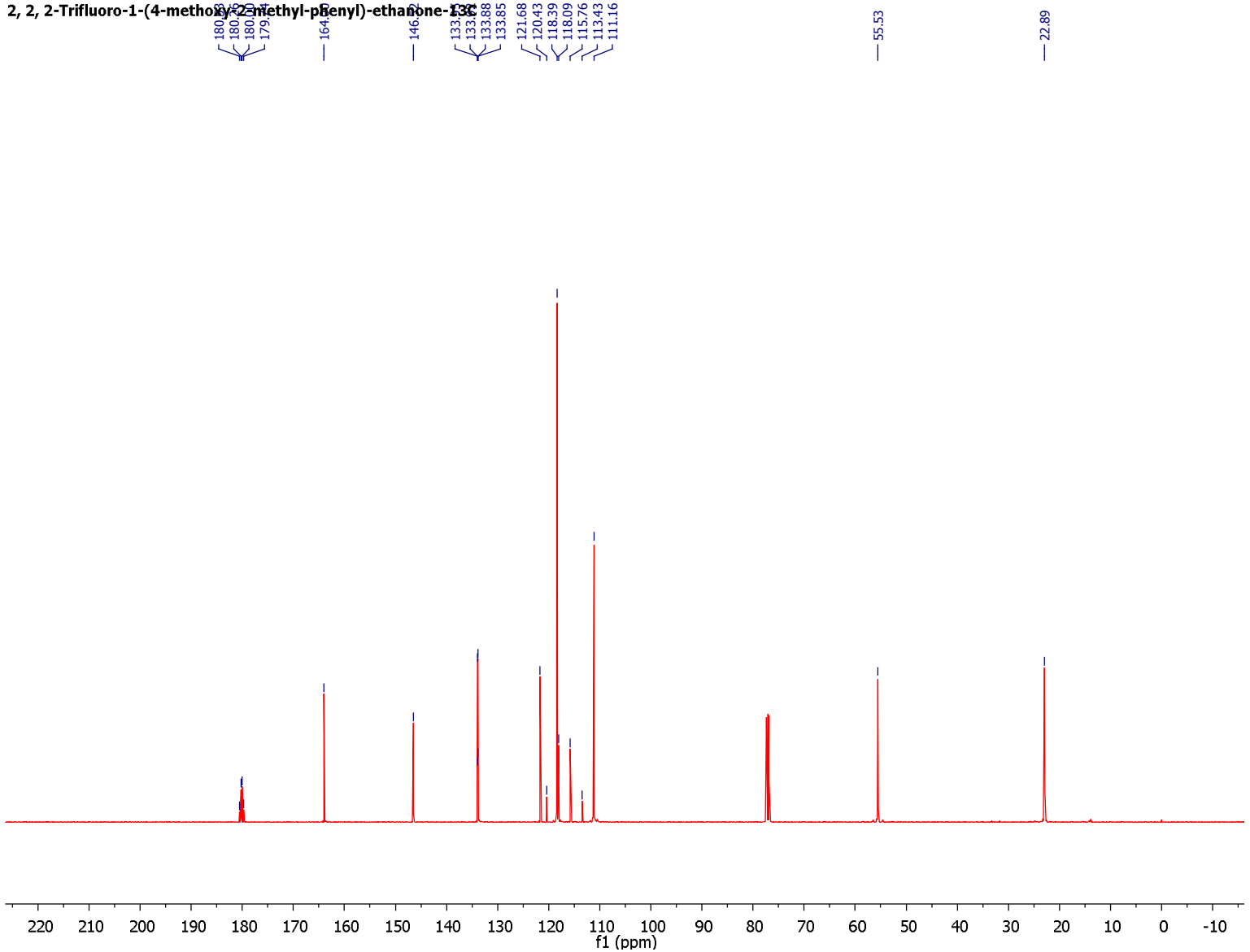

2, 2, 2-Trifluoro-1-(4-methoxy-2-methyl-phenyl)-ethanone oxime-1H

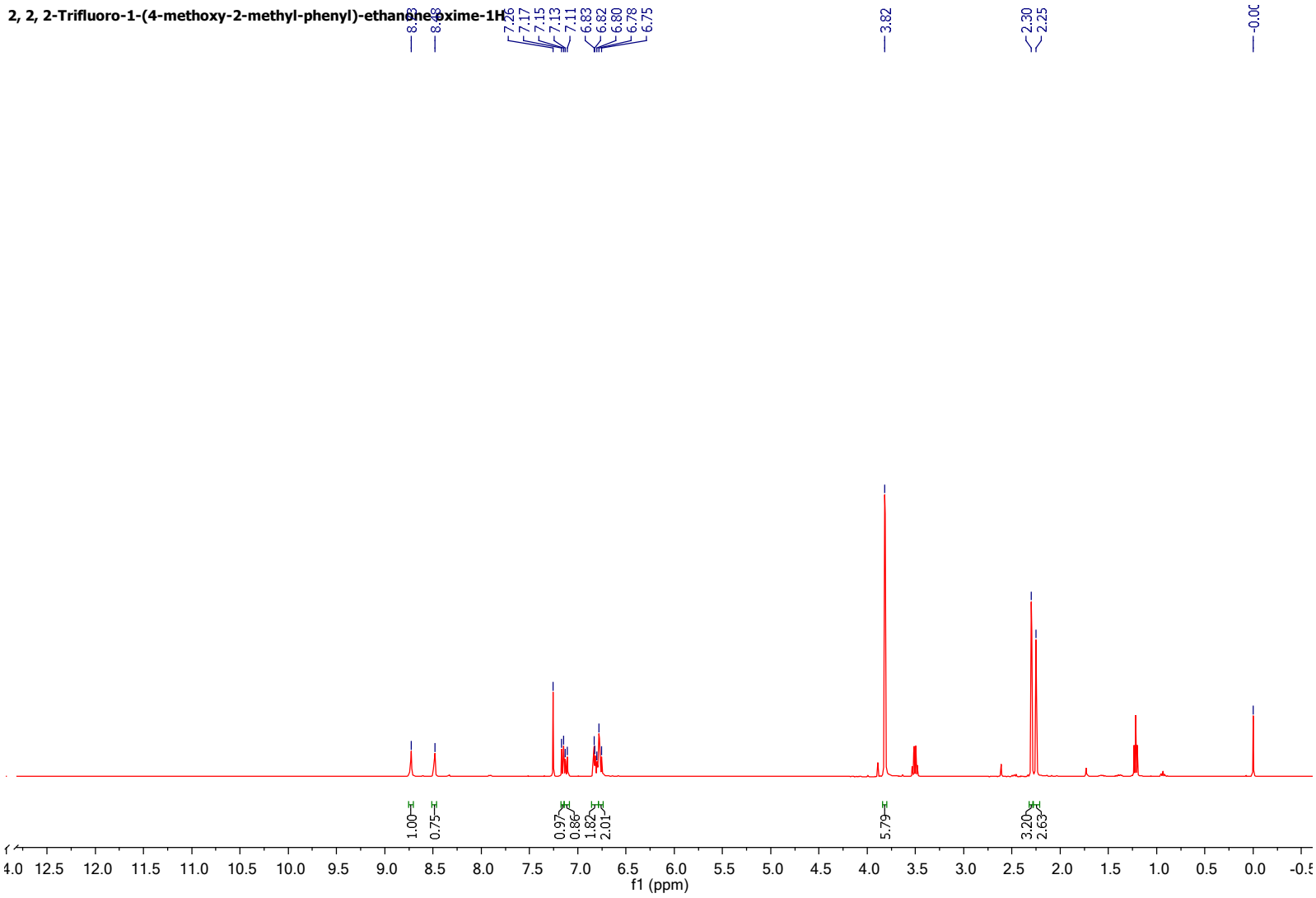

2, 2, 2-Trifluoro-1-(4-methoxy-2-methyl-phenyl)-ethanone methanesulfonic oxime-1H

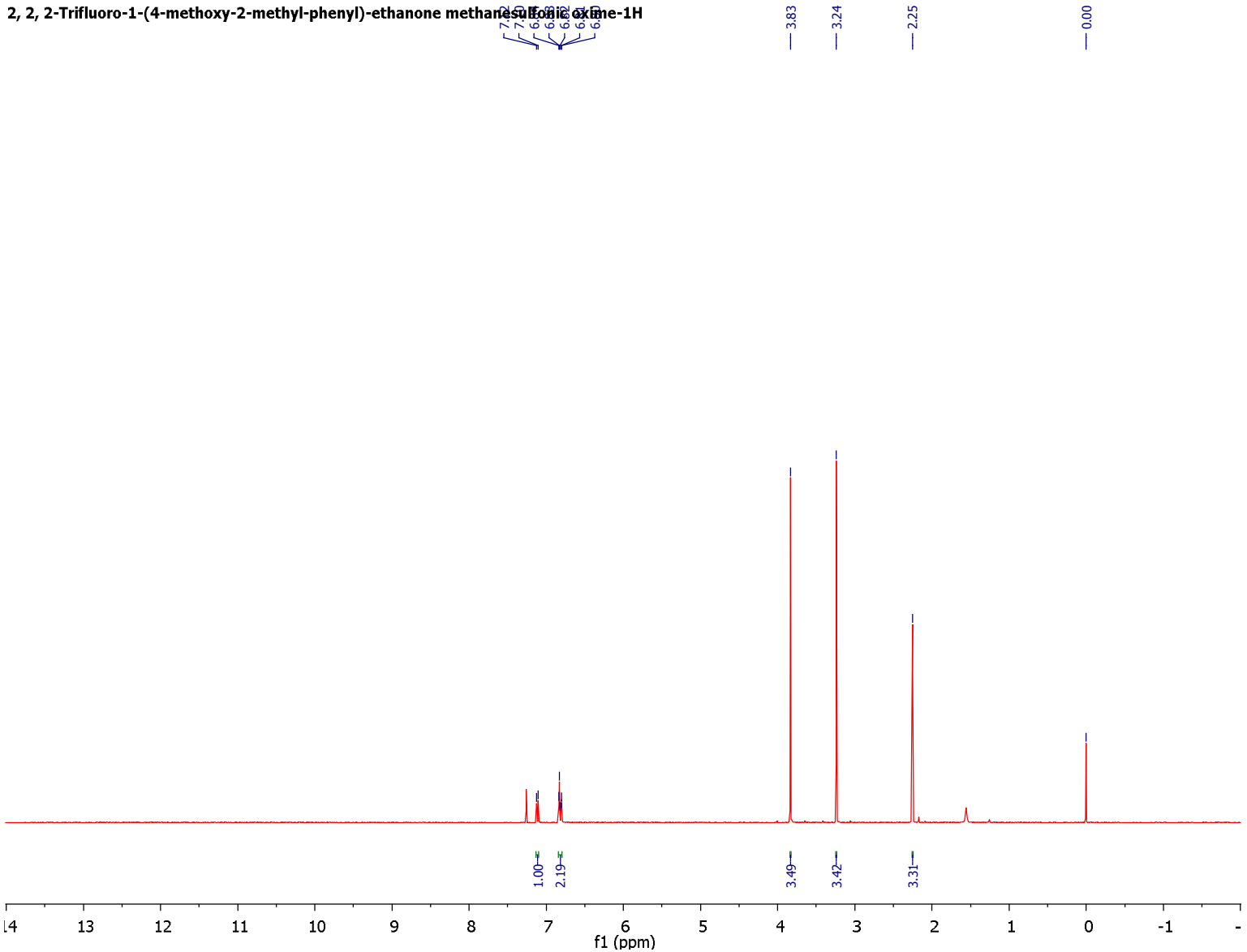

2, 2, 2-Trifluoro-1-(4-methoxy-2-methyl-phenyl)-ethanone methanesulfonic oxime-19F

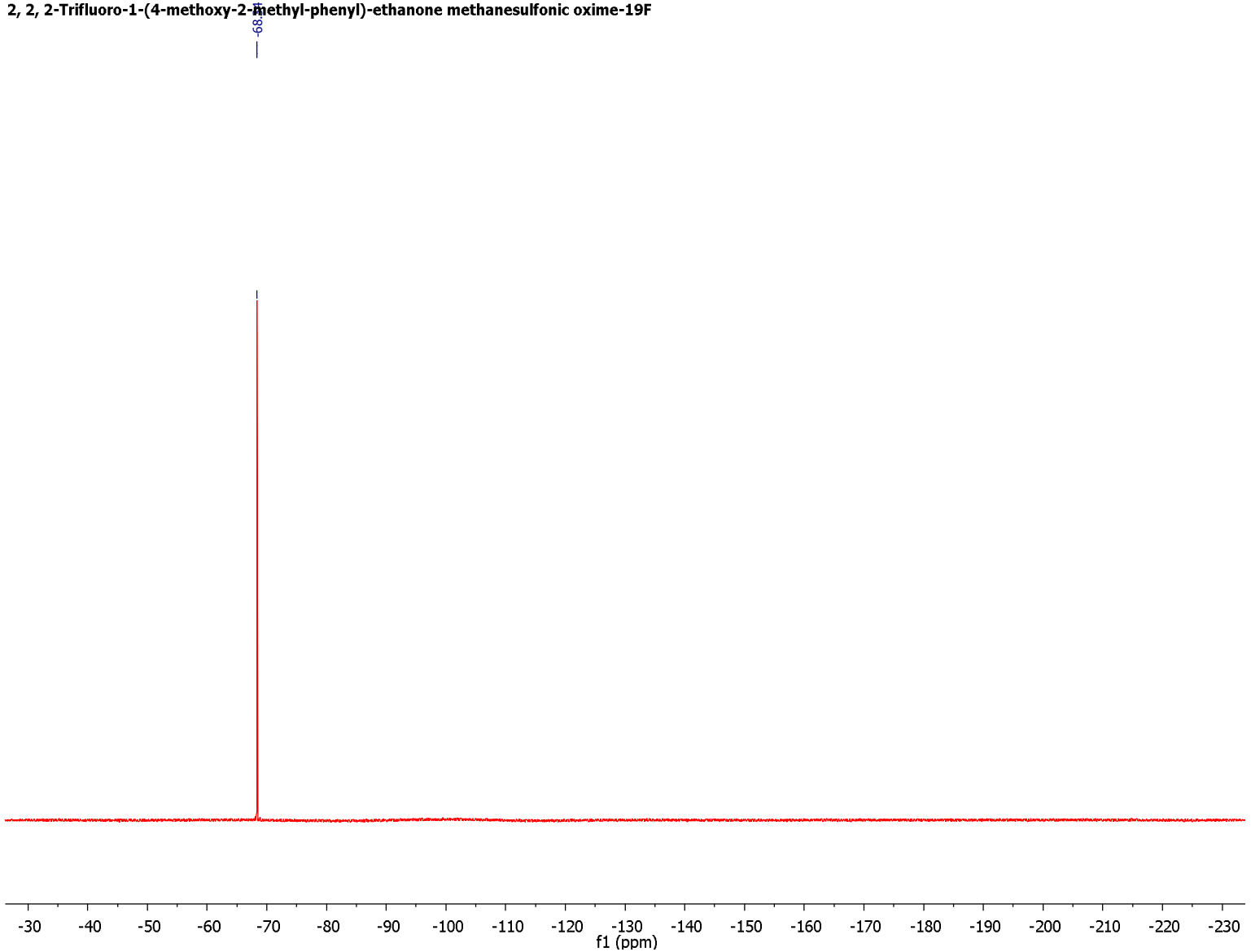

3-(4-Methoxy-2-methyl-phenyl)-3-trifluoromethyl-diaziridine-1H

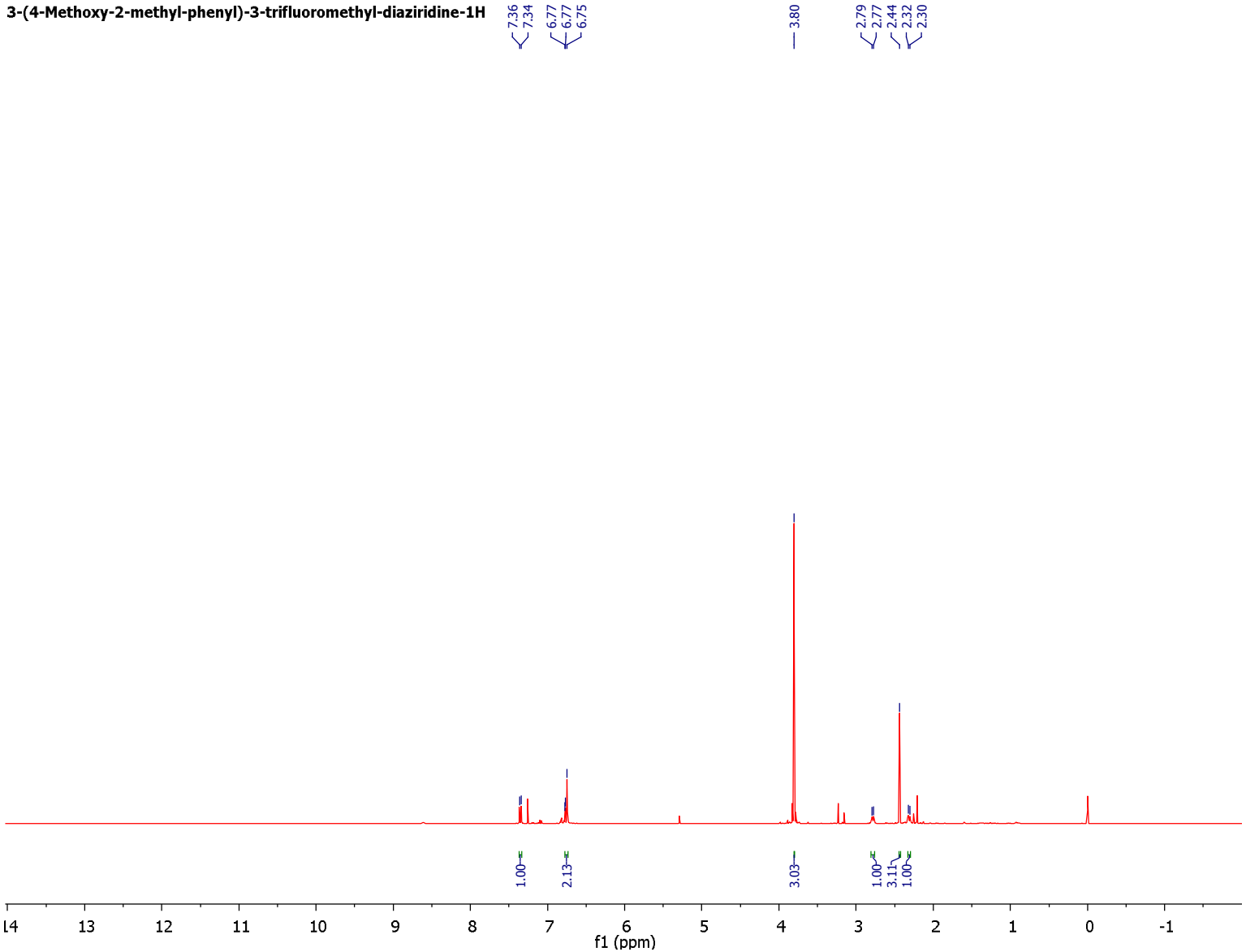

3-(4-Methoxy-2-methyl-phenyl)-3-trifluoromethyl-diaziridine-coexist with oxime-19F

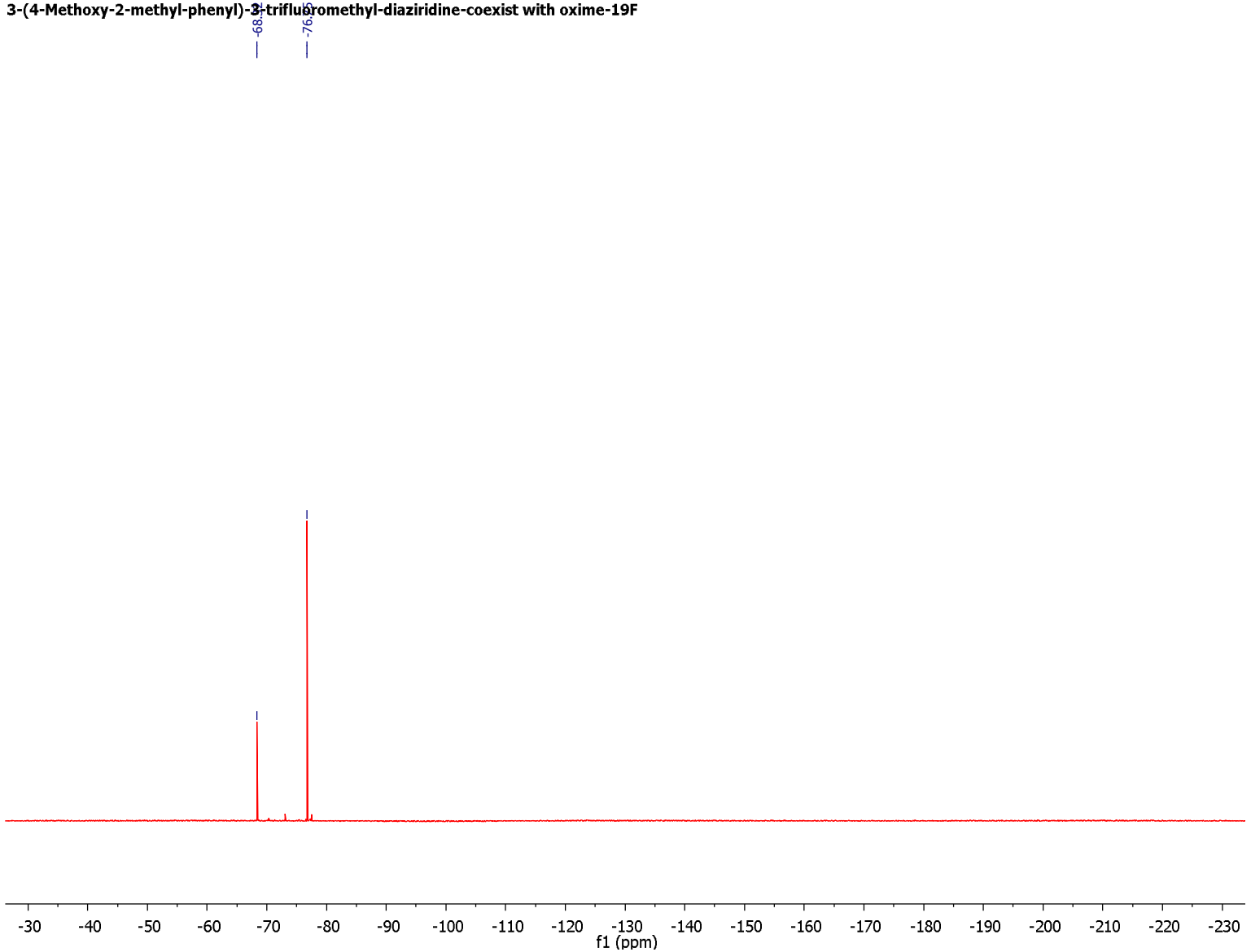

3-(4-Methoxy-2-methyl-phenyl)-3-trifluoromethyl-diazirine-1H

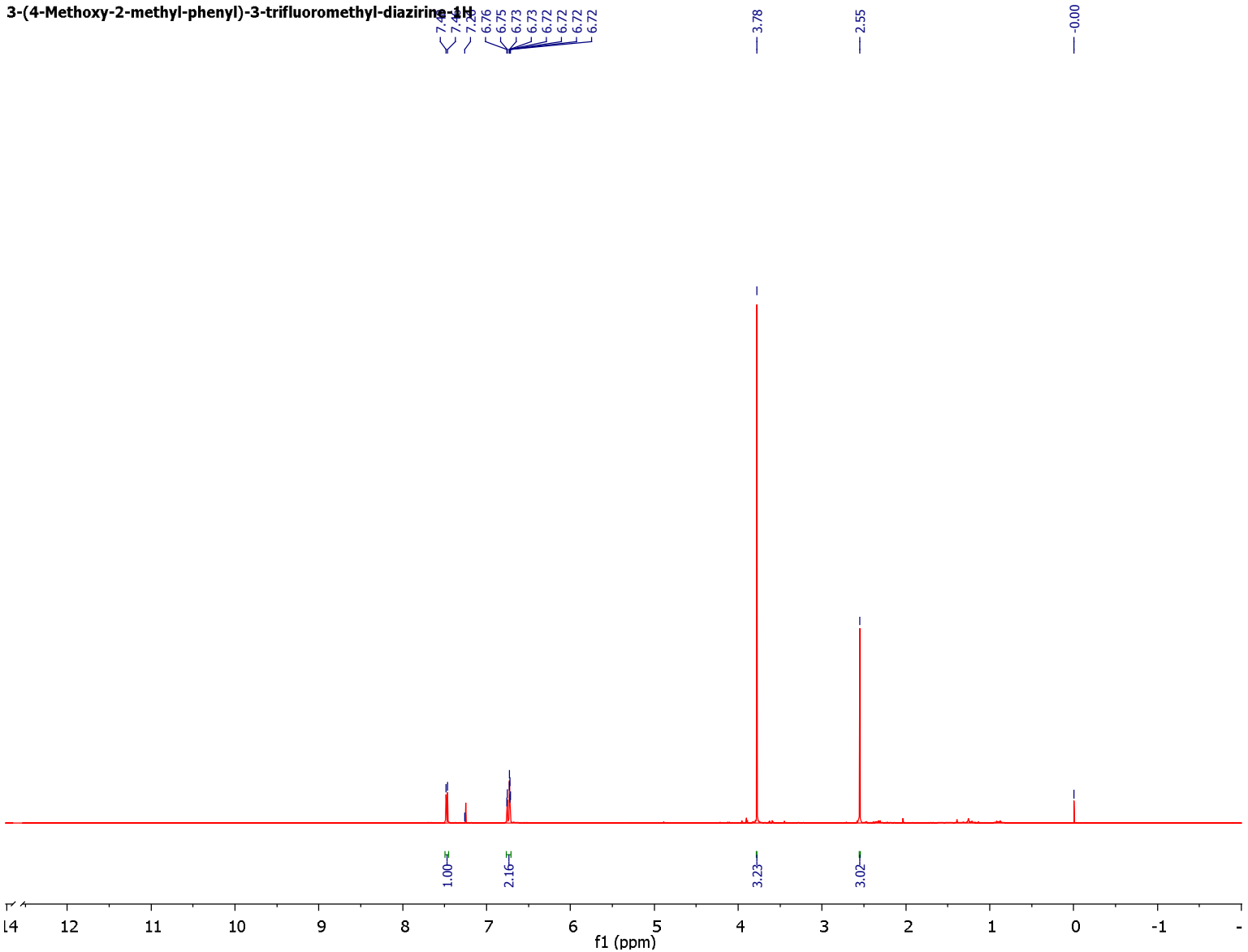

3-(4-Methoxy-2-methyl-phenyl)-3-trifluoromethyl-diazirine-19F

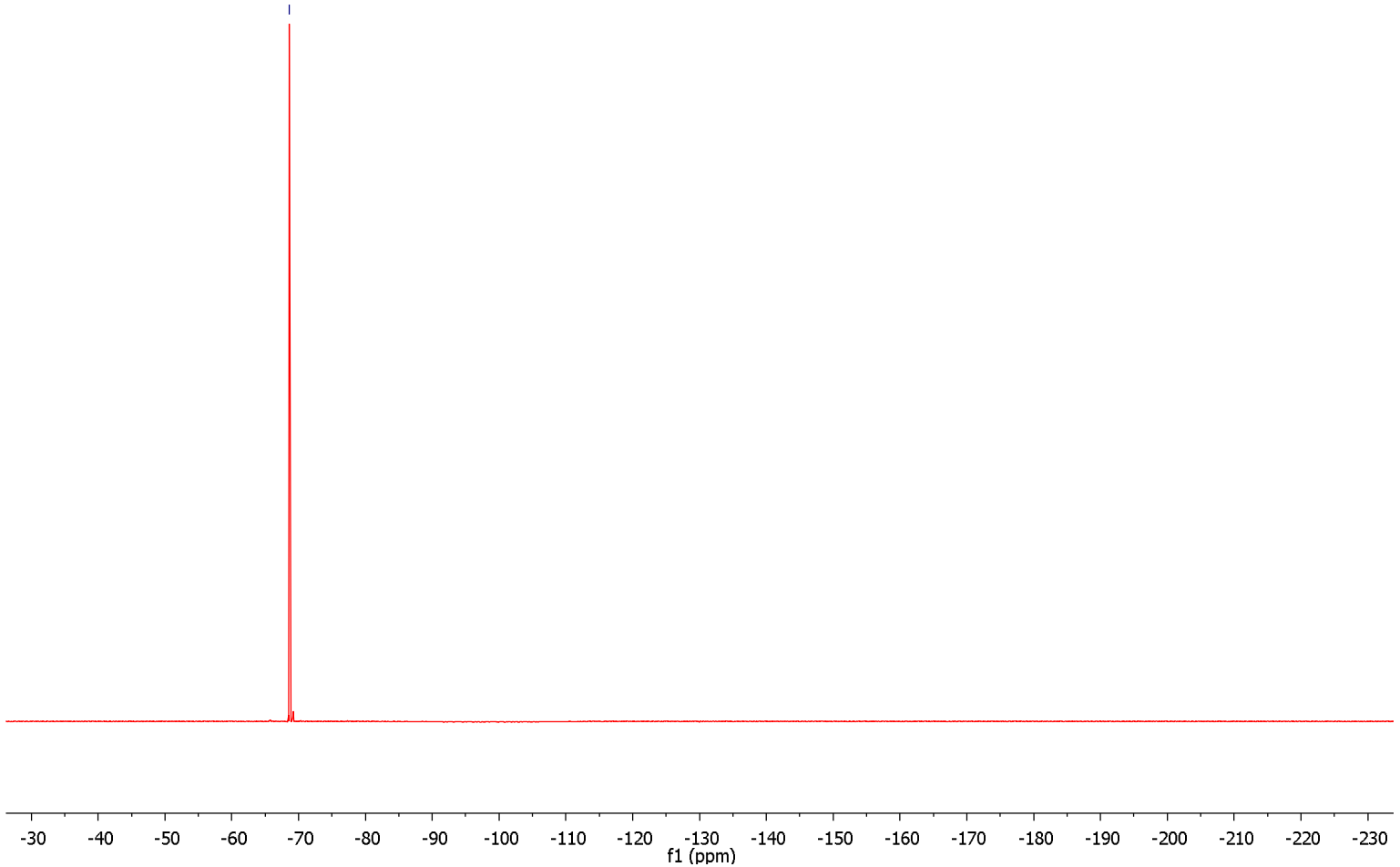

3-(4-Methoxy-2-methyl-phenyl)-3-trifluoromethyl-diazirine-13C

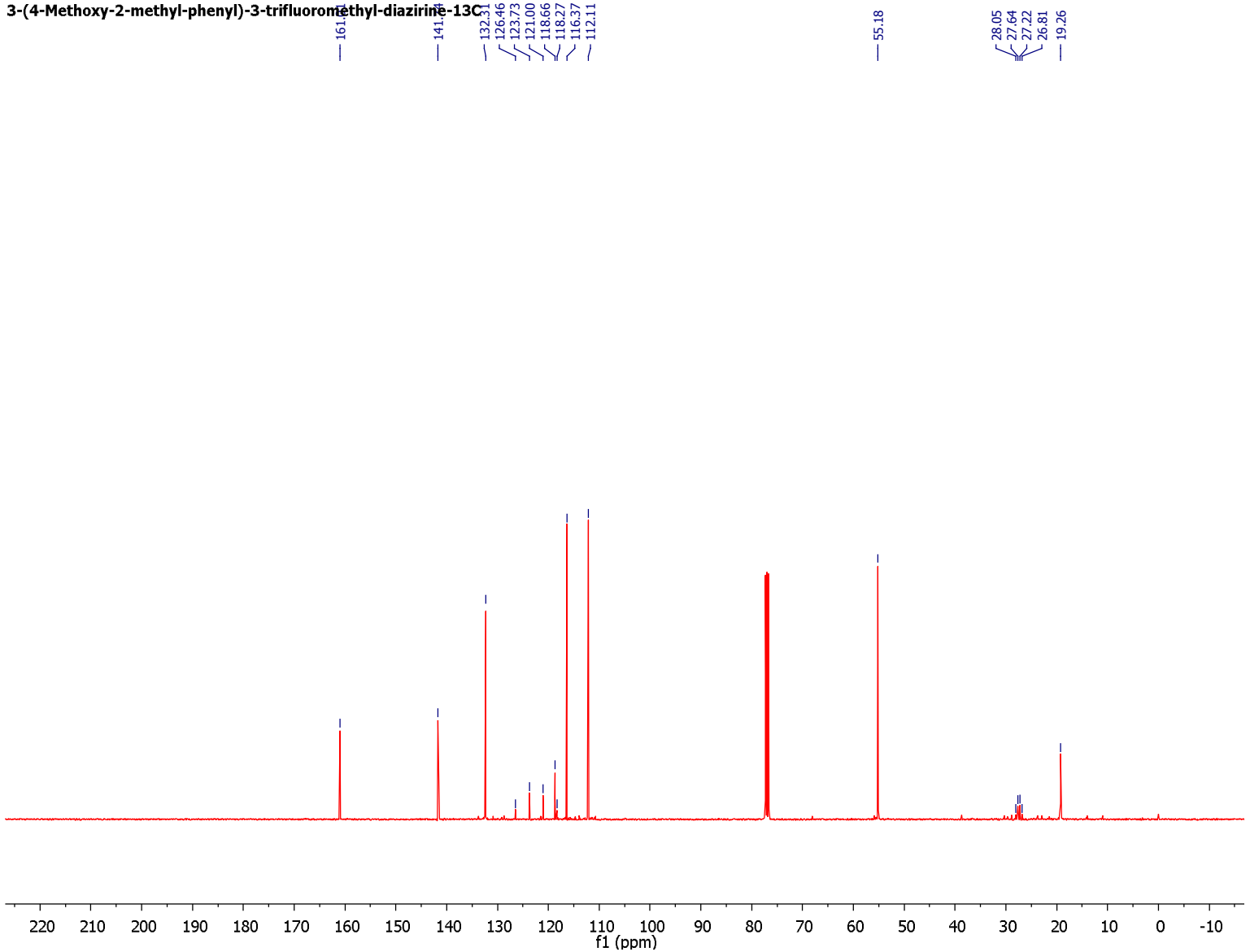

1-trifluoroacetyl piperidine-1H

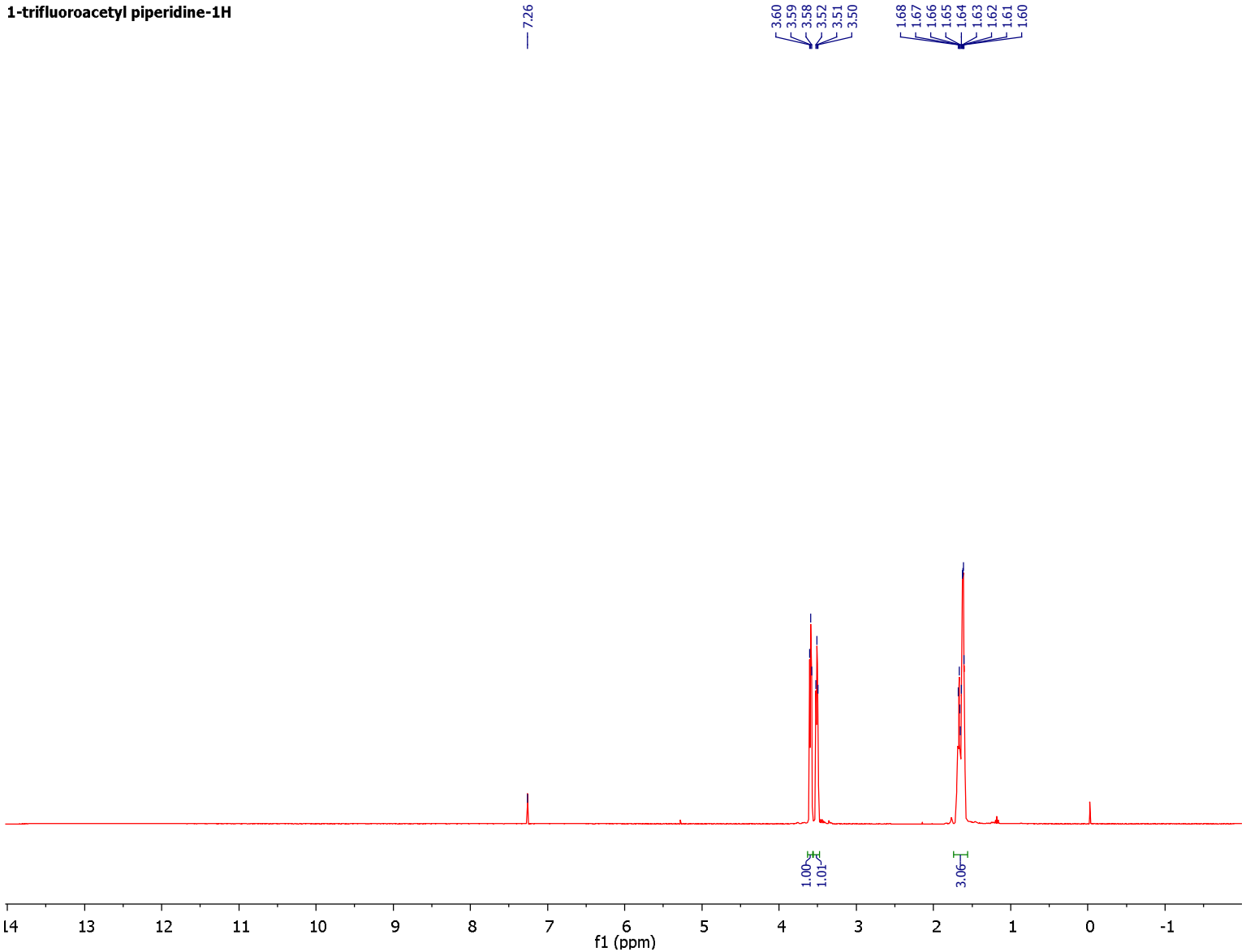

1-trifluoroacetyl piperidine-19F

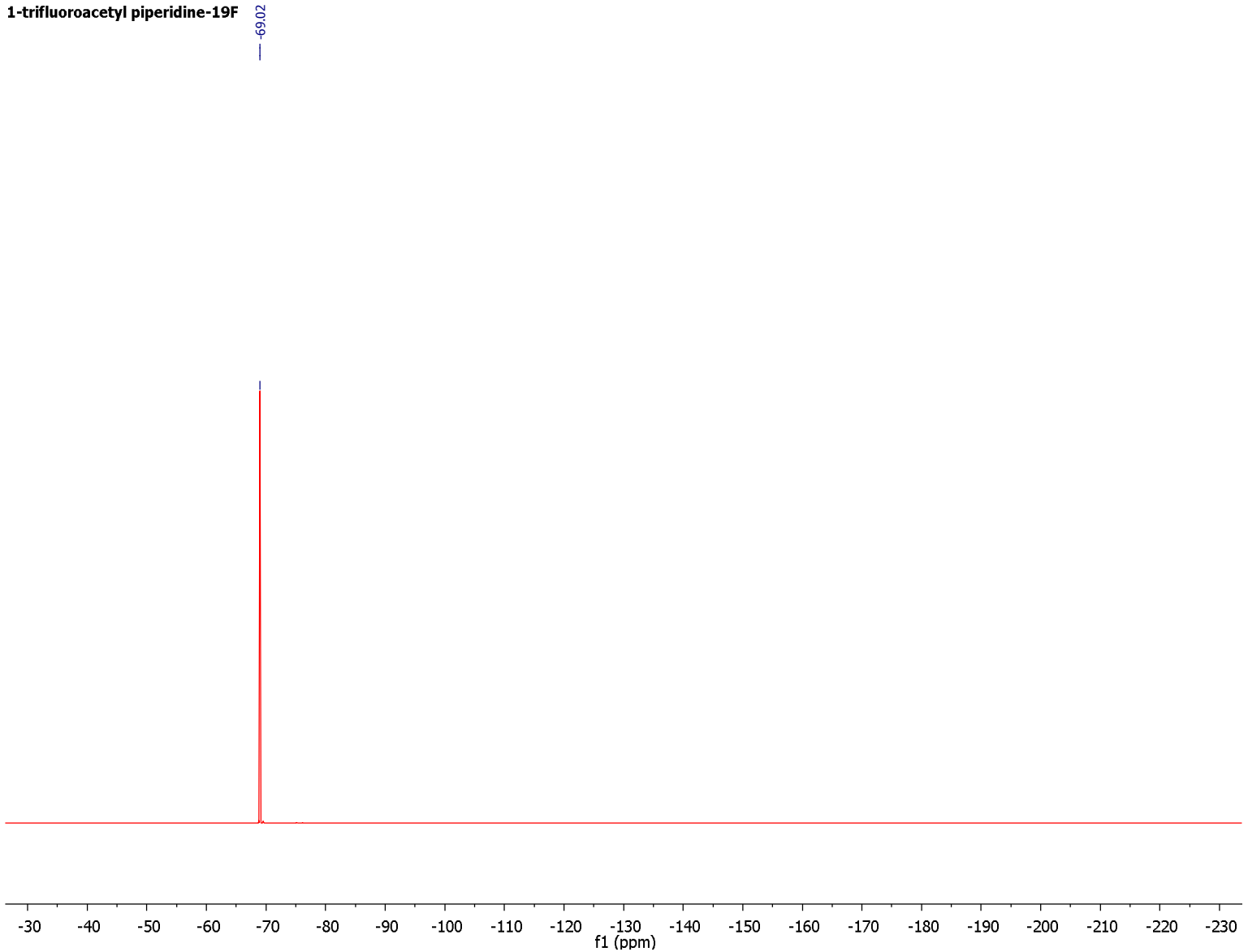

2, 2, 2-Trifluoro-1-o-tolyl-ethanone-1H

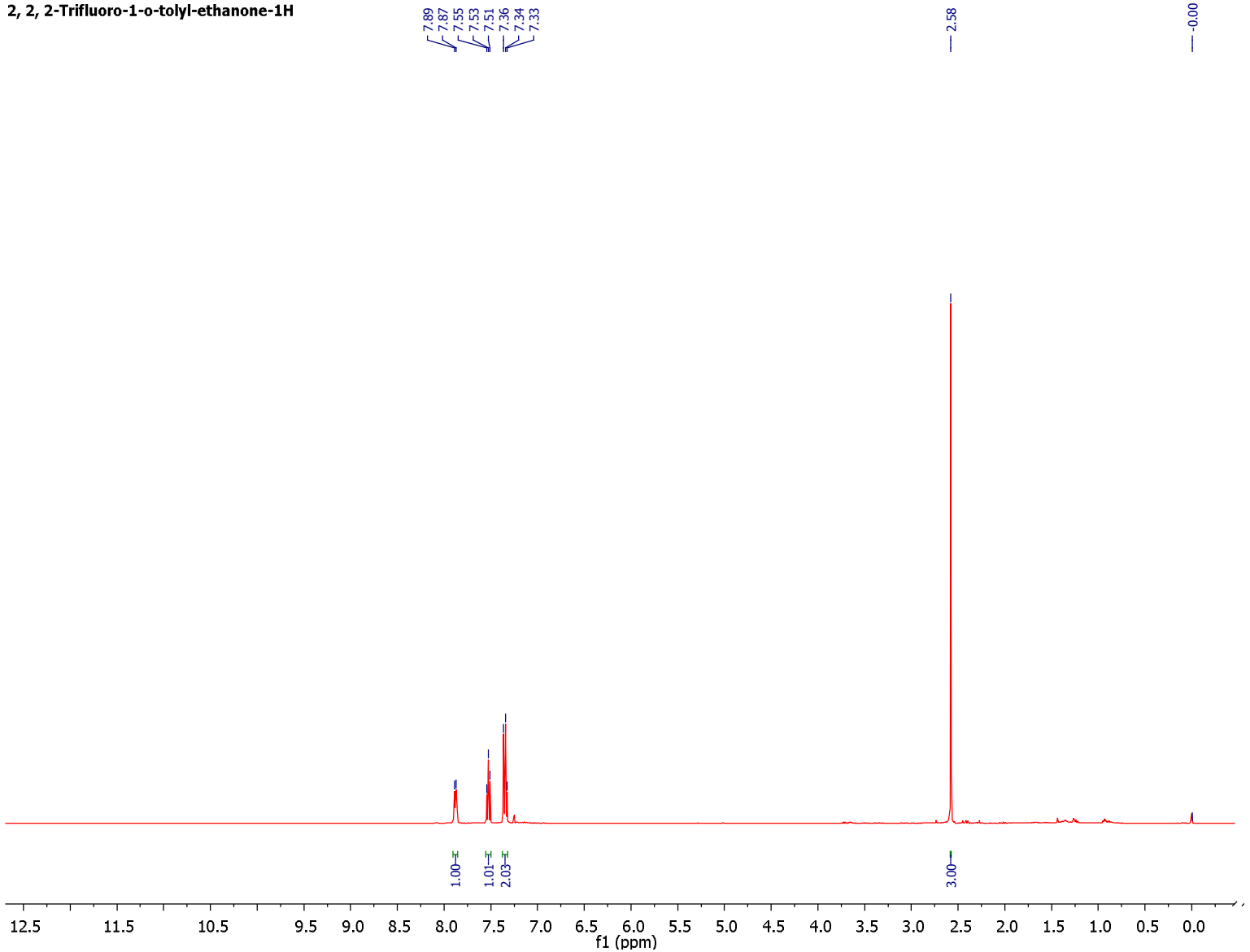

2, 2, 2-Trifluoro-1-o-tolyl-ethanone-19F

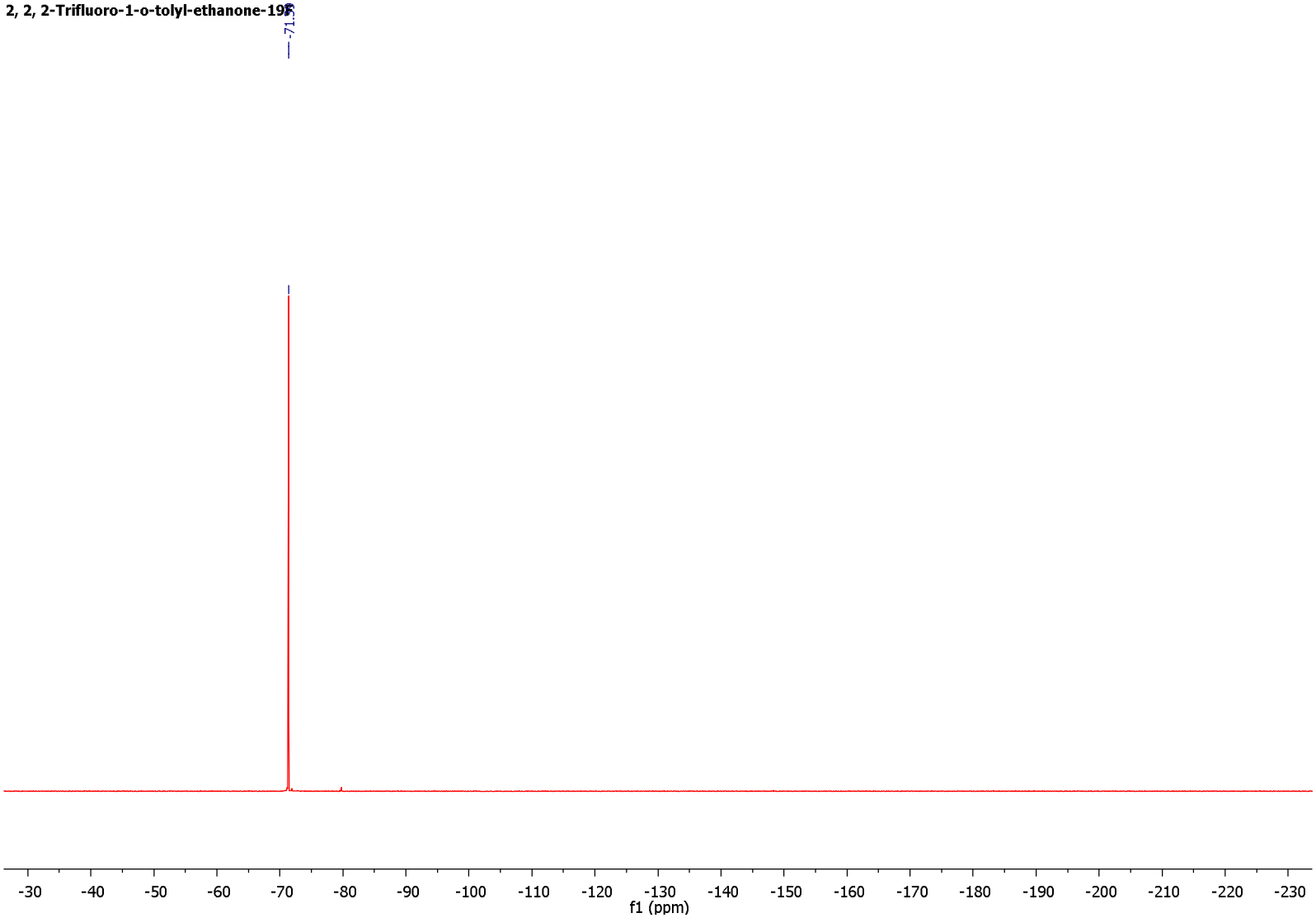

2, 2, 2-Trifluoro-1-o-tolyl-ethanone-13C

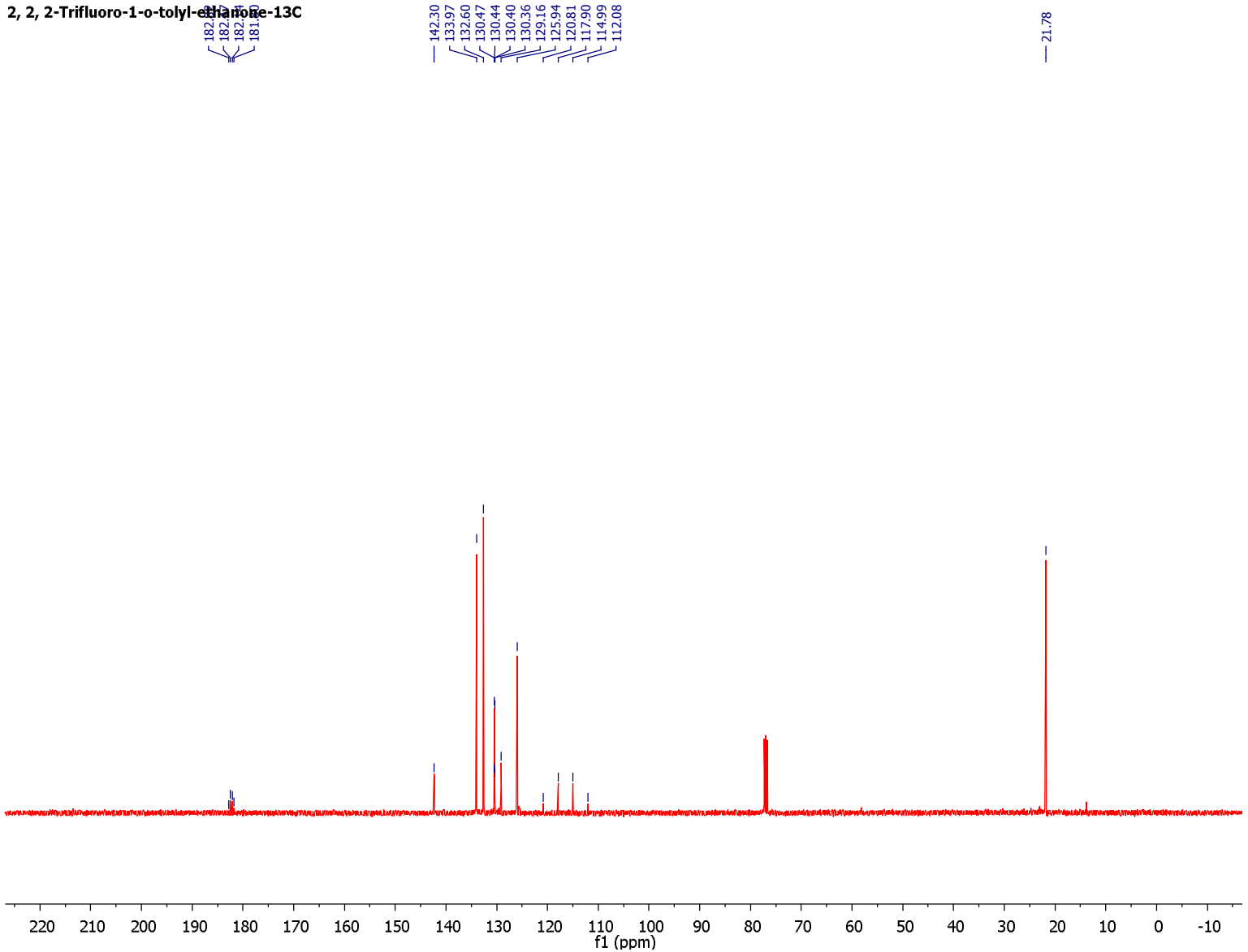

2, 2, 2-Trifluoro-1-o-tolyl-ethanone oxime-1H (two isomers)

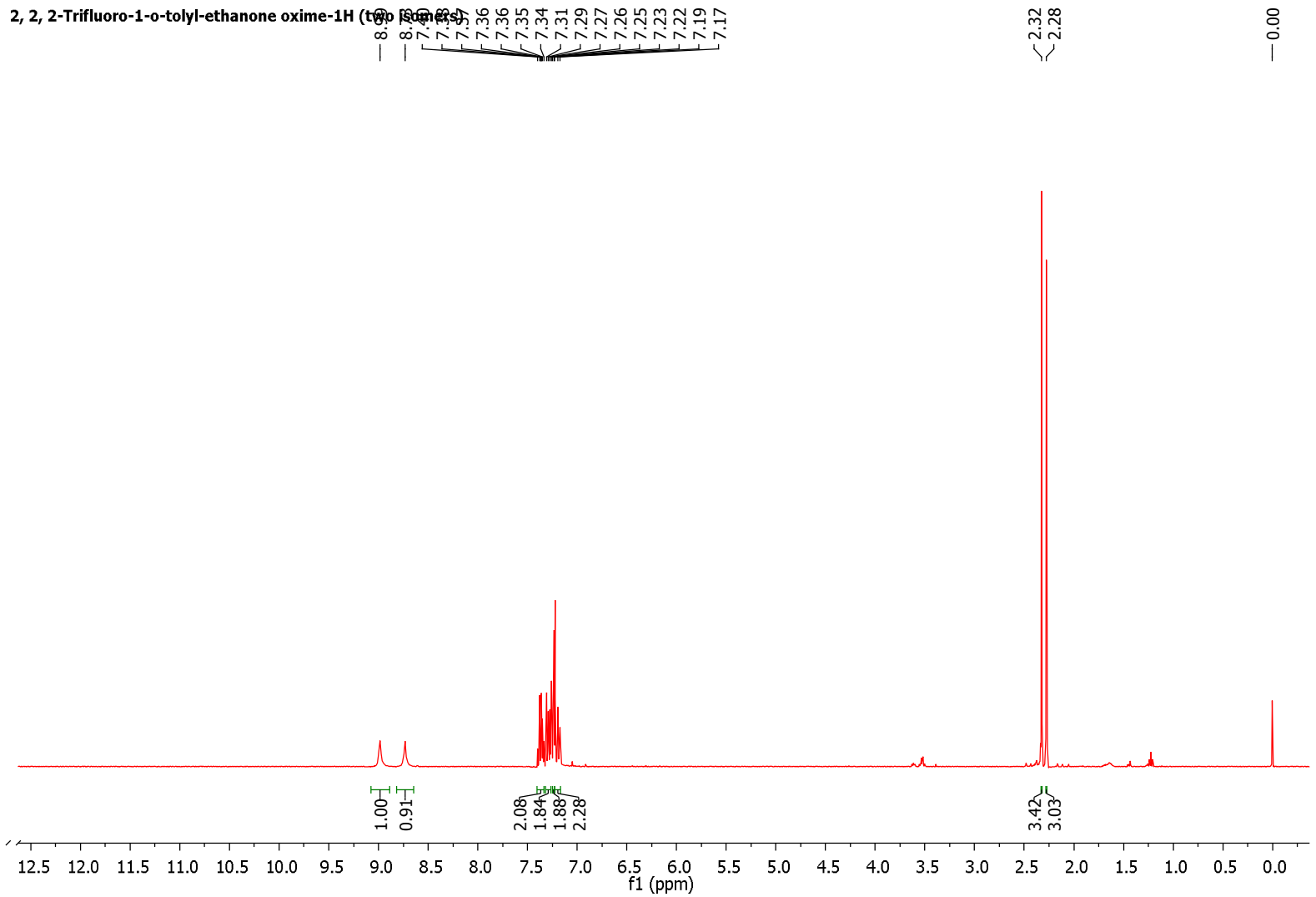

2, 2, 2-Trifluoro-1-o-tolyl-ethanone oxime-19F (two isomers)

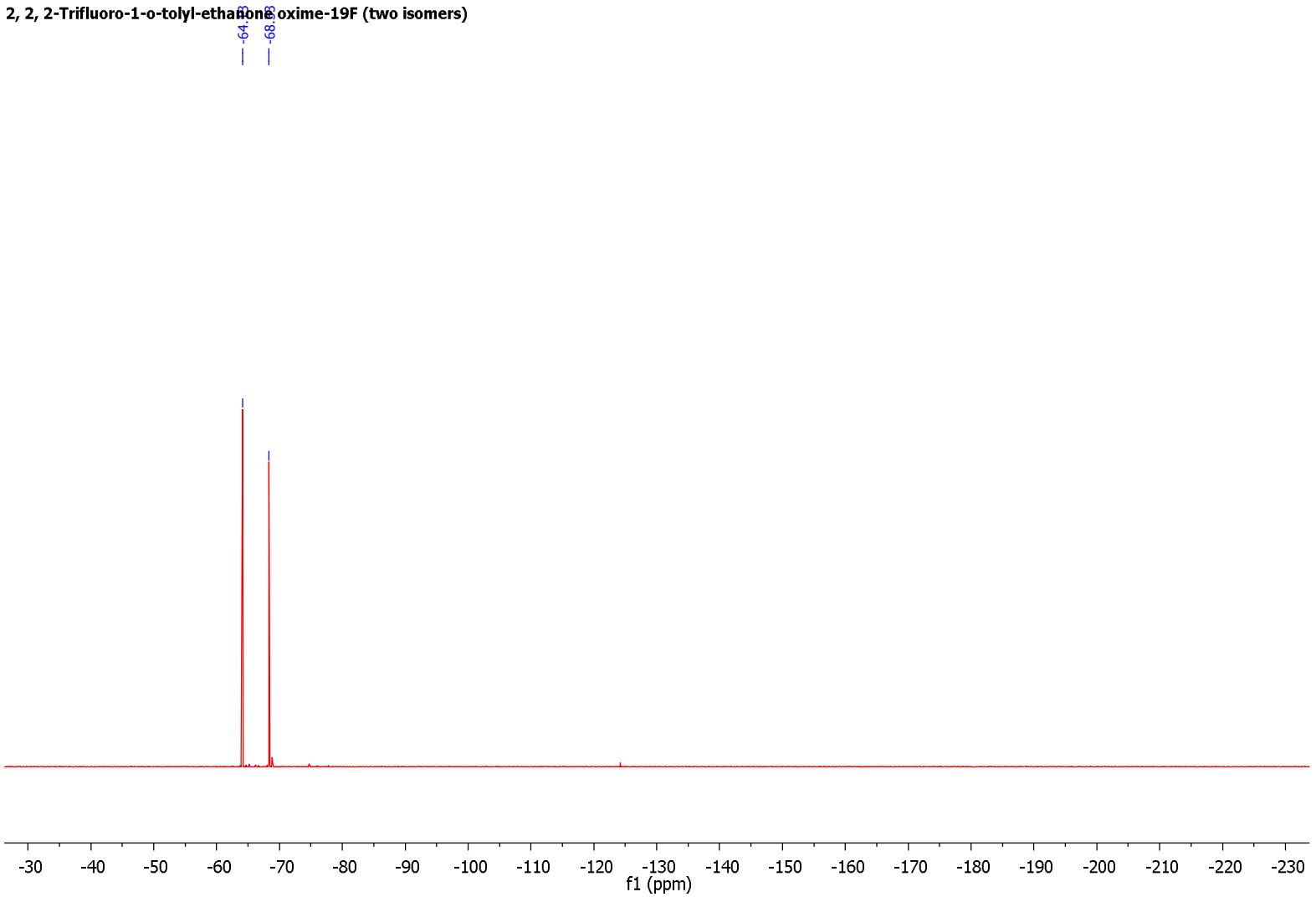

2, 2, 2-Trifluoro-1-o-tolyl-ethanone methanesulfonic oxime-1H

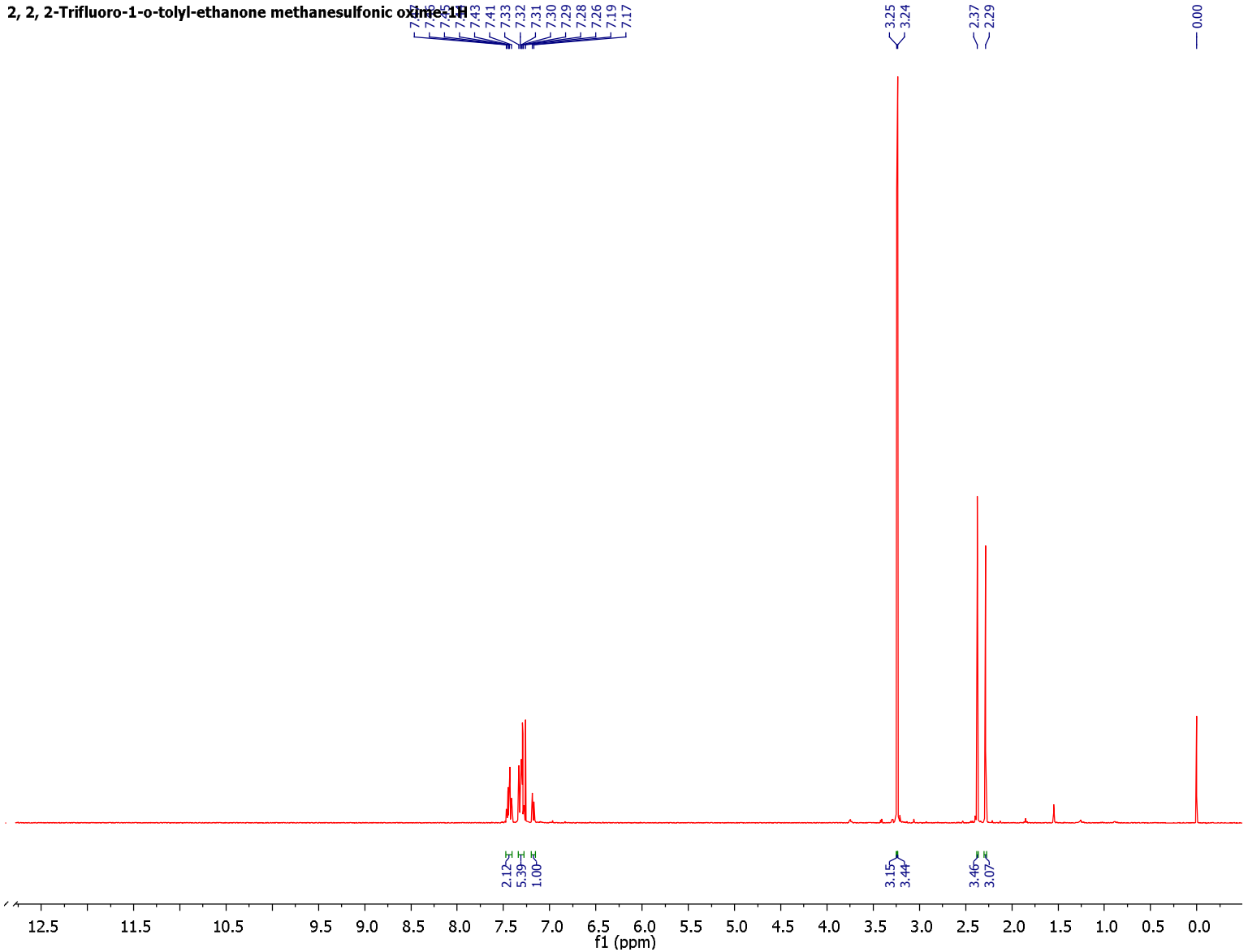

2, 2, 2-Trifluoro-1-o-tolyl-ethanone methanesulfonic oxime-19F

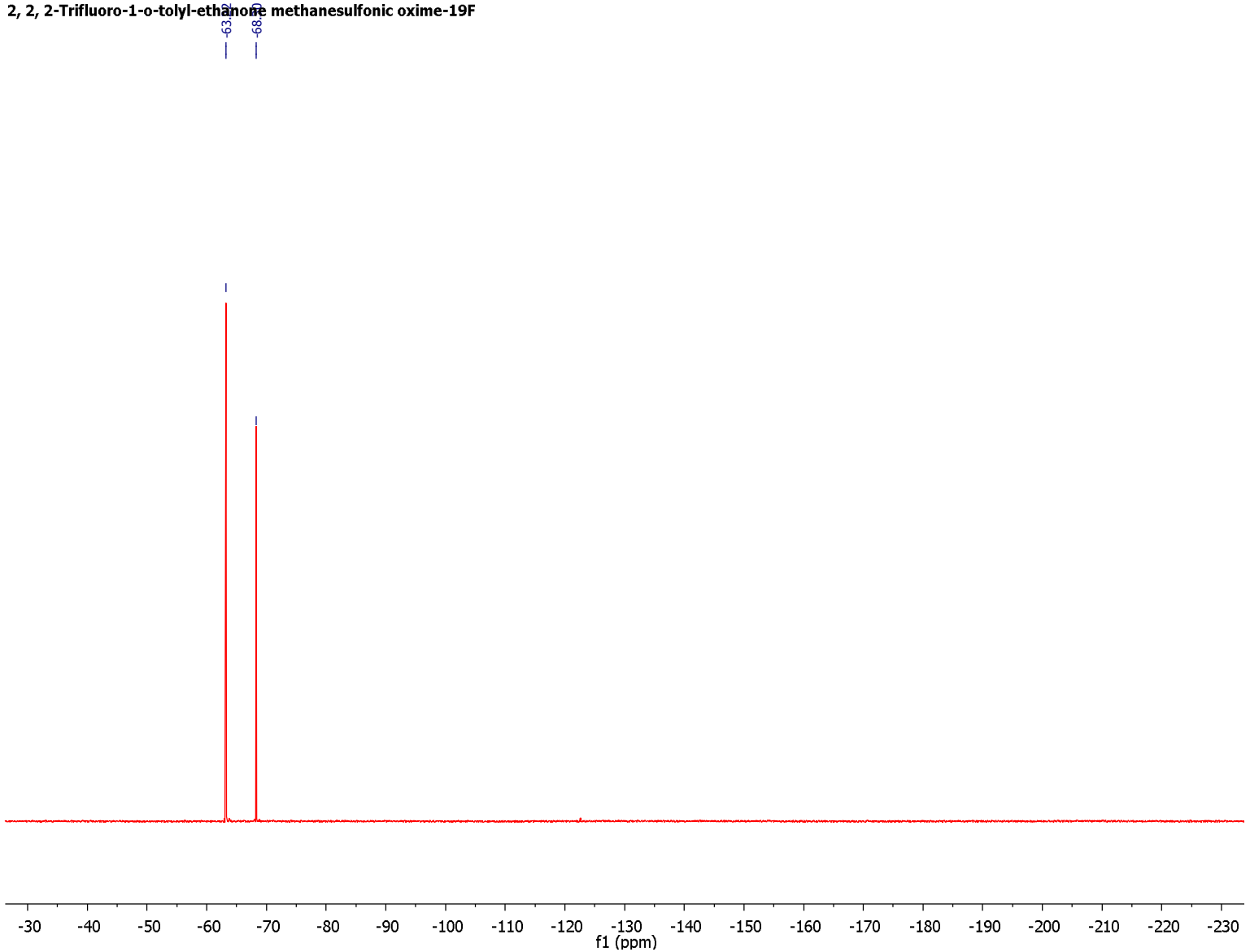

3-o-Tolyl-3-trifluoromethyl-diaziridine-1H (coexist with oxime)

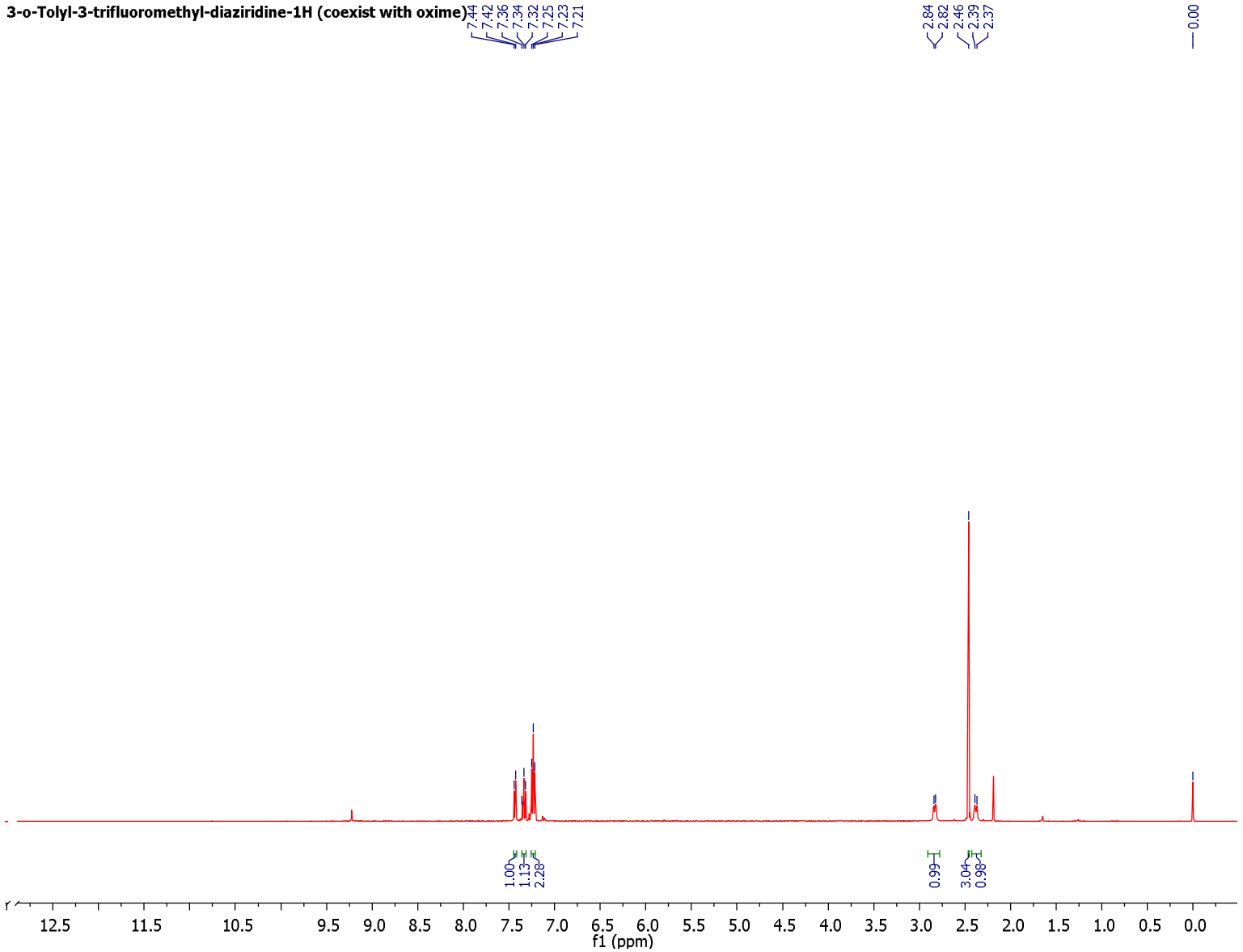

3-o-Tolyl-3-trifluoromethyl-diaziridine-19F (coexist with oxime)

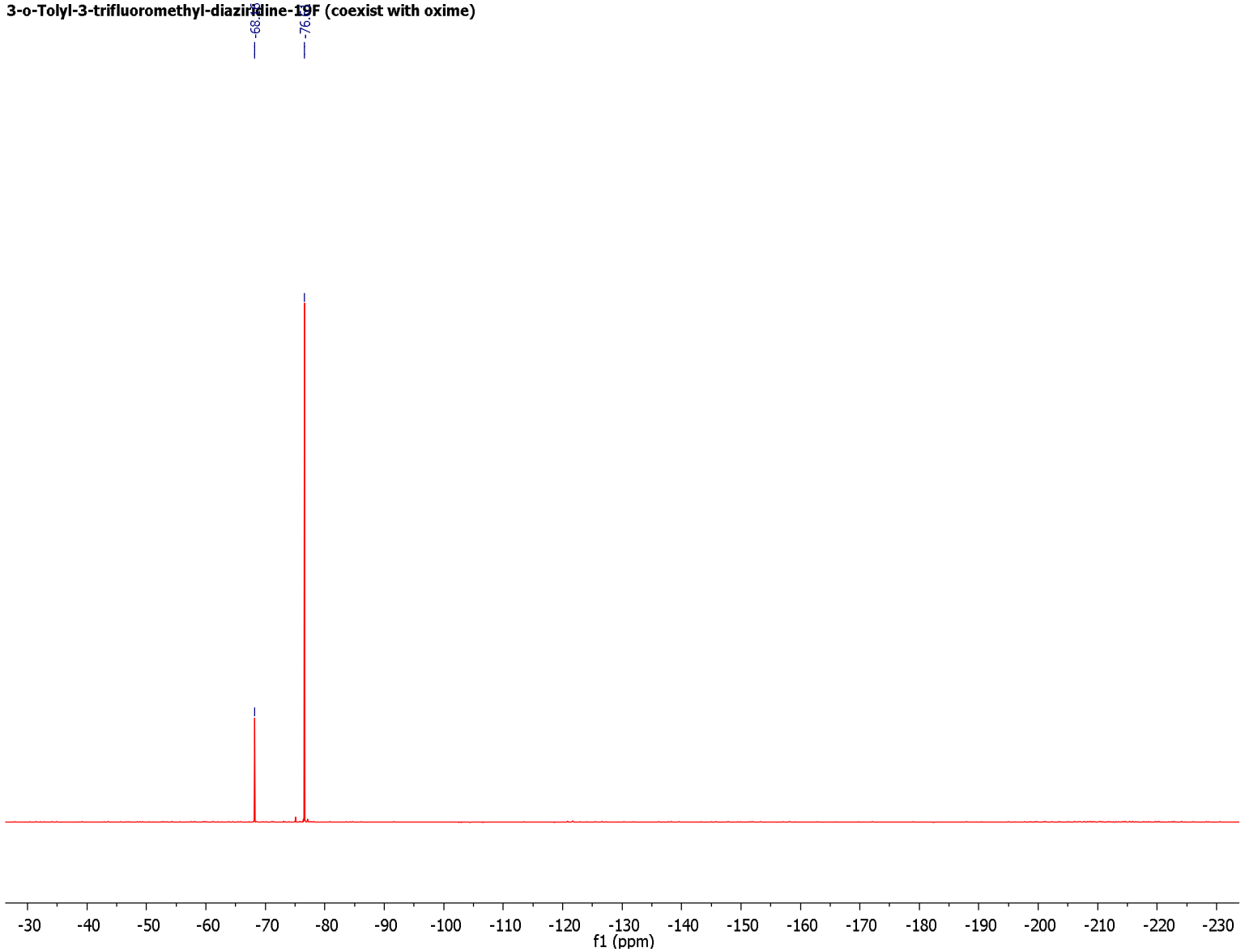

3-o-Tolyl-3-trifluoromethyl-diazirine-1H

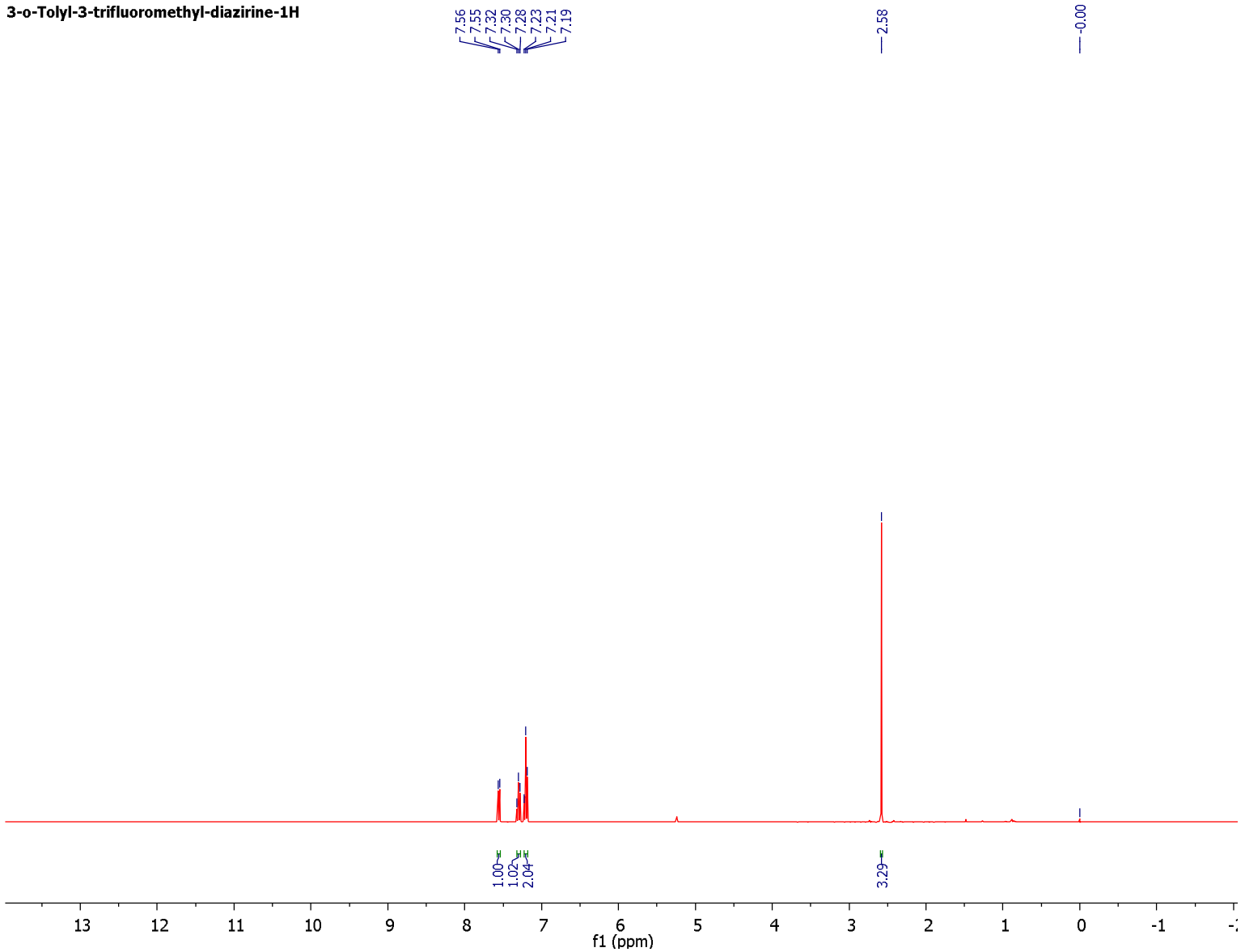

3-o-Tolyl-3-trifluoromethyl-diazirine-19F

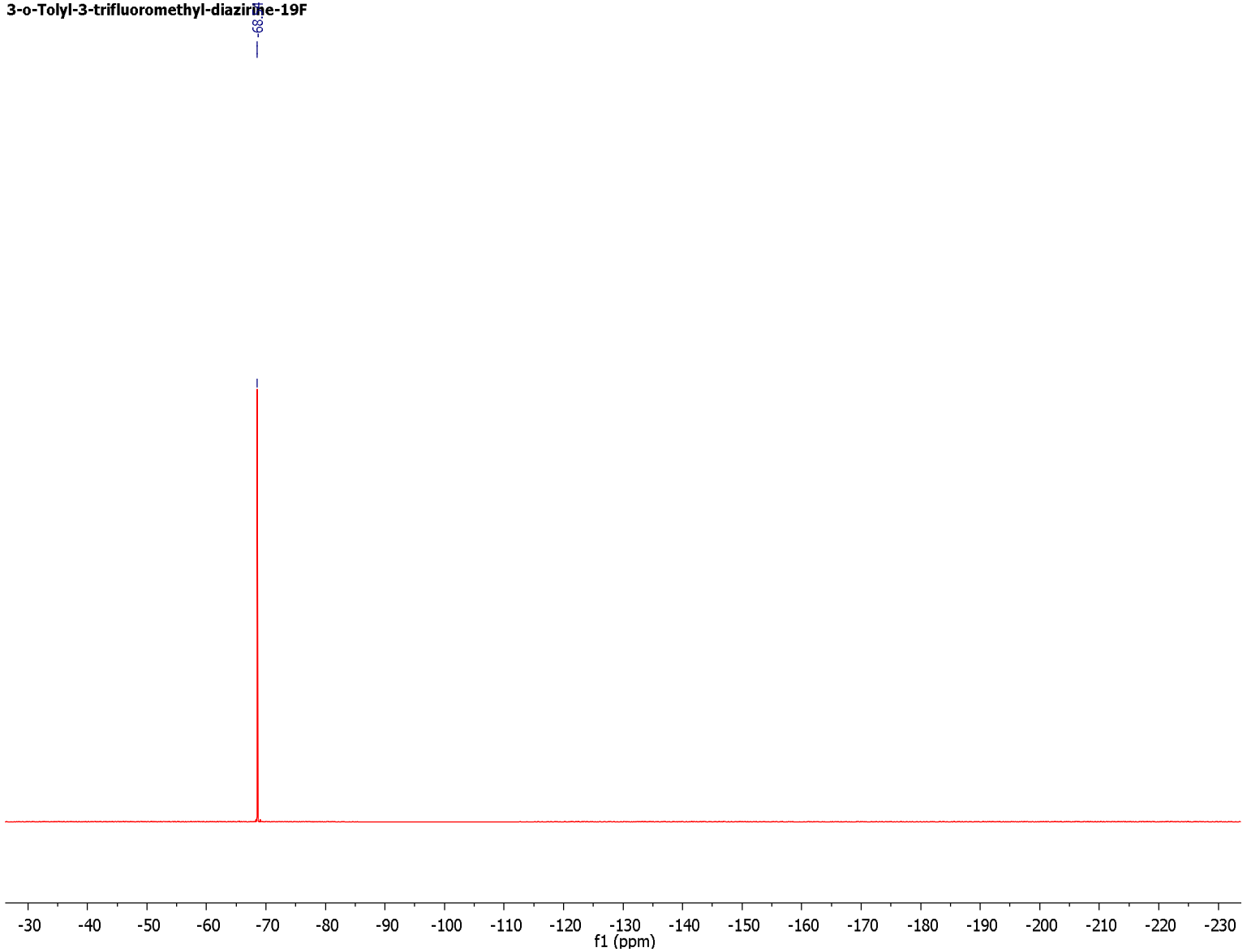

3-o-Tolyl-3-trifluoromethyl-diazirine-13C

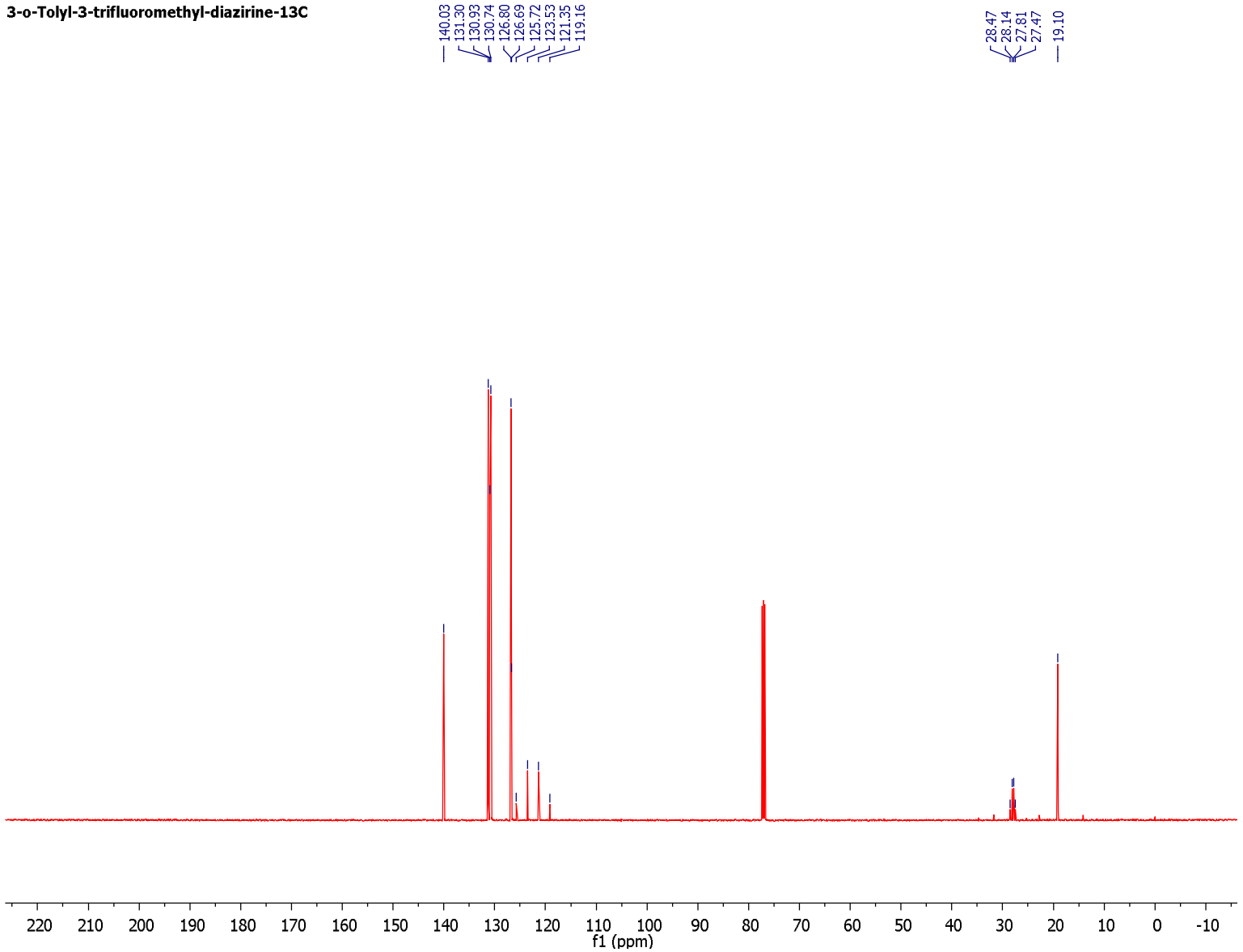

2-Bromo-(methyl-d3)-toluene-1H

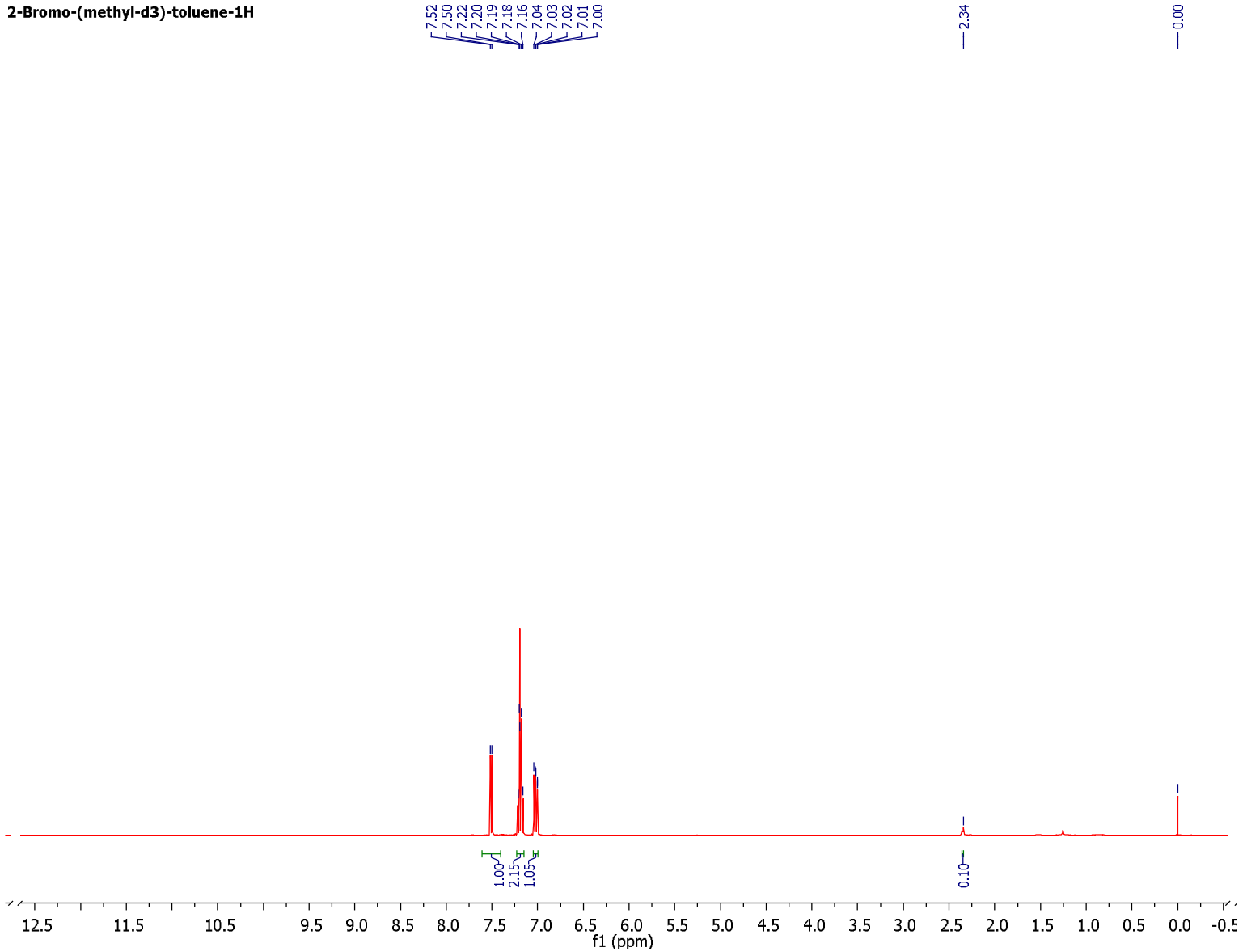

2-Bromo-(methyl-d3)-toluene-13C

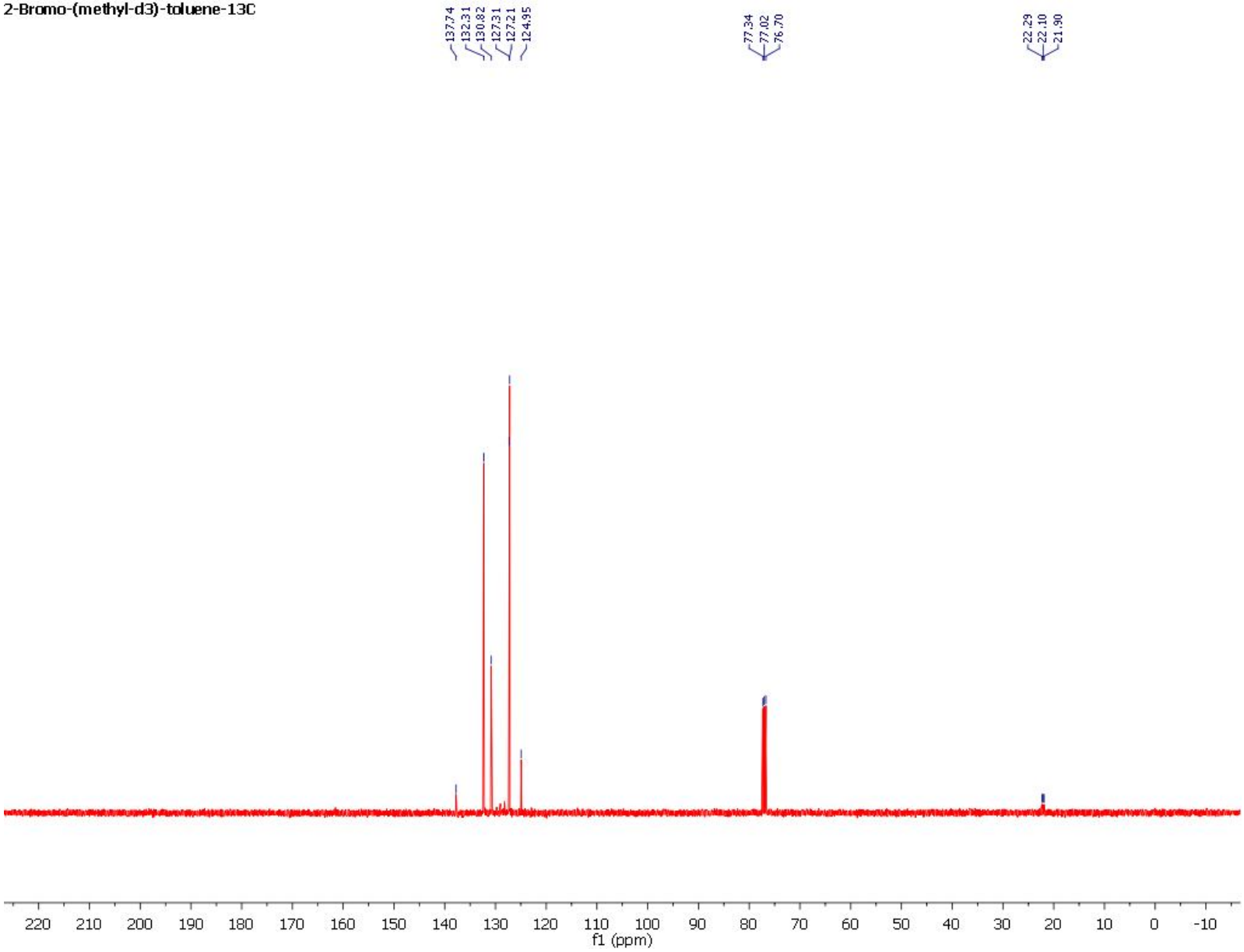

2, 2, 2-Trifluoro-1-(2-methyl-(d3)-phenyl) ethanone-1H (coexist with 1-trifluoroacetyl piperidine)

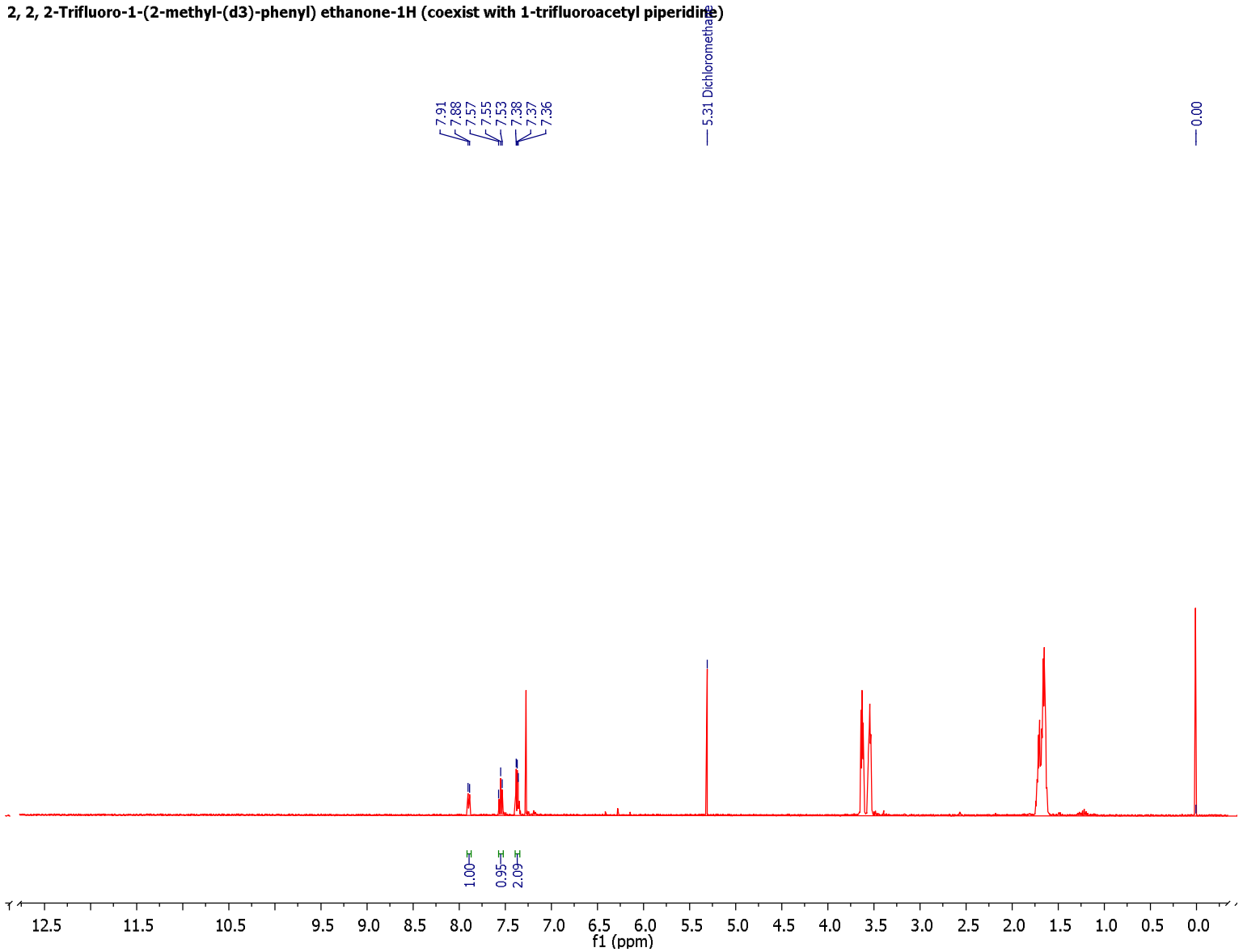

2, 2, 2-Trifluoro-1-(2-methyl-(d3)-phenyl) ethanone (coexist with 1-trifluoroacetyl piperidine)-19F

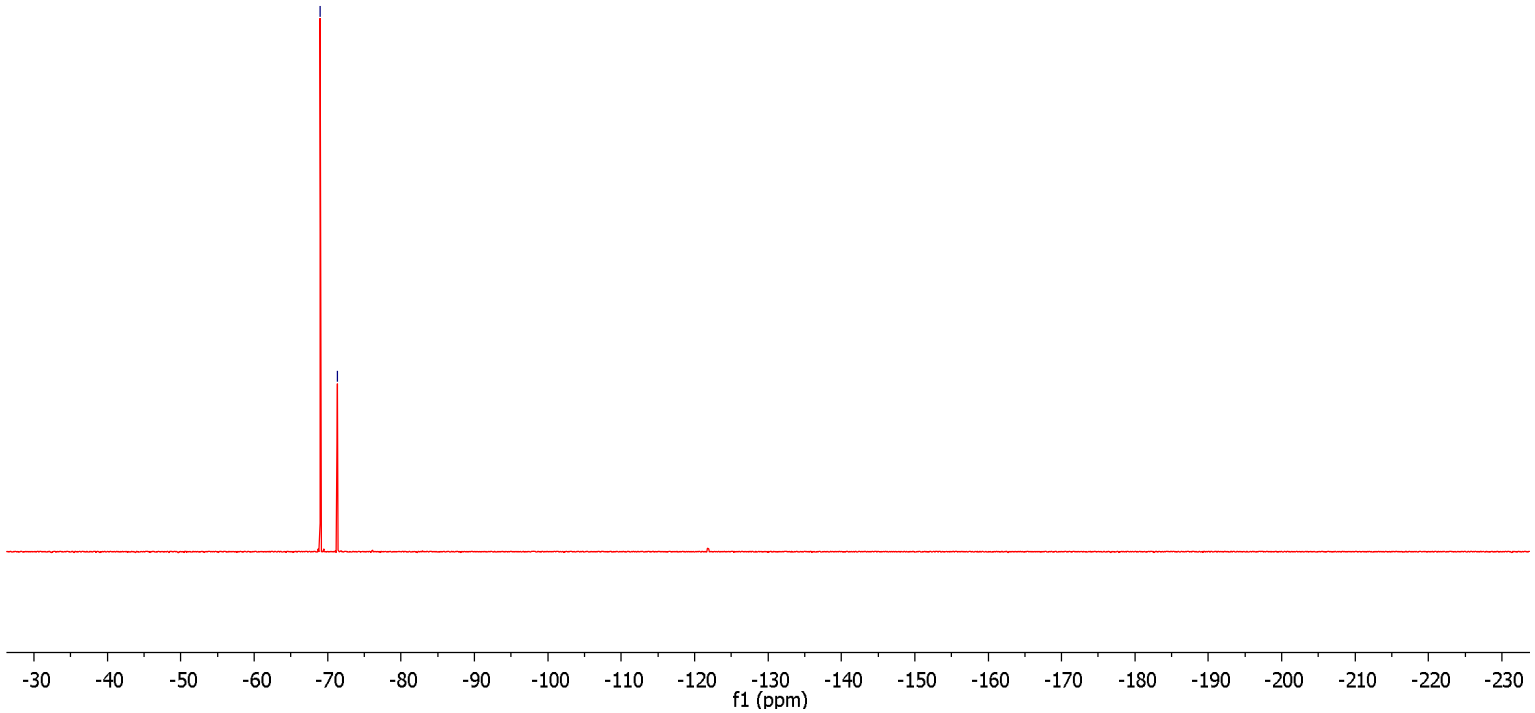

2, 2, 2-Trifluoro-1-(2-methyl-(d3)-phenyl) ethanone oxime (two isomers)-1H

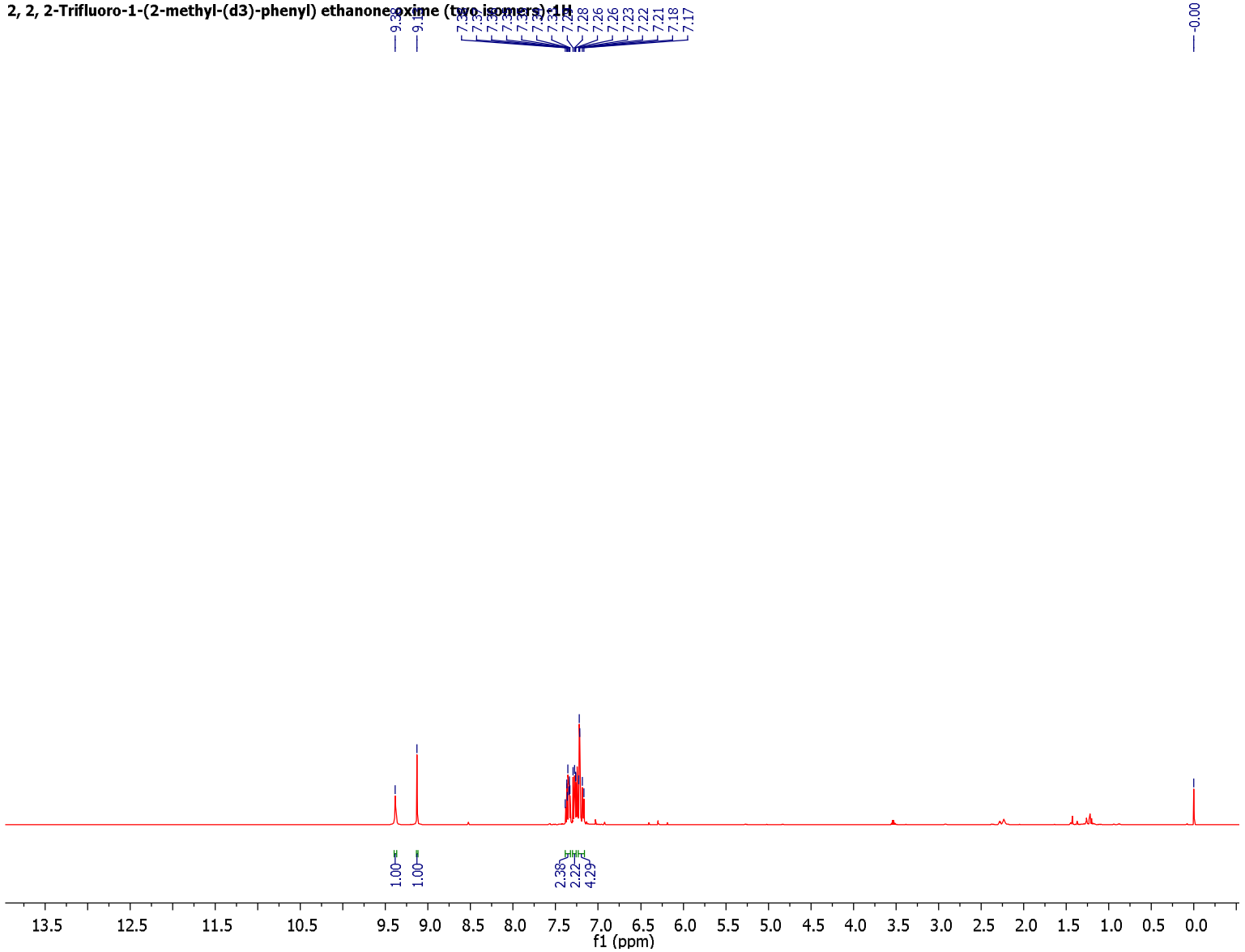

2, 2, 2-Trifluoro-1-(2-methyl-(d3)-phenyl) ethanone methanesulfonic oxime (two isomers) -19F

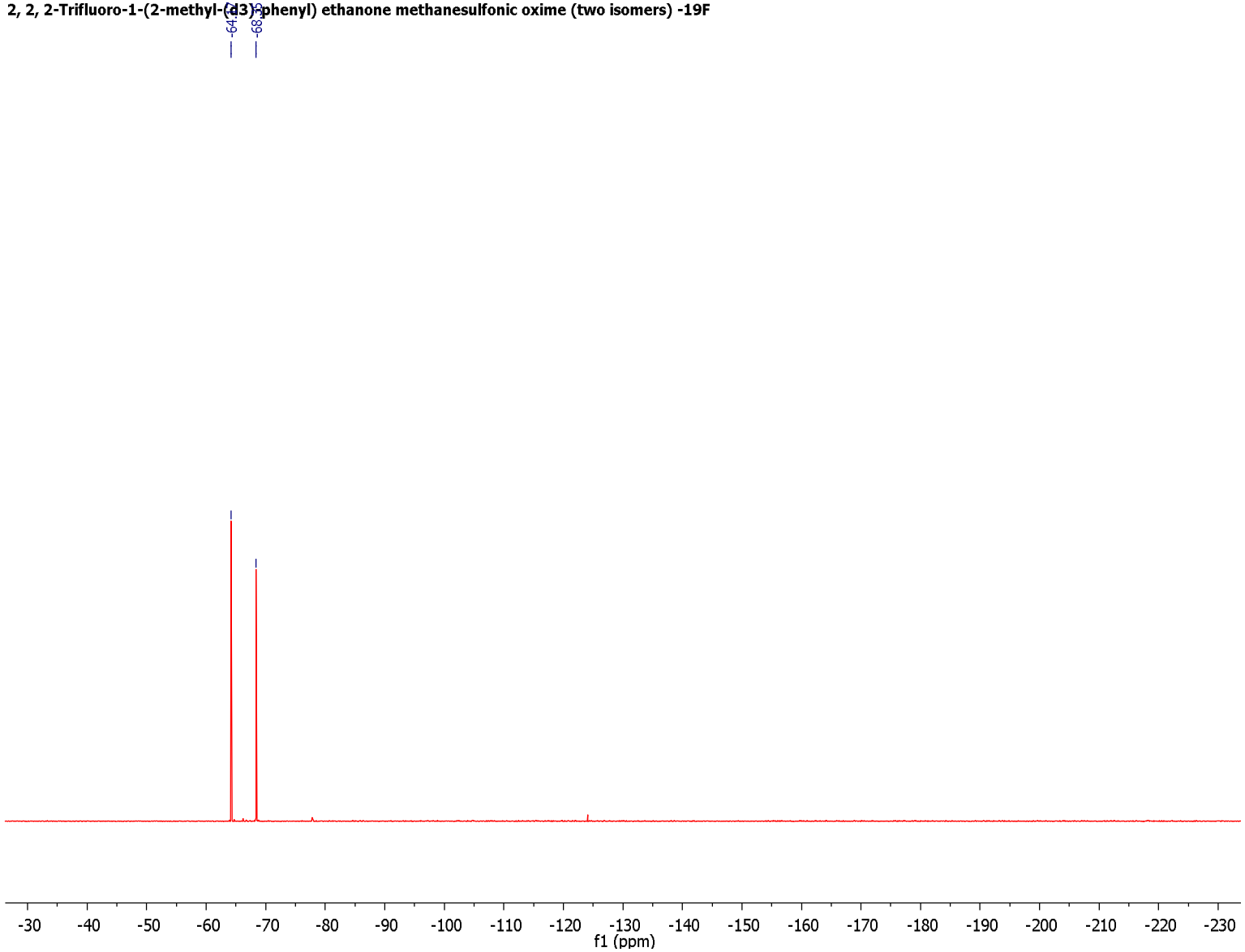

2, 2, 2-Trifluoro-1-(2-methyl-(d3)-phenyl) ethanone methanesulfonic oxime (two isomers)-1H

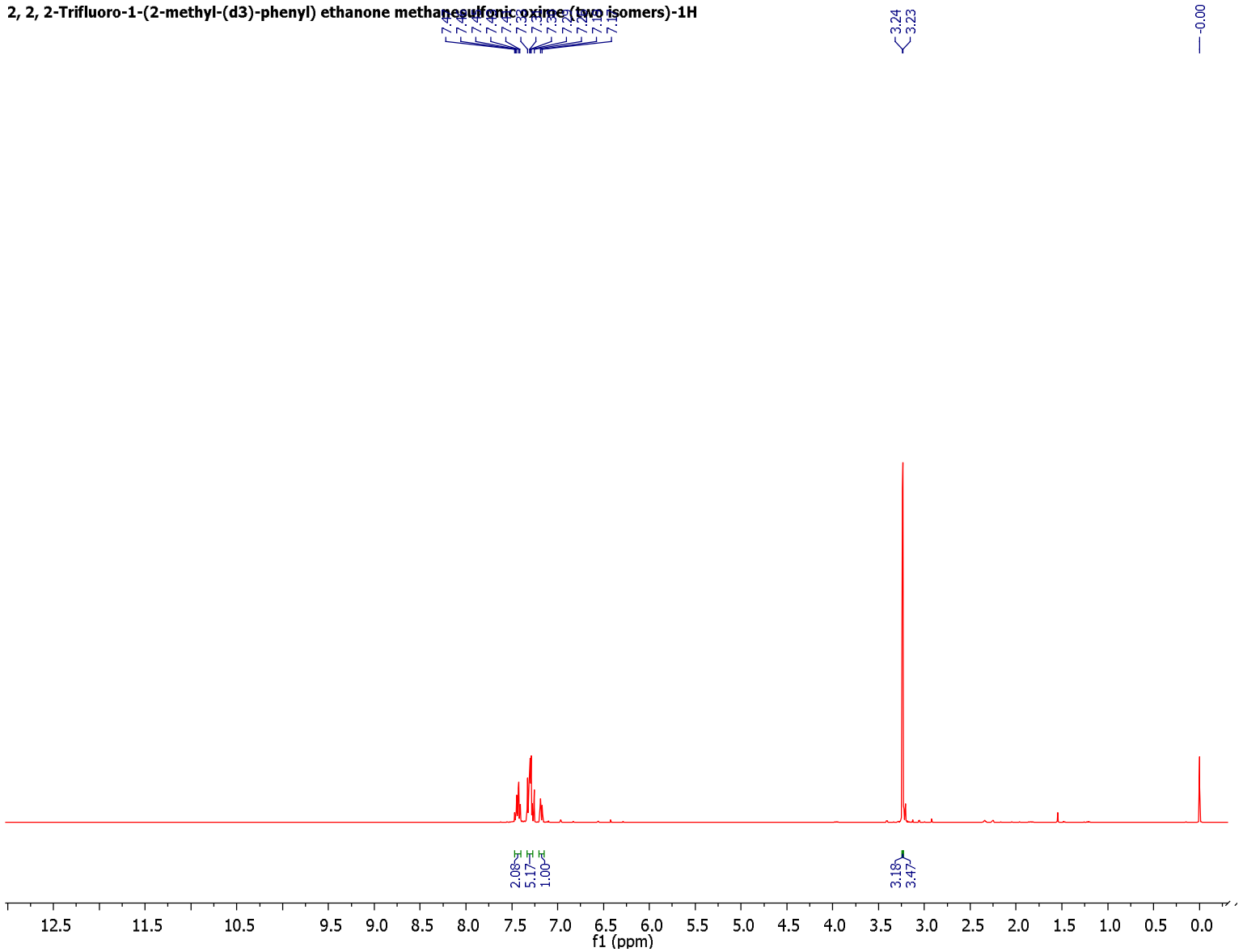

2, 2, 2-Trifluoro-1-(2-methyl-(d3)-phenyl) ethanone methanesulfonic oxime (two isomers)-19F

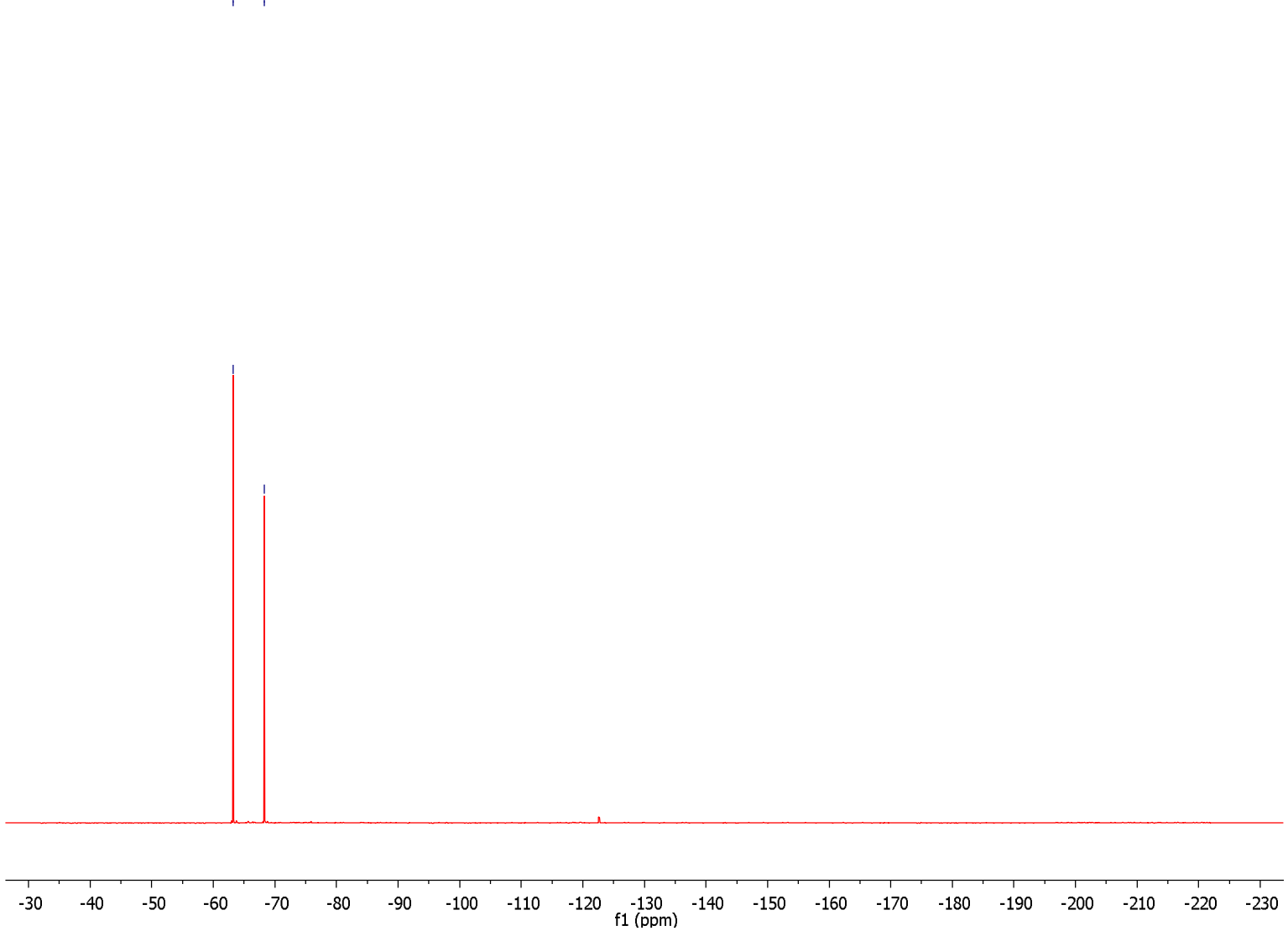

3-(2-Methyl-(d3)-phenyl)-3-(trifluoromethyl) diaziridine-1H

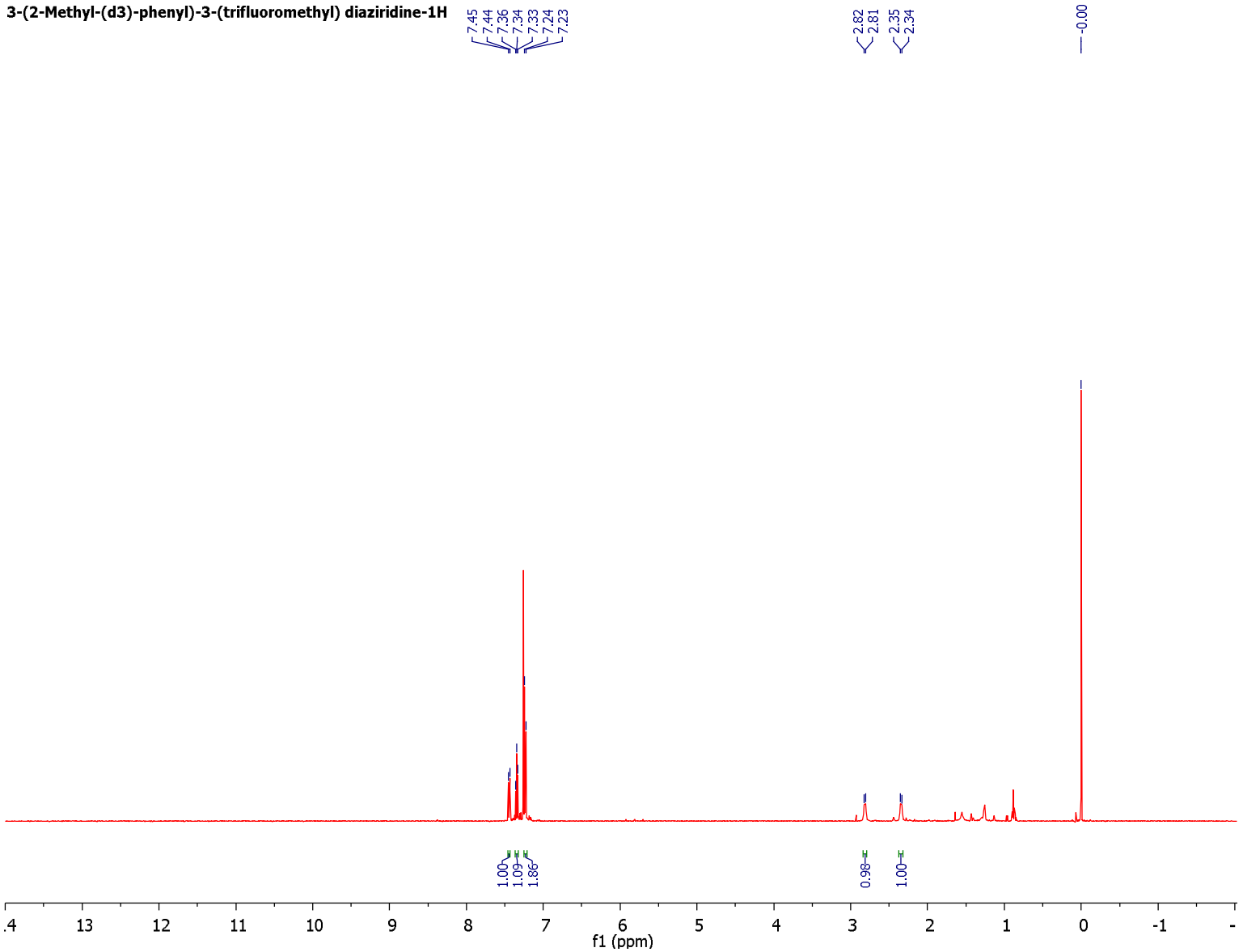

3-(2-Methyl-(d3)-phenyl)-3-(trifluoromethyl) diaziridine (coexist with oxime)-19F

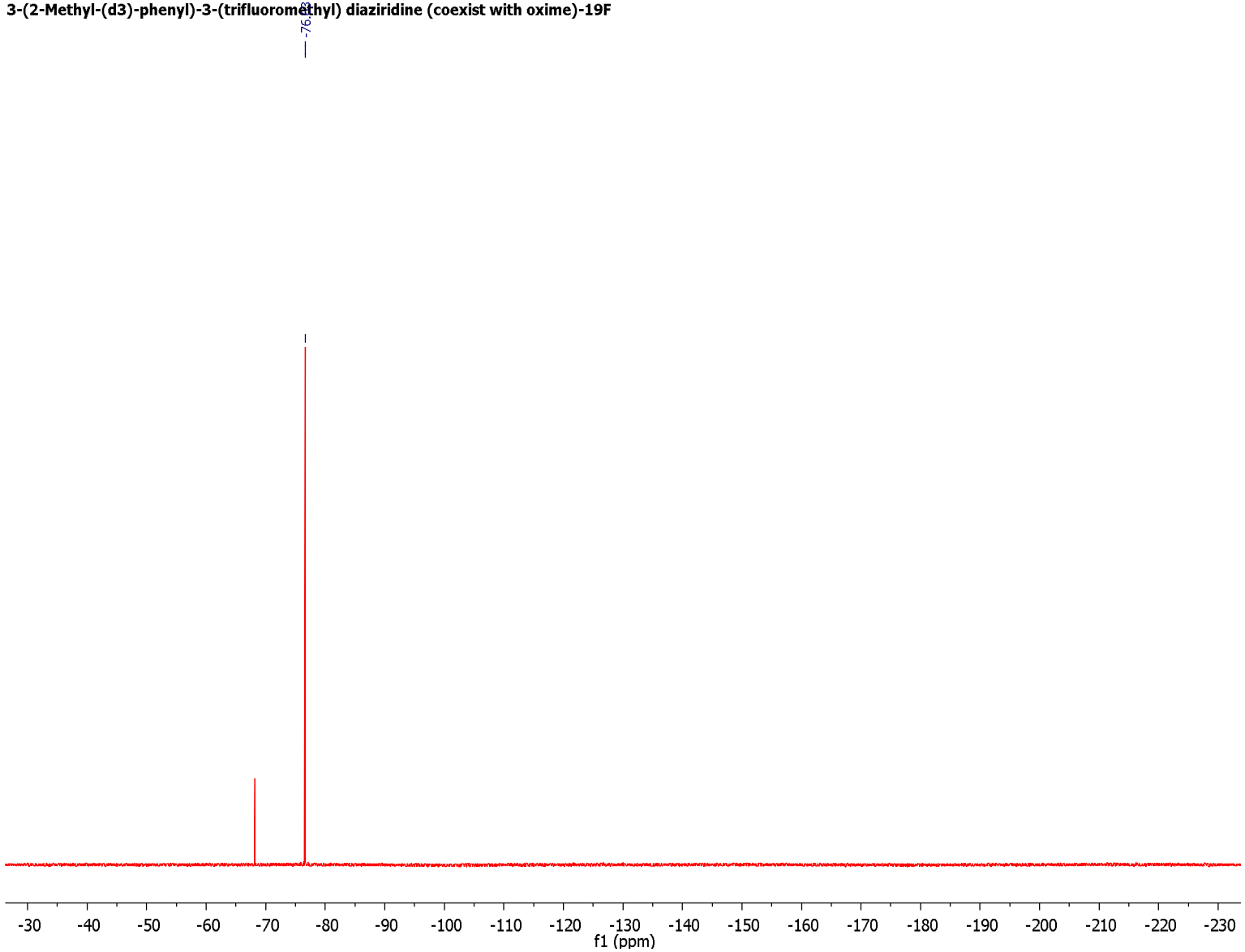

3-(2-Methyl-(d3)-phenyl)-3-(trifluoromethyl) diazirine-1H

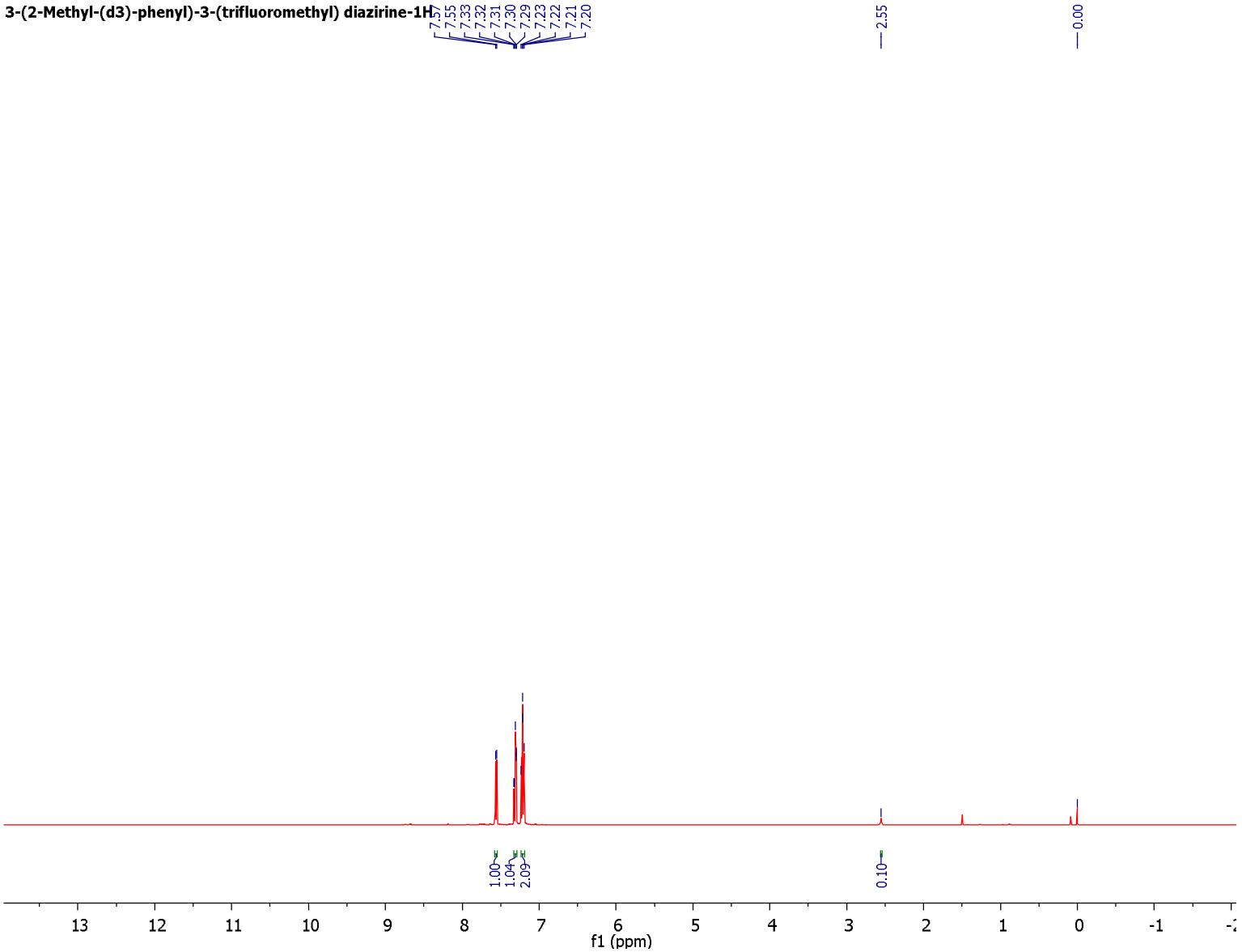

3-(2-Methyl-(d3)-phenyl)-3-(trifluoromethyl) diazirine-19F

3-(2-Methyl-(d3)-phenyl)-3-(trifluoromethyl) diazirine-13C